Dissertation

Submitted to the

Combined Faculties for Natural Sciences and Mathematics

of the

Ruprecht-Karls-University of Heidelberg, Germany

for the degree of

Doctor of Natural Sciences (Dr. rer. nat)

Presented by

Maximilian Breuer, M.Sc.

Born in Bonn, Germany

Date of Examination:_____

Characterizing the function and role of three dihydropteridine reductase homologs, Qdpra, Qdprb1 and Qdprb2 in the embryonic development of *Danio rerio*

1st Referee: Prof. Dr. Andreas Draguhn

2nd Referee: Prof. Dr. Ana Martin-Villalba

I hereby declare that this thesis is my own work and that, to the best of my knowledge and belief, contains no material previously published or written by another person, except for those explicitly acknowledged in my thesis.

Maximilian Breuer: _____

City and Date: _____

Believe those who are seeking the truth, doubt those who find it!

- André Gide -

Contents

Figures

Supplemental Figures

Tables

Abstract

Recycling of the cofactor tetrahydrobiopterin (BH_4) via dihydropteridine reductase (DHPR) is required for the synthesis of tyrosine from phenylalanine, as well as dopamine and serotonin precursors, L-Dopa and 5-HT, respectively. Patients with DHPR deficiency have severe neurological symptoms, including brain atrophy, dystonia and epilepsy. The pathophysiology remains mostly unknown.

In order to model the disorder to better understand its pathophysiology we characterized all three homologs of the zebrafish (*Danio rerio*), Qdpra, Qdprb1 and Qdprb2 in the developing embryo. We analyzed the genes' temporal expression during development using whole mount *in situ* hybridization and qRT-PCR and investigated their functional relevance using morpholino mediated knockdown. We further used a diagnostic approach to examine amino acid levels in both wildtype and morphant embryos.

We were able to identify the homolog Qdpra to be involved in the production of melanin in the early embryo, likely due to its conserved BH_4 recycling function. Morphants showed hyperphenylalaninemia and significantly depleted melanin levels. We could show that *qdpra* is co-expressed with the BH_4 dependent enzyme Phenylalanine hydroxylase and is active in the liver post 3 days of development. Qdprb2 was found to be not required, nor expressed in the early embryo. *qdprb1* was detected in the early proliferative regions of the eye and midbrain. We could show that Qdprb1 influences glial development, while neuronal development was unaffected. Intriguingly, Qdprb1 inhibits glutamine production. We discovered that similar to Qdprb1 morphant embryos exposed to high levels of glutamine, exhibit a depletion of astroglial markers in eye and midbrain. We could not detect any involvement in BH_4 and therefore conclude glia differentiation by regulating glutamine as a novel function. Although the underlying mechanisms remain to be explored, we were able to observe high glutamine levels in a severe DHPR patient, just as we observed in Qdprb1 morphants.

Our study is the first to give insights into the pathophysiology of DHPR deficiency, by modeling the disorder in zebrafish and unraveling a novel role for the homolog Qdprb1 in regulating gliogenesis.

Abstract - Deutsch

Der Kofaktor Tetrahydrobiopterin (BH_4) wird recycled durch die Dihydrobiopteridin Reduktase (DHPR). BH_4 wird benötigt für die Synthese von Tyrosin von Phenylalanin sowie für die Vorstufen der Neurotransmitter Dopamin und Serotonin: L-Dopa und 5-HT. Eine DHPR-Defizienz geht zumeist einher mit schweren neurologischen Symptomen. Diese beinhalten unter anderem: Hirnatrophie, Dystonie und Epilepsie. Die Pathophysiologie ist weitestgehend unbekannt.

Mit dem Zebrabärbling (*Danio rerio*) als Modellorganismus, charakterisieren wir die drei Homologe Qdpra, Qdprb1 und Qdprb2, mit Hilfe von Morpholinos, *in situ* Hybridisierungen und qRT-PCR. Mit diagnostischen Methoden haben wir die Aminosäuren bestimmt und die Wildtypen mit Defizienten Fischen verglichen. Wir haben die Embryos hohen Konzentrationen von Glutamin ausgesetzt um den Phänotypen zu reproduzieren und haben Transgene, sowie Antikörperfärbungen als visuelles Ergebnis.

Es ist uns gelungen, den Homolog Qdpra der Produktion von Melanin im frühen Embryo zuzuweisen, durch die Supplementierung von BH_4 für das Enzym Pah. Eine Defizienz führte zu einer Hyperphenylalaninämie und signifikant erniedrigtem Melanin-Spiegel. Nach 3 Tagen der Entwicklung konnten wir *qdpra* Ko-lokalisiert zur Pah in der Leber aufzeigen. Für Qdprb2 wurde keine relevante Funktion in der frühen Embryonalentwicklung erkannt. *qdprb1* wurde detektiert in den frühen proliferativen Zonen des Auges und Mittelhirns. Es beeinflusst die Gliazell Entwicklung, während neuronale Entwicklung unbeeinflusst war. Qdprb1 reguliert Glutamin, welches bei hoher Exposition die Gliazellmarker des Auges und Mittelhirn runter reguliert. Wir konnten keine Verbindung zur traditionellen Funktion und BH_4 bestimmen und folgern daher die Regulation von Glutamin und der Gliazell-differenzierung als neue, bisher unbeschriebene, Funktion der Qdprb1. Des Weiteren konnten wir, wie bei Qdprb1 in Zebrafisch, erhöhte Glutamin-Spiegel in einem Patienten mit schwerer DHPR-Defizienz nachweisen

Unsere Ergebnisse sind die ersten, die Einblicke in die Pathophysiologie der DHPR-Defizienz ermöglichen, durch die erfolgreiche Charakterisierung der Qdpr im Zebrabärbling, sowie die Bestimmung einer neuen Funktion des Homologes Qdprb1 in der Gliogenese.

Abbreviations

Table 1. Abbreviations

Abbreviation	Full Name
°C	Degrees Celsius
µ	Micro
3-OMD	3-O-Methyldopa
5-HT	5-Hydroxytryptophan
AP	Alkaline phosphatase
BCAA	Branched chain amino acids
BCIP	5-bromo-4-chloro-3-indoyl-phosphate
BH_2	Dihydrobiopterin
BH_4	Tetrahydrobiopterin
bp	Base pairs
BSA	Bovine serum albumin
CMZ	Ciliary marginal zone
CNS	Central nervous system
CRISPR	Clustered regularly interspaced short palindromic repeats
CSF	Cerebrospinal fluid
Da	Dalton
DAPI	4,6-Diamidin-2-phenylindol
DHKA	Dihydrokainic acid
DMEM	Dulbecco modified eagle medium
DMSO	Dimethylsulfoxide
DNA	Deoxyribonucleic acid
DOB	Date of birth
dpf	days post fertilization
ECL	Enhanced chemiluminescence
ECM	Extracellular matrix
EDTA	Ethylenediaminetetraacetic acid
ETBR	Ethidium bromide
FCS	Fetal calf serum
Fig.	Figure

g	Gram / g-force
GCL	Ganglion cell layer
GFP	Green fluorescent protein
GTP	Guanosine triphosphate
HIAA	5-hydroxyindolacetic acid
HPA	Hyperphenylalaninemia
Hpf	Hours post fertilization
HPLC	High performance liquid chromatography
HRP	Horseradish peroxidase
HVA	Homovanillic acid
INL	Inner nuclear layer
IP	Immunoprecipitation
IPL	Inner peripheral layer
(W)ISH	(Whole mount) *In situ* hybridization
kb	Kilobases
l	Liter
L-Dopa	Levodopa
LMSO	L-methionine S-sulphoximine
m	Meter
M	Molar
m	Milli
MBT	Mid-blastula transition
MHB	Mid-hindbrain boundary
min	Minutes
MO	Morpholino
MOPS	3-(N-Morpholino)propansulfonic acid
mRNA	Messenger RNA
n	Nano
NADH	Nicotinamide adenine dinucleotide
NBT	Nitro blue tetrazolium chloride
NCC	Neural crest cells
NO	Nitric oxide
ONL	Outer nuclear layer

ONL	Outer nuclear layer
OPC	Oligodendrocyte precursor cell
p	p-value
PAGE	Polyacrylamide gel electrophoresis
PBS	Phosphate buffered saline
PBST	Phosphate buffered Saline with Tween
PBTr	Phosphate buffered Saline with Triton
PCR	Polymerase chain reaction
PFA	Paraformaldehyde
pH3	Phoshpo-histone 3
PKU	Phenylketonuria
PNK	Polynucleotide kinase
PTR	Proliferative tectum region
PVDF	Polyvinylidenfluorid
q-BH_2	Quinoid dihydrobiopterin
qRT-PCR	Quantitative real time - polymerase chain reaction
RBP	RNA binding protein
RNA	Ribonucleic acid
rpm	Rounds per minute
RT-PCR	Reverse transcription polymerase chain reaction
S	Siemens (Conductance)
SDS	Sodium dodecyl sulfate
Som	Somites
siRNA	Silencing RNA
TAE	Tris-acetate-EDTA buffer
TALEN	Transcription activator-like effector nuclease
TEMED	N,N,N,N-Tetramethylethylendiamine
tg	Transgene
Tris	Tris(hydroxymethyl)-aminomethane
V	Volt
wt	Wildtype

Nomenclature

Considering the comparisons between gene expression and protein function between human, mouse and zebrafish in this study, nomenclature is based on Trends in Genetics "Genetic Nomenclature Guide"; Hester et al., 2002; the committee of standardized genetic nomenclature of mice (1962) and the zebrafish nomenclature committee (zfin.org; accessed 9.1.2017; Howe et al., 2013).

e.g. QDPR

Species	Gene	Protein
Human	*QDPR*	DHPR
Mouse	*Qdpr*	QDPR
Zebrafish	*qdpra*	Qdpra

1. Introduction

1.1 BH_4 pathway

The proper homeostasis of neurotransmitters, cofactors and gene expression in a neuron are of the utmost important for proper functioning of the cell. Neurons, neuronal network, development and structure have been in the focus of science for many years, especially since the works of Santiago Ramon y Cajal (1852-1934), who has set the basis for identifying the morphology of the nervous system (Cajal 1899). The knowledge about this field has rapidly accumulated to the understanding and function of neurons. Two major neuronal subtypes, that have been focus of these studies, are dopaminergic and serotonergic neurons. While serotonin is majorly expressed in the periphery of the gut and acts as a hormone (Walther et al., 2003), it is also a strong neurotransmitter that is present in a variety of neurological networks of the brain and spinal cord (Alanina et al., 2006). Depletion of serotonin is associated with epilepsy and seizures (Tripathi and Bozzi, 2015). Dopaminergic neurons however are majorly found in the midbrain, more specifically in the substantia nigra, which was named due to the present neuromelanin in these cells (Zucca et al., 2014). Dopaminergic neurons are required for many functions such as addiction, mood and stress (Chinta and Andersen., 2004). On one hand, loss of these neurons is associated with the extensively studied Parkinson's disease (German et al., 1989), first described 200 years ago (Parkinson, 1817). On the other hand, overproduction of dopamine is associated with schizophrenia (Seeman and Kapur, 2000). It is therefore essential to tightly control neurotransmitter synthesis.

The cofactor tetrahydrobiopterin (BH_4) is a heterocyclic compound (Fig. 1) which is necessary for the enzymatic reactions that are required to produce the neurotransmitter precursors of dopamine and serotonin, as well as for nitric oxide synthase (NOS) activity. As presented in Fig. 2, BH_4 is involved in numerous pathways. The BH_4 pathway consists of a 3-step *de novo* pathway and a 2-step recycling pathway. During *de novo* synthesis, BH_4 is produced from GTP via the enzyme GTP-cyclohydrolase 1 (GTPCH), 6-pyruvoyl-tetrahydropterin synthase (PTPS) and sepiapterin reductase (SPR) resulting in 7,8 Dihydroneopterin phosphate, 6-pyruvoyltetrahydropterin and BH_4, respectively. BH_4 is then used up in the hydrolysis reactions of tyrosine hydroxylase (TH), tryptophan hydroxylase (TPH) and phenylalanine hydroxylase (PAH) producing Levodopa (L-Dopa), 5-hydroxytryptophan (5-HT) and tyrosine, respectively. For NOS activity it is required in the direct generation of citrulline and NO from arginine (Fig 2.)

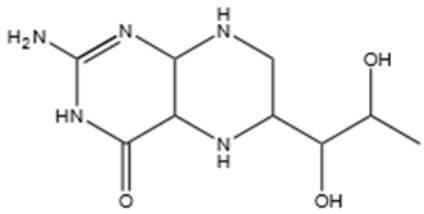

Figure 1. Chemical structure of BH_4

Chemical Structure of BH_4 made with ChemDraw©

The level of phenylalanine can also regulate a feedback mechanism via GTP cyclohydrolase feedback regulator (GFRP), which regulates the activity of GTPCH via direct binding (Werner et al. 2011; Ponzone et al. 2004). Increased Phenylalanine supports synthesis of BH_4, while reduced phenylalanine slows down synthesis (Maita et al., 2002). After the hydrolysis BH_2 is then turned to q-BH_2 by pterin-4-alpha-carbinolamine dehydratase (PCD) and finally recycled back to BH_4 via dihydropteridine reductase (DHPR) (Gross et al. 1992, Thöny et al., 2000). BH_4 can then be used again as cofactor. It is to note that from the closely related folate pathway, the dihydrofolate reductase (DHFR) can perform the same enzymatic reaction in the salvage pathway with q-BH_2 and the tetrahydrofolate reductase from BH_2 (Ponzone et al., 1993; Matthews et al., 1980; Scriver et al., 2001, Pollock et al., 1978).

As shown in Fig. 2, the pathway is directly required for the production of tyrosine from phenylalanine. Furthermore, it is directly involved in the generation of L-Dopa and 5-HT, the precursors of dopamine and serotonin, respectively. Therefore, neurotransmission is indirectly dependent on BH_4. Additionally, NOS generate nitric oxide for various important functions including neurotransmission, antimicrobial agent and reproduction (Roselli et al., 1998; Gross et al., 1992). BH_4 misregulation has even been linked to autism (Schnetz-Boutad et al., 2009) and cardiovascular disease (Bendall et al., 2014). During *de novo* synthesis a sidetrack via Spr can produce pteridines that serve as yellow pigments, i.e. xantophores, in zebrafish (Odenthal et al., 1996, Ziegler et al., 2000). Since BH_4 is required in such a variety of mechanisms, deficiencies have been associated with the regulation of neurotransmitter levels, pigmentation, immune response, liver function and cell metabolism.

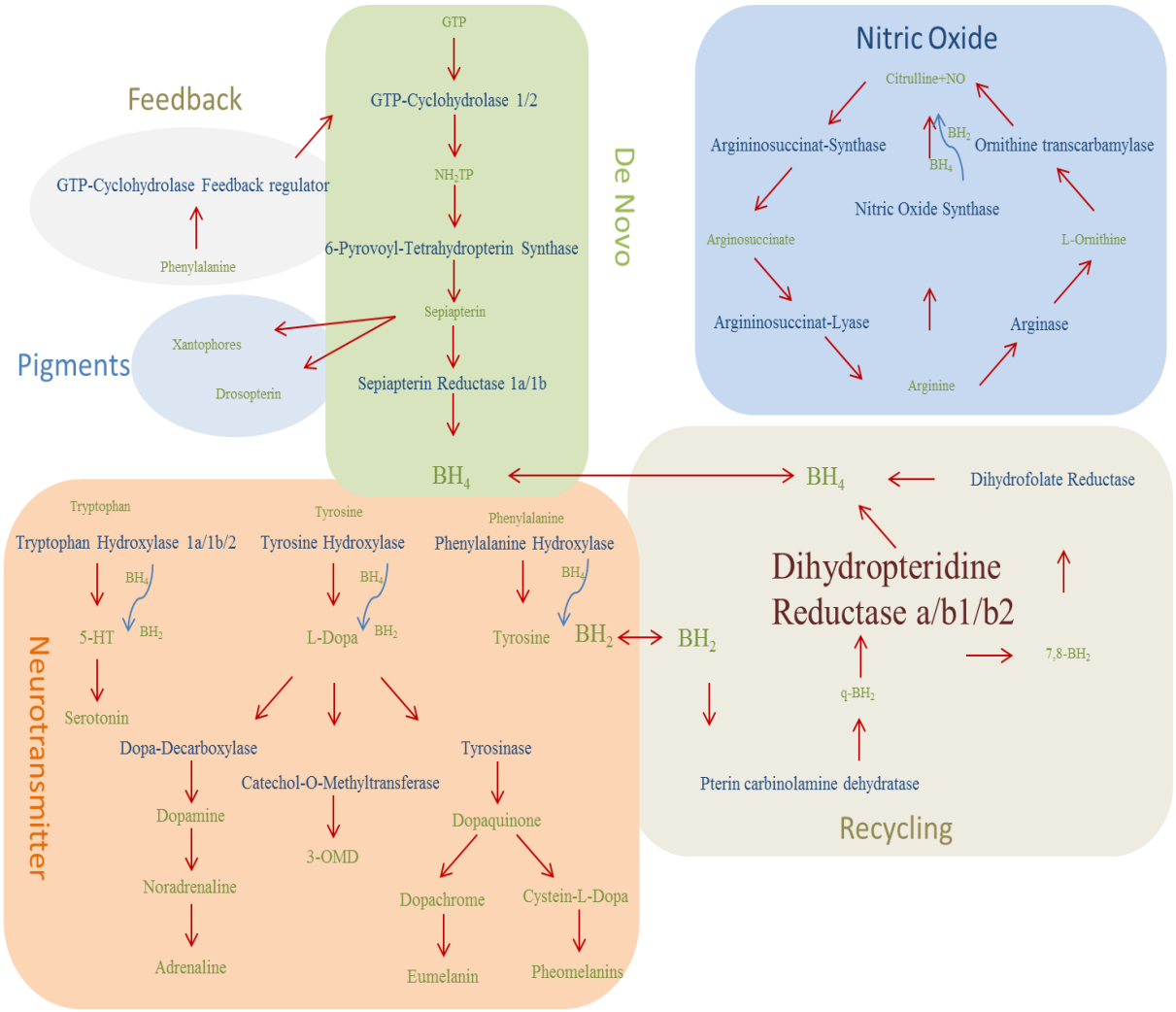

Figure 2. BH_4 synthesis and related pathways

Overview of the BH_4 *de novo*, recycling and Nos pathway. De novo synthesis shown in green, neurotransmitter related pathway in orange, recycling pathway in pale brown, NOS pathway in blue. Related pathways for pigmentation in zebrafish shown in pale blue and feedback mechanism in grey. Enzymes are shown in blue while compounds are shown in green. All reactions that require BH_4 as a cofactor are shown by a blue arrow, all related steps by red arrows.

1.2 Most prevalent BH_4 deficiencies

The first described defect related to the BH_4 pathway and the most common inborn error of metabolism is phenylketonuria (PKU) (Camp et al., 2014). Even though not directly a deficiency of the cofactor BH_4, it pathed the way for the diagnosis of BH_4 related deficiencies. PKU classically presents as a PAH deficiency resulting in a severe increase in phenylalanine (hyperphenylalaninemia (HPA)) (Blau., 2015). It is often diagnosed during diagnostic newborn screening (Blau et al. 2014). It has a prevalence of 1:10'000 to 1:15'000 in Caucasians and East Asians (Williams et al., 2008). In Turkey and Northern Ireland however, the prevalence is 1:4000 births (Ozalp et al., 2001). PKU needs to be treated with reduced phenylalanine uptake to prevent toxic levels to accumulate, which has been linked to the neuropsychological defects in patients (Fölling, 1934). This low-phenylalanine diet treatment was pioneered by Horst Bickel in the 1950's (Bickel et al., 1953) and today has led to a wide variety of low-phenylalanine products (van Calcar and Ney, 2012; Ney et al., 2014).

The diagnosis of HPA also led to the discovery of PAH related disorders involving BH_4 (Blau et al., 2014). BH_4 deficiencies present a rare inborn error of neurotransmitter metabolism. Of all HPAs diagnosed only 2% are caused by BH_4 deficiencies (Blau 2006; Thöny and Blau 2006). Worldwide, the highest diagnosis and incident rate is observed in Turkey (Fig. 3). The most common case is a deficiency in the enzyme PTPS (Fig. 3.; Opladen et al, 2012). As this is a defect in the *de novo* synthesis pathway it causes a loss in BH_4 and in turn an increase in neopterin, the compound produced by GTPCH (Fig 2.). In parallel, the lack of BH_4 causes a lack of TH, TPH and PAH function. Therewith results a drop of dopamine and serotonin precursors, and a sharp increase in phenylalanine. Additionally, the downstream compounds such as homovanillic acid (HVA) and 5-hydroxyindolacetic acid (HIAA) are depleted in the cerebrospinal fluid (CSF) (Blau, 2006). Similar to PKU, this symptom can be treated by reduced phenylalanine uptake and BH_4 given as treatment (Blau et al., 2001). BH_4 responsiveness is analyzed by a loading test, in which BH_4 is supplemented and the phenylalanine levels are screened. A drop in phenylalanine indicates BH_4 responsiveness (Bernegger and Blau, 2002). Furthermore, the supplementation of neurotransmitter precursors was shown to improve neurological symptoms (Longo., 2009; Porta et al., 2009; Burlina and Blau, 2014). Gene therapy has been recently advancing as treatment option for inborn errors of metabolism. Most recently iPSCs from patients of PTPS and DHPR were rescued using CRISPR/Cas9 and showed improvement of phenotype and corrected BH_4 and TH protein levels in the then differentiated cells (Ishikawa et al., 2016).

1.2.1 Least prevalent BH_4 Deficiencies

Mutations in the genes of GTPCH, termed *GCH1*, and SPR deficiencies also cause a *de novo* synthesis defect. GTPCH and SPR deficiencies however do not cause HPA, can be difficult to diagnose (Thöny and Blau, 2001) and make up less than 10% of worldwide diagnoses BH_4 deficiency cases (Fig. 3). In newborn screening, SPR deficiency diagnosis can be done by an increase in total biopterin and depletion of HIAA and HVA in the CSF (Blau, 2006). SPR deficiency results in a dopa-responsive movement disorder and can present with growth hormone deficiency and hypothyroidism, which improve upon treatment (Zielonka et al., 2015). GTPCH deficiency has previously been diagnosed as Segawa disease (Segawa et al., 1976; Ichinose et al., 1994). Similar to SPR deficiency, mutations in *GCH1* also present without HPA and are dopa-responsive (Thöny and Blau, 2006). Additionally, a depletion in neopterin, biopterin, HIAA and HVA can be detected in the CSF. GTPCH deficiency has been previously been linked to disorders such as Parkinson's (Menacci et al., 2014).

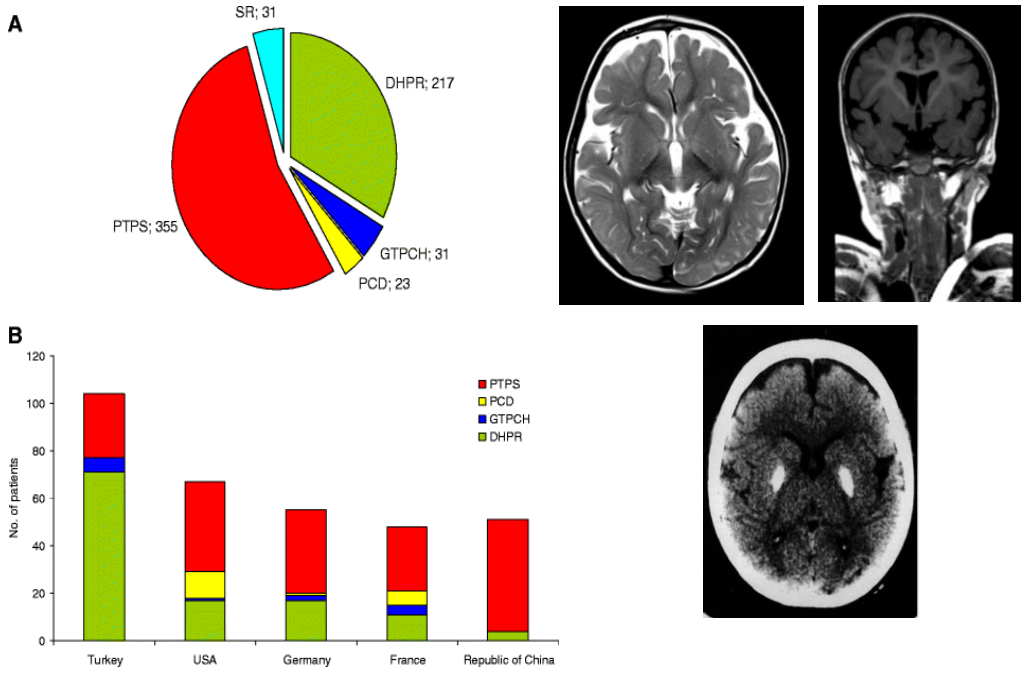

Figure 3. BH_4 deficiencies

Adapted from Opladen et al., 2012. A. Statistical analysis of BH_4 deficiencies as piechart and total case numbers worldwide. B. Statistical representation of BH_4 deficiencies linked to country of origin, Right: MRI top left and right (left liquor: white; right liquor: black) shows brain atrophy of 3 year old female DHPR patient. Bottom shows textbook example of a CT scan of calcification of basal ganglia

PCBD mutations set a special class of mutations due to its function. PCBD deficiency causes primapterinuria and a similar pattern of pterins as PTPS, with an increased level of 7-biopterin (Thöny et al., 1998a, Thöny et al., 1998b, Blau, 2006). PCBD also has been shown to have other functions, i.e. a moonlighting function that involves the dimerization of the hepatic nuclear factor 1 (HNF-1) and therefore termed dimerization cofactor of HNF-1 (DCoH) (Ficner et al 1995, Lei et al., 1999). In multiple studies it has been shown to act as a transcriptional activator (Johnen et al., 1997). Furthermore, a role on pigment cell development has been suggested in xenopus (Pogge v. Strandmann et al., 2000). It has later been found to be expressed in human melanocytes and affect tyrosinase transcription (Schallreuter et al., 2003). The same research group suggested before that the accumulation of 7-BH_4 due to lack of PCBD activity causes an inhibition of PAH activity and therefore can cause vitiligo (Schallreuter et al., 1994). Recently, computational reconstruction of the structure of PAH, also suggests BH_4 as pharmacological chaperones for the resting-state PAH, this would make recycling and BH_4/BH_2 homeostasis even more relevant (Jaffe., 2017).

1.3 QDPR/DHPR deficiency

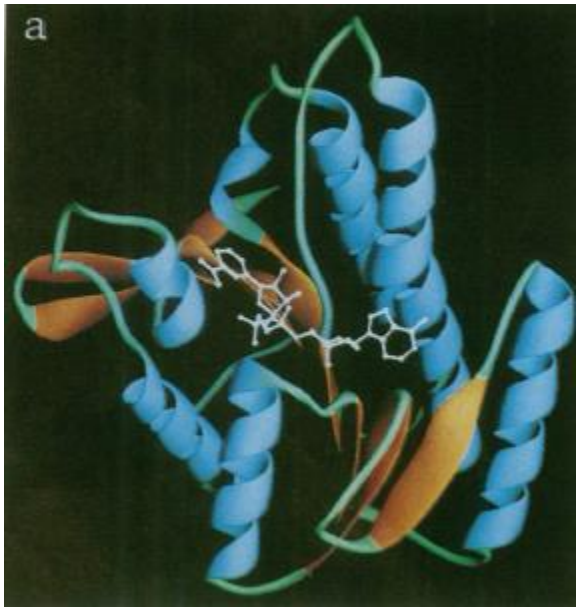

Figure 4. DHPR protein structure

Taken from Varughese et al., 1992. Three-dimensional protein structure of Qdpr from rat liver with NADH binding site. Alpha helices are shown in blue and beta sheets in yellow.

DHPR is a 26kDA large enzyme that acts in form of a homodimer to turn BH_2 into BH_4, by the use of NADH. The gene is located on 4p15.3 and contains 7 exons (Dianzani et al., 1998). The protein structure was resolved first in rat liver (Fig. 4) and confirms the binding site for NADH, as well as four-helix bundle motif for dimerization (Varughese et al., 1992). Its role has been linked to keeping BH_4/BH_2 homeostasis for BH_4 dependent reactions in the CNS and liver. DHPR mediates the reaction as cofactor by resupplying the two lost hydrogen atoms via NADH (Fig. 5). It contains a conserved short chain dehydrogenase sequence, a NAD binding site at position 14-38 and a conserved tyrosine (Y150) in the proton acceptor active site.

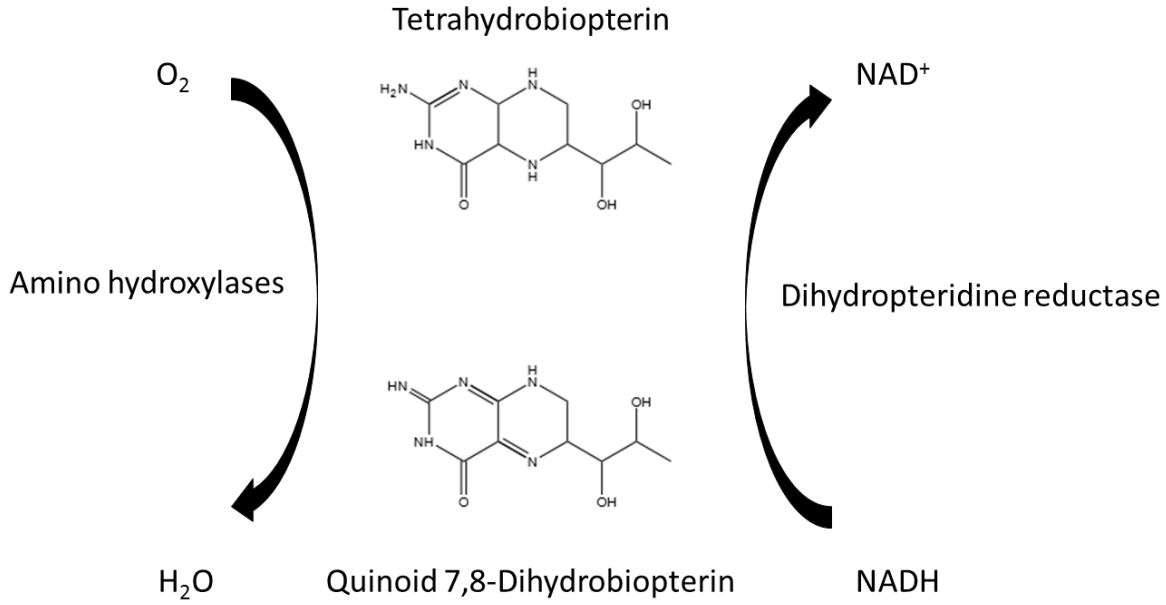

Figure 5. Chemical reaction of BH_4

Chemical structure and reaction of BH_4 to q-7,8 BH_2, which is performed by the amino hydroxylases and is reversed by DHPR with the use of NADH. The hydrogen from two nitrogens are removed by the hydrolysis and replaced by DHPR in recycling. Structure drawn with ChemDraw©.

As shown before the BH_4 deficiencies are divided into two major groups: synthesis and recycling. The major representative of the recycling defects is the DHPR deficiency and second largest cohort overall (Fig. 2; Opladen et al., 2012; Blau, 2006). Most cases have been identified in Turkey and very few in China (Fig. 2). The numbers of identified mutations have steadily increased in time with rapid improvement and standardization of newborn screening. While 34 different mutations had been detected in 2006 (Thöny and Blau, 2006 (a,b)), a total of 82 mutations have been identified for DHPR deficiency today (<<BioPKU Database>> accessed 23.8.2017)

The patients present with decreased neurotransmitters, depleted HIAA, HVA and a strong increase in BH_2 levels (Longo., 2008, Blau, 2006). BH_4 itself may be normal or close to, as synthesis is unaffected, yet folate levels are significantly reduced (Ponzone et al., 2004). Patients also show calcification of the basal ganglia and dystonia (Fig. 2.; Longhi et al., 1985; Woody et al., 1989). Hair may appear light coloured and some show muscular hypotonia. Many patients also have a microcephaly, while few, mostly untreated patients, show general brain atrophy (Fig. 2; Longo., 2008, Opladen et al., 2012). Deficiency can only be confirmed via an enzymatic assay, as the patient may present with normal pterin levels (Blau, 2006). Mutations can cause severe and mild phenotypes. In fact, DHPR deficiency presents with such great variety that some patients do not show any morphological phenotype and have exclusively an influence on the serotonergic pathway (Blau et al., 1992), while others are not responsive to any treatment and have severe brain atrophy, epilepsy and dystonia (Thöny and Blau, 2006). Yet others have a very mild phenotype with some remaining enzymatic activity (Blau, 2006).

Often complete loss of enzymatic function leads to severe phenotype, while remaining activity correlates with a mild phenotype (Dianzanie et al., 1998). Treatment involves neurotransmitter precursors L-Dopa and 5-HT, as well as dopadecarboxylase blocker and folinic acid supplementation (Thöny et al., 2006). Although some patients receive BH_4 with some improvement (Coughlin et al., 2013) patients are in general BH_4 unresponsive and treatment does not improve neurotransmitter levels or symptoms (Coughlin et al., 2013, Jäggi et al., 2007). Therefore, phenylalanine levels are commonly regulated by a controlled diet (Jäggi et al., 2007). This genotype-phenotype correlation has been partially described for several mutations (de Sanctis et al., 2000). However, the pathophysiology of this deficiency is not fully explained as the phenotype is more severe than a complete lack of BH_4 as in PTPS deficiency and devises a worse outcome than PTPS deficiencies (Jäggi et al., 2007). It is proposed that BH_2 may be causative as neurotoxic agent by interfering with NOS and hydroxylase activity, although the direct link has never been shown (Longo., 2008; Opladen et al. 2012).

To unravel the pathophysiology, studies have attempted to find a matching animal model. The homolog QDPR in mouse has been previously studied to determine the pathophysiology (Xu et al. 2014). The *Qdpr* knockout mouse shows all biochemical features of the DHPR deficient patients including a sharp increase in BH_2 and increase in phenylalanine. However, the mouse has no morphological or neurological phenotype. The hypothesis proposes that due to the conserved function of DHFR, which commonly regulates folate homeostasis, the BH_4 pool is maintained in the brain. However, this compensation may be inefficient in humans, due to low

DHFR activity and consequently cannot compensate the loss of DHPR (Whitsett et al., 2013). Therefore, the lack of a phenotype in mice was accredited to the function of DHFR to link the folate and pterin pathways and take over the QDPR function (Xu et al., 2014). Although the mouse shows the biochemical features of DHPR deficiency and could convincingly connect DHFR and QDPR function, it does not serve as a model for elucidating the pathophysiology of the disorder.

1.4 Zebrafish as model organism

Figure 6. Adult zebrafish

Image taken from Zebrafish atlas (zfatlas.pdu.edu)

Thanks to the works of George Streisinger (1927-1984), who was among the first to work with zebrafish in a laboratory and has revolutionized the analysis of mutants and cloning of vertebrates (Streisinger et al., 1981, Kimmel et al., 1985), the zebrafish has evolved as an indispensable vertebrate model system. Zebrafish have been used in developmental biology as a very useful tool to observe embryonic development. The development occurs *ex utero* and as the embryo is translucent, the early developmental and morphological changes can be observed with use of a microscope. Large clutches of up to 300 embryos and the rapid development of 1-cell stage to early larvae at 5 days post fertilization (dpf) allow for excellent comparative studies. Developmental stages have been clearly described (Kimmel et al., 1995) and most processes of gastrulation to somitogenesis and neurogenesis are well studied. The organism has become an excellent tool in pharmacological drug discovery, in describing affectivity and toxicity of small molecules and chemicals (Lieschke et al.2007). By simple exposure to these compounds one can screen for developmental changes or genetic and biological responses.

For the last decades the zebrafish model organism has proven very useful in the fields of developmental biology and embryology. Especially metabolic disorders profit from the easy manipulation and readouts (Seth et al., 2013). The use of simple manipulation methods such as

morpholinos that can be injected into the 1-cell stage makes for straight-forward modeling of genetic deficiencies. Morpholinos are short oligonucleotides with an uncharged backbone. As morpholinos specifically target the mRNA at either the start codon or a splice site, it results in a lack of translation or a lack of properly spliced mRNA, respectively, therewith resulting in a drop of protein levels (Eisen et al., 2008). Specificity of these effects is tested by rescuing the developmental phenotypes with injection of mRNA of e.g. humans or mice, which will additionally confirm functional conservation between species. As off-targets have been a concern for morpholinos, one must consider a set of controls and tests to exclude such risks (Eisen et al., 2008).

Advances of genome editing via TALENs (Kawahara et al., 2016) and more recently the CRISPR/Cas9 method (Doudna et al., 2014) has enabled us to specifically knock-out or knock-in genes of interest and look at the developmental effects. Zebrafish have also the great advantage of transgenic lines. These lines express a fluorescent protein under a specific promotor, which allow for a visual readout of specific cell types or change in gene expression. Most commonly the new fish lines are generated via the GATEWAY system that makes use of the proficient Tol2 mechanism (Kwan et al., 2007). The plasmid containing the Tol2 sites, promotor, fluorescent protein and sometimes a second readout fluorescent protein, is co-injected with a transposase which randomly integrates the plasmid into the genome. This method can create a large variety of useful readouts for experiments that have become of great use for the study of neurodegenerative disorders (Don et al., 2016).

D.rerio is of great advantage to characterize genetic functions and related disorders. In fact, most recently our working group used data from zebrafish, yeast and calf to identify a novel mutation in the human isoleucyl-tRNA synthetase (IARS), which causes growth retardation, intellectual developmental disorder, hypotonia and hepatopathy (Kopaijtich et al., 2016).

1.5 BH_4 pathway in zebrafish (Pigmentation)

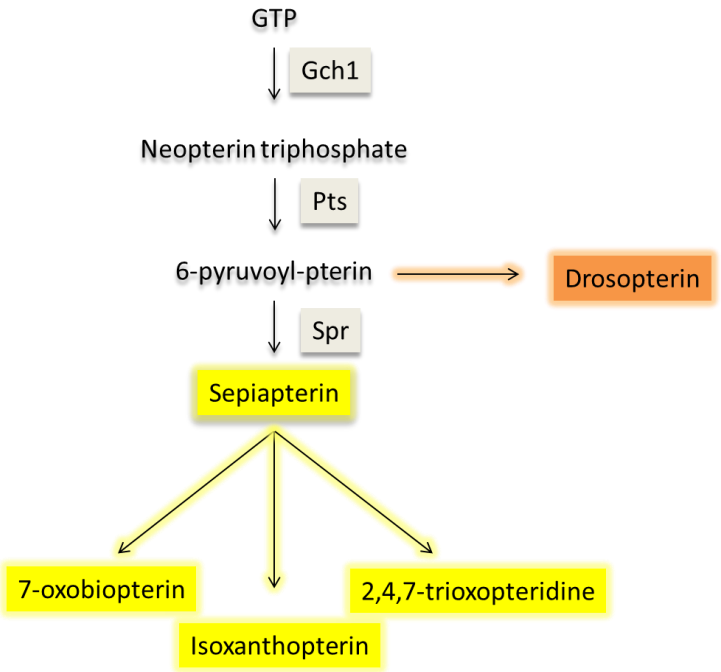

Figure 7. Overview of pterin dependent pigment synthesis of xantophores

Overview of xantophore pigment synthesis dependent on de novo synthesis of BH_4 (adapted from Braasch et al., 2007). Red pigment drosopterin shown in orange and yellow pigments shown in yellow. Required genes in grey and compounds in black.

The BH_4 pathway has been extensively studied in zebrafish in association with the pterin pathway and the production of all pigments in the embryo (Fig. 7). Pterins are connected to pigments and named after the colourful wings of butterflies (pteron = wing) (Schöpf 1964). Pterins account for the yellow and red pigments in zebrafish and are dependent on sepiapterin (Odenthal et al. 1996, Ziegler et al. 2000) and are therefore dependent on the *de novo* pathway of BH_4. This was also shown for the red pigments in the eye of drosophila (Kim et al. 2013). Melanin on the other hand is produced from tyrosine via L-Dopa and is therewith indirectly dependent on BH_4 recycling. Melanophores, which arise from the neural crest (Braasch et al, 2007), require sufficient BH_4 levels, which were previously shown to express the second recycling enzyme Pcbd (Schallreuter et al., 2003). If one would only consider pigmentation, then one would expect only the production of melanin to be reduced by a deficiency in recycling enzymes, which is seen in the reduced pigmentation in DHPR patients (Blau et al., 2005).

1.6 Neurological advantage

A major topic of zebrafish research concentrates on neuronal development. Its unparalleled advantages for neural imaging and cell tracking in the living embryo under physiological conditions has been widely exploited (Pan et al., 2011; Gerlai., 2012; Beretta et al., 2017). Transgenic lines such as the brainbow zebrafish (Fig. 8) allow for single cell fate tracking, by integrating different fluorescence cassettes into each neuron, allowing the identification of single neurons from others (Pan et al., 2011). The mapping of neuronal pathways has become additionally interesting for understanding of behavioral genetics (Parker et al., 2013). The developing zebrafish contains highly conserved neuronal networks in its CNS, which develop rapidly. For instance, already at 72 hpf (hours post fertilization), dopaminergic neurons cluster in the diencephalon and noradrenergic neurons mature in the locus coeruleus of the metencephalon (Kastenhuber et al., 2010).

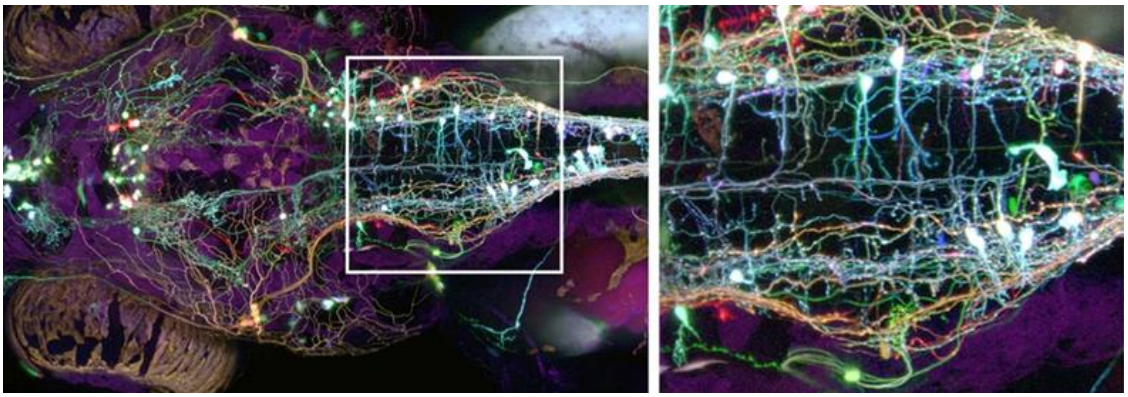

Figure 8. Brainbow zebrafish

Taken from Pan et al., 2011. Dorsal image and close up of fluorescing neurons in a brainbow zebrafish

The neuronal development of the embryo has been extensively studied and described. Along the anterior-posterior axis of the developing embryo, key organizing centers such as the midhindbrain boundary (MHB) pattern the brain and influence neuronal development. The underlying genetic network has been unraveled mainly by the study of mutants such as the *acerebellar/fgf8* (Reifers et al., 1998), *MHB gone* (Shima et al., 2009) and *no isthmus/pax2* (Brand et al. 1996). Cells at the MHB are often proliferative and a network of transcription factors and secreted molecules influence the early neurogenesis in this region, which commences as early as 10 hpf as judged by marker gene expression (Geling et al., 2003; Stigloher et al., 2008). Two other proliferative regions in which neurons are born are the proliferative tectum region (PTR) of the midbrain in close vicinity of the MHB and the ciliary

marginal zone (CMZ) in the eye (Fig. 9.). These regions have been extensively studied in teleost fish and other vertebrates (Avanesov and Malicki, 2010; Chow and Lang, 2001; Dyer an Cepko et al., 2001; Jean et al., 1998; Pujic and Malicki, 2004) and have been defined as conserved sister regions (Aldiri et al., 2013; Alunni et al., 2010; Cerveny et al., 2010; Imai et al., 2014; Malo et al., 2017; Recher et al., 2013). Here, for instance tightly controlled gene expression can distinguish between different areas such as a stem cell region, a cell cycle exit region and a differentiation zone (Cerveny et al., 2010; Wehman et al., 2005). Mutations in genes expressed in these regions can severely influence the proliferation and differentiation of neuronal and glia cells (Cerveny et al., 2015; Hu et al., 2015; Kubo et al., 2003; Reinhardt et al., 2015)

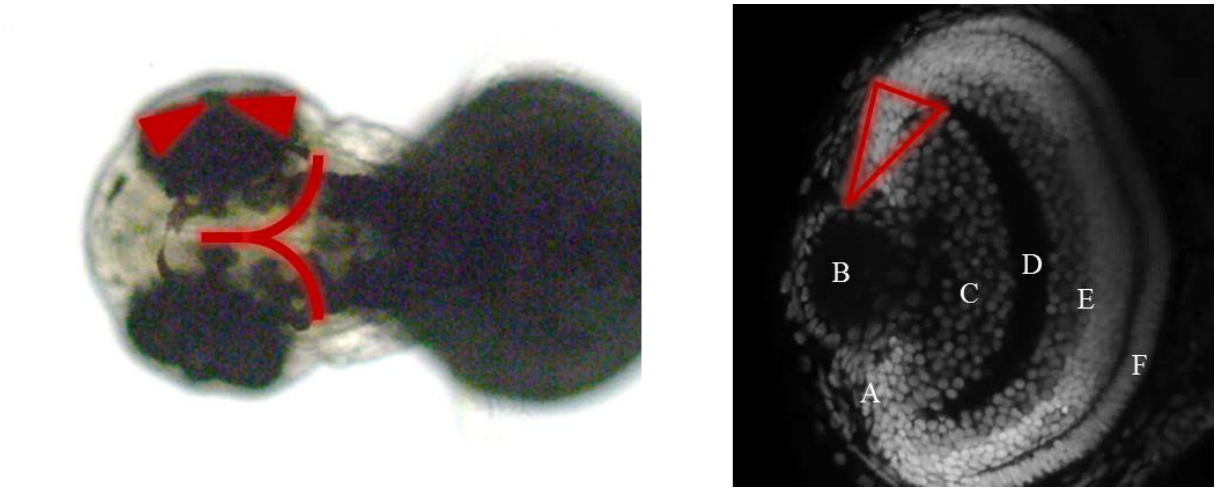

Figure 9. Proliferative regions of the zebrafish

Left: Presentation of zebrafish proliferative regions in 3dpf zebrafish (dorsal view). Proliferative regions marked in red in the midbrain and CMZ of the eye; Right: Presentation of the eye at 3dpf. Proliferative region from left (CMZ), marked in red. A: CMZ, B: Lens; C: Ganglion cell layer (GCL); D: Inner peripheral layer (IPL); E: inner nuclear layer (INL), F: Outer nuclear layer (ONL)

1.7 Glial cells of the zebrafish brain

Apart from neurons, the main cell lineage, composing the mass of the brain, are glial cells. Glial cells were originally named after the term “glue”, since they have been first considered supportive cells for neurons. They now have been determined as major regulators of neuronal networks and have become one of the major focuses for disease and neuronal development (Taber et al., 2012). In mammals, the majority of glial cells belong to the cell line of astrocytes, which are named after their shape “star-like”. They have a distinct order of gene expression patterns during their development and are shown to influence the extracellular matrix (ECM)

(Wiese et al., 2012). The second major type of glial cells are oligodendrocytes, which act as myelinating cells for neurons and are positive for the expression of Olig2 (Park et al., 2002). Oligodendrocytes also arise from the same precursors as motor neurons (Wiese et al., 2012; Lyons et al., 2015). The third cell line termed glia are microglial cells, although these arise from the hematopoietic lineage and not the neuronal lineage (Chan et al., 2007).

In teleost fish, the astrocyte-like cells are termed radial glia, because of their extended shape, rather than the star-like appearance (Kalman et al., 1998). They share many commonalities to the mammalian astrocytes (Grupp et al., 2010), which include conservation of typical astrocyte markers: glutamine synthetase (Glul), glial fibrillary acidic protein (Gfap) and Aquaporin (Aqp4) (Grupp et al., 2010). Furthermore, radial glia cells and the eye specific Müller glia cells have regenerative capacity and are capable to generate and replace lost cells after injury (Bernardos et al., 2007; Nagashina et al., 2013). Upon injury to the CNS, these glial cells therefore act as neuronal stem cells (Kroehne et al., 2011). For continuity in this study we will refer to these zebrafish astrocyte-like, *glula* positive cells, as astroglial cells.

Astroglial cells in zebrafish, as in mammals, are necessary for the functional ionic and metabolic homeostasis in the brain and within neuronal networks. One of the most studied mechanisms involves uptake of glutamate (Bacci et al., 1999; Bringmann et al, 2013). Astrocytes at the glutamatergic synapse are required for rapidly clearing the synapse of the neurotransmitter to prevent neuronal toxicity and glutamate accumulation. Glutamate is taken up via the transporters EEAT1/SLC1a3 and EAAT2/SLC1a2, from which the latter is necessary for 95% of the rapid uptake (Haugeto et al., 1996). The cell then metabolizes the glutamate to glutamine by GLUL and the glutamine then in turn gets transported back to the neurons. The neurons then complete the cycle by metabolizing glutamine back to glutamate for neurotransmission. Both glutamate transporters are conserved in the teleost midbrain (Gesemann et al., 2010) and have been linked to a conserved function (McKeown et al., 2012).

Alterations of astrocytes and their function have been linked to numerous disorders, including epilepsy and early death, due to neurotoxic extracellular glutamate in case of a loss in GLT-1 (Tanaka et al., 1997). More specifically a knockout of Glt-1 in $Gfap^{+}$ astrocytes was shown linked to high lethality in mice and a neuron specific knockout of Glt-1 to have none (Petr et al., 2015). High levels of glutamate are neurotoxic and therefore proper astrocyte uptake and transport is extremely important (Choi., 1988). Glutamate and ammonia overload the synapse and become neurotoxic. One of our recent studies models this effect in zebrafish and shows that

high levels of glutamate are the pathophysiological source and that inhibition of the ornithine amino transferase (OAT) is highly effective as protective remedy (Zielonka et al. 2018, unpublished). In the "Trojan horse theory" high levels of glutamine are taken up by the cell and turned into ammonia and glutamate in mitochondria. This in turn results in dysfunction and swelling of mitochondria (Rao et al., 2003; Zieminska et al., 2000; Albrecht and Norenberg, 2007).

In zebrafish many genes have been linked to gliogenesis, glia patterning and axon guidance (Barresi et al., 2010). Many of these genes are related to diseases. For example, mutations in GFAP are correlated to Alexander's disease, which affects astrocyte development and causes severe neurological symptoms (Brenner et al., 2010). Alexander's disease is also listed as differential diagnosis for DHPR deficiency (*Orphanet* <<accessed 20.9.2017>>; Ng et al., 2015).

1.8 RNA binding proteins

Beside the function of BH_4 recycling, large-scale screens for RNA binding proteins, detected DHPR as an RNA-binding enzyme (Castello et al., 2013). The protein function of binding RNAs has been described for numerous proteins and is required for the regulation of cell metabolism and regulation of RNA fate (Castello et al., 2012). Expression of these RNA-binding proteins (RBPs) may give insight into the state of the cell (Castello et al., 2016). Large scale screens have identified a large number of proteins capable of this function (Castello et al., 2013). An extensively analyzed protein, the human nuclear ribonucleoprotein particle C (hnRNPC), has been shown to form complexes, regulate splicing and change conformation when bound to heterogeneous nuclear RNAs (Swanson et al., 1987). Commonly RBPs make use of specific RNA binding domains (RBD), but even non-canonical RBDs have been described (Lee and Hong 2004). Many RBPs are conserved among species and are highly important for RNA regulation (Beckmann et al., 2015).

In addition to RNA binding proteins that have this function as their main role, other enzymes have been detected that can bind RNA. Since many proteins contain unknown mode of function for their RNA binding and its role (Castello et al., 2016), it offers the opportunity of studying the role of RNA binding as supportive role, regulatory or novel function for the enzyme and possible insight into the unknown pathophysiology.

1.9 Unraveling the pathophysiology

This thesis focuses on the unknown pathophysiology of DHPR deficiency modeled in zebrafish that presents with an atypical severity of BH_4 deficiencies including brain atrophy and microcephaly. It characterizes all three homologs Qdpra, Qdprb1 and Qdprb2. Our data defines the role of Qdpra in early pigment synthesis and Pah activity, while Qdprb1 activity influences the gliogenesis in the proliferative regions of midbrain and eye. We find that Qdprb1 functions in regulating glutamine production in this process. Intriguingly, our studies of human patients implicate the evolutionary conservation of this mechanism. This study is the first to explain, at least in part, the pathophysiology of DHPR deficiency via a novel function for Qdpr, linking it to neuronal differentiation in the proliferation zones of the eye and midbrain.

2. Materials and Methods

2a. Chemicals

Table 2. Chemicals

Company	Chemical
Carl Roth, Karlsruhe (Germany)	Acetic acid 100% Chloroform > 99%, Denatured ethanol > 99.8% + 1% MEK Ethanol > 99.8%, Ethylenediaminetetraacetic acid Dihydrate > 99%, Methanol > 99%, Milkpowder D+ sucrose >99.5, Tris-(hydroxymethyl)-amniomethan > 99.5% Triton Tween® 20,Ph.Eur. Sulfosalicyclic acid >99%
Roche, Basel (Switzerland)	10x Dig-RNA labeling Mix Complete, EDTA free protease inhibitor DNAse 1 NBT/BCIP solution RNAse inhibitor SP6 polymerase T7 polymerase
SIGMA, St. Louis, Missouri (United States)	10X Dulbecco's phosphate buffered saline 20X SSC Buffer concentrate Agarose for molecular biology Bacteriological agar Bovine serum albumin (BSA) >98% Citric acid monohydrate >99% ACS Diethyl pyrocarbonate (DEPC) >97%

Dimethylsulfoxide (DMSO) >99%

Eukitt

Ethidium bromide solution 10mg/ml

Formamide >99.5%

Heparin sodium salt from porcine

Hydrochloric acid solution (37%)

Isopropanol >99.7%

Lithium chloride >99.0%

Magnesium chloride hexahydrate >98%

Magnesium sulfate

Methyl cellulose

Methylene blue, dye >82%

Paraformaldehyde, reagent grade

1-phenyl-2-thiourea (PTU) >98%

Potassium chloride >99%

Proteinase K

RNAseAway®

Sodium chloride >99.5%

Sodium hydroxide

Tricholaracetic acid

TRI Reagent®

tRNA from wheat germ Type V

2b. Antibodies

Table 3. Antibodies

Company	Chemical
Jackson Immuno Research Laboratories Inc., West Grove, Pennsylvania (United States)	Cy™2 Affinipure donkey anti rabbit IgG (H+L) Cy™3 Affinipure goat anti mouse IgG (H+L)
Roche, Basel (Switzerland)	Anti-Dig-AP Fragments
Merck Millipore, Billerica, Massachusetts (United States)	Polyclonal anti- GFP (rabbit) Polyclonal anti-pH3 (rabbit)
Proteintech Group, Manchsester (United Kingdom)	Polyclonal anti- QDPR (rabbit)
Santa Cruz Biotechnologies, Heidelberg (Germany)	Monoclonal anti-QDPR (mouse)
SIGMA, St. Louis, Missouri (United States)	Monoclonal anti- acetylated-tubulin (rabbit) Monoclonal anti-FLAG® M2 (mouse)

2c. Kits

Table 4. Kits

Company	Kit or Component
QIAGEN, Hilden (Germany)	QIAprep® Spin Midiprep kit QIAprep® Spin Miniprep kit One-Step RT-PCR kit RNeasy® Mini Extraction kit
Bioline, London (United Kingdom)	MyTaq® 2x HS Red Mix SensiFast SYBR® Hi-Rox 2x
New England Biolabs, Frankfurt (Germany)	GeneRuler DNA 1kb Ladder GeneRuler DNA 100bp Ladder Quick-load® Purple DNA 2-log Ladder Quick-load® Purple DNA loading dye High-Fidelity® Restriction endonucleases: *Bam*H1, *Not*1, *Xba*I, *Xho*I, *Spe*1, *Eco*R1 Q5® High- fidelity polymerase
SIGMA, St. Louis, Missouri (United States)	GenElute™ Gel extraction kit
Bio-Rad Laboratories, Inc., Hercules, California (United States)	Protein Reagent A&B
Invitrogen, Carlsbad, California (United States)	mMessage mMachine® SP6
Thermo Fisher Scientific, Waltham, Massachusetts (United States)	Maxima first strand cDNA synthesis for RT-qPCR SuperSignal™ West Pico Chemiluminscent Substrate

2d. Equipment and materials

Table 5. Equipment and materials

Company	Equipment
Ansell, Richmond (Australia)	Gloves L (Touch'nTuff)
Beckman Coulter GmbH, Sinsheim (Germany)	Avanti J-26S XP Centrifuge
Binder GmbH, Tuttlingen (Germany)	"Series C" CO_2 Incubator
Biochrom GmbH, Berlin (Germany)	Biochrom 30 + (Cation exchange Chromaography)
Bio-Rad Laboratories, Inc., Hercules, California (United States)	4-15% Mini-Protean® TGX™ Precast Gel Agarose gel Chamber Sub-Cell GT C1000 Touch™ Thermal Cycler CFX Connect™ Real-Time System SDS Gel Chamber Criterion™ Cell Trans-Blot® Turbo™ Mini PVDF Transfer Western blotter Trans-Blot® Turbo™
Brand GMBH & Co KG, Wertheim (Germany)	Pasteurpipettes PE-LD 3ml
Carl Roth, Karlsruhe (Germany)	Petri dishes
Carl Zeiss, Jena (Germany)	Stemi 305 Microscope
Consort bvba, Turnhout (Belgium)	Power Source E835
Corning, Corning, New York (United States)	Serological Pipettes (5ml, 10ml, 25m)

Emerson Electric Co., St.Louis, Missouri (United States)	Branson Sonifier 450
Eppendorf, Hamburg (Germany)	Gelloader Tips (20µl) Femtojet 4i Pipettes (0.1-1,5µl, 0,5-10µl, 20-200µl, 100-1000µl)
Goebel, Au in der Hallertau (Germany)	S5200 HPLC Autosampler
Harvard Apaparatus, Holliston, Massachusetts (United States)	Capillaries G-100F-3
Heraeus GmbH, Hanau (Germany)	Biofuge pico Centrifuge
Knauer, Berlin (Germany)	HPLC pump smartline pump 1050
Leica Camera AG, Wetzlar (Germany)	CM1900 Cryotome Leica DMI 4000B Microscope
Mettler Toledo, Columbus, Ohio (United States)	Ph204L Fine Scale
Molecular Devices, LLC, Sunnyvale, California (United States)	Spectrophotometer SpectraMax Plus
MWG Biotech, Ebersberg (germany)	UV Transilluminator
Narishige GROUP, Tokyo (Japan)	Microinjector
Neolab Laborbedarf, Heidelberg (Germany)	Tweezers Dumont Dumoxel #5

Ohaus Europe GmbH, Greifensee (Switzerland)	Precision Advanced Scale
Sarstedt AG&Co, Nümbrecht (Germany)	Tissue culture 24-well plate 1,5ml/2ml Eppendorf Tubes Falcon tubes (15ml, 50ml) Filter pipette tips (10µl, 200µl, 1000µl) Pipette Tips (10µl, 200µl, 1000µl)
SIGMA, St. Louis, Missouri (United States)	Cover glasses 22mmx22mm
Techlab, Braunschweig (Germany)	Jetstream 2+ for HPLC
Thermo Fisher Scientific, Waltham, Massachusetts (United States)	Superfrost® Plus microscope slides HeraSafe™ HS 12 Laminar flow hood
Sutter Instruments, Novato, California (United States)	Needle Puller P97
Terumo, Tokyo (Japan)	Butterfly needle 27G

2.1 Zebrafish maintenance

Zebrafish were kept in a unit of the "Interfakultäre Biomedizinische Forschungseinrichtung" (IBF) of the University Heidelberg. Animals were kept at 28.5 °C with a 14/10 light/dark cycle, ~700µS osmolarity conductance and a pH of 6.8 - 7.5. All in accordance with Westerfield et al. (2000). Animals were kept in regulation with Regierungspräsidium Karlsruhe (Az. 35-9185.81/G-85/16). Animals were fed daily with dry food in form of flakes and live artemia. Husbandry for experiments using wildtype embryos was done by outcrossing of AB/AB wildtype line. Husbandry of transgenic lines used for experiments was done by incrossing heterozygous animals of the respective lines.

The lines used were:

- AB/AB wildtype
- Tg(HuC/D:GFP)
- Tg(NBT/lyn:GFP)
- Tg(mpeg:GFP)

The lines were supplied from the Wittbrodt Lab (University Heidelberg) (AB/AB), Carl Lab (CBTM Mannheim) (HuC/D:GFP), Gilmour Lab (EMBL Heidelberg) (NBT/lyn:GFP) and Peri Lab (EMBL Heidelberg) (mpeg:GFP).

2.2 MO knockdown

MOs are short oligonucleotides that are used to bind specific regions of RNA to inhibit the correct splicing or translation entirely. The uncharged Morpholino backbone of these oligonucleotides makes them specifically stable and can last in embryos for up to 3 days. MOs are designed and distributed by "GeneTools, LLC" and are used at a range of concentration that need to be titrated for each MO before using it.

Although MOs have been recently discussed to contain possible off target effects one has to use efficient controls to confirm the results. Every control to confirm the specificity was run, which included multiple morpholinos with different targets, multiple rescues with different species mRNA, p53 morpholino co-injections and RT-PCR or qRT-PCR analysis.

2.2.1 Targeting

Morpholinos are either designed as translation inhibiting (targeting the start codon) or splice blocking (targeting intron/exon boundary). I used both possible targets for *qdpra* and *qdprb1*.

Table 6. Qdpr MO sequences and working concentrations

Mismatches in morpholino controls (MOCO) are labelled as lowercase letters, while matches are labelled as capital letters

MO	Sequence	Target	Used concentration
Qdpra 1	ATGGCTTTTCTCCGCTGTGAGACGC	ATG	0,3 mM
Qdpra 2	CTTAGGTGTCCTAACCTTTCGAGCT	Splice site exon3/intron3	0,3 mM
Qdprb1 1	TAGCTGCCATTCTGTCTTCACGAGC	ATG	0,1 mM
Qdprb1 2	TATTAGGCGAGTACCAACTTTTGGC	Splice site exon4/intron4	0,3 mM
Qdprb2 1	CCAAAAGTAAGCATGATTCTGACAC	ATG	0,3 mM
Qdpra 1 MOCO	ATaGCTTTTaTCCGaTGTaAGACaC	5bp mismatch	0,3 mM
Qdpra 2 MOCO	CTTAcGTcTCCTAAaCTTTCcAGaT	5bp mismatch	0,3 mM
Qdprb1 MOCO	TAaCTGaCATTCTaTCTTaACGAaC	5bp mismatch	0,1 mM
Qdprb1 2 MOCO	TATTAcGCcAGTAaCAAaTTTTGcC	5bp mismatch	0,3 mM
Qdprb2 MOCO	CaAAAAaTAAGaATGATTaTGAaAC	5bp mismatch	0,3 mM

2.2.2 Infections

Embryos were injected at the 1-cell stage. Morpholinos and mRNAs were injected always into the yolk, as close as possible to the cell. Injection volume was adjusted to 1/5th of the cell volume which accounts to roughly 2 nl (Yuan and Sun, 2009).

MOs were injected at a concentration gradient to determine the lowest concentration at which a stable morphological phenotype could be observed. The related control morpholinos were injected at the corresponding concentration. Embryos were placed in E3 Medium after injections and were incubated at 28.5 °C until the desired stage. Embryos that were to grow older than 24 hpf and analyzed via WISH, were placed in PTU containing E3 medium after gastrulation to inhibit pigment synthesis.

2.2.3 Phenotype determination

The phenotype was analyzed by the correct concentration that caused no toxicity but a stable phenotype. Embryos were directly compared to wildtype and control injected embryos. To determine no unspecific effects, we used a p53 MO at 0,2 mM co-injected, which inhibits apoptosis. This is to account for unspecific cell death due to MO toxicity and will show if the morphological change is apoptosis dependent (Robu et al., 2007). Further controls were performed by direct rescues with zebrafish or mouse mRNA.

2.2.4 Rescues

Rescues were generated in a similar fashion as described in 2.2 with minor adjustments. Rescues were designed from mRNA of *qdprb1*(NM_001020698.1) from zebrafish, QDPR 201(NM_024236.2) and 204 (ENSMUST00000120867.7) from mice. The sequences were amplified by PCR using Q5 polymerase and cloned into pCS2^{+} Vector. After sequence confirmation by sequencing the plasmids were linearized and *in vitro* transcription performed using the SP6 mMessageMachine transcription kit (Ambion) to produce 5'methylcapped mRNA.

This mRNA was injected along with the morpholino and alone. Concentration was varied to find a non-toxic but rescue effective range of mRNA. Only mRNA was injected as a control.

Table 7. Rescue mRNA concentration

mRNA	Concentration Qdpra MO	Concentration Qdprb1 MO
qdprb1 mRNA	/	80 pg/µl
Qdpr 201 mRNA	80 pg/µl	500pg/µl
Qdpr 204 mRNA	/	500pg/µl

2.2.5 RT-PCR

To determine, if splice morpholinos are acting specifically at the target side one can run an RT-PCR to determine, if an intron remains in the mRNA or an exon is removed. RNA is isolated as previously described (2.2.1) and then specific primers that flank the binding site of the MO are used for One-Step RT-PCR kit (Qiagen). Samples are then run on an agarose gel and visualized to observe a single band in control-injected embryos and a secondary band in MO injected embryos.

2.3 *In situ* probe preparation

Whole mount *in situ* hybridization (WISH) is a method that allows visualization of specific mRNAs in the whole mount embryo using sequence specific RNA probes. General procedure for preparing *in situ* probes is shown by Figure 10.

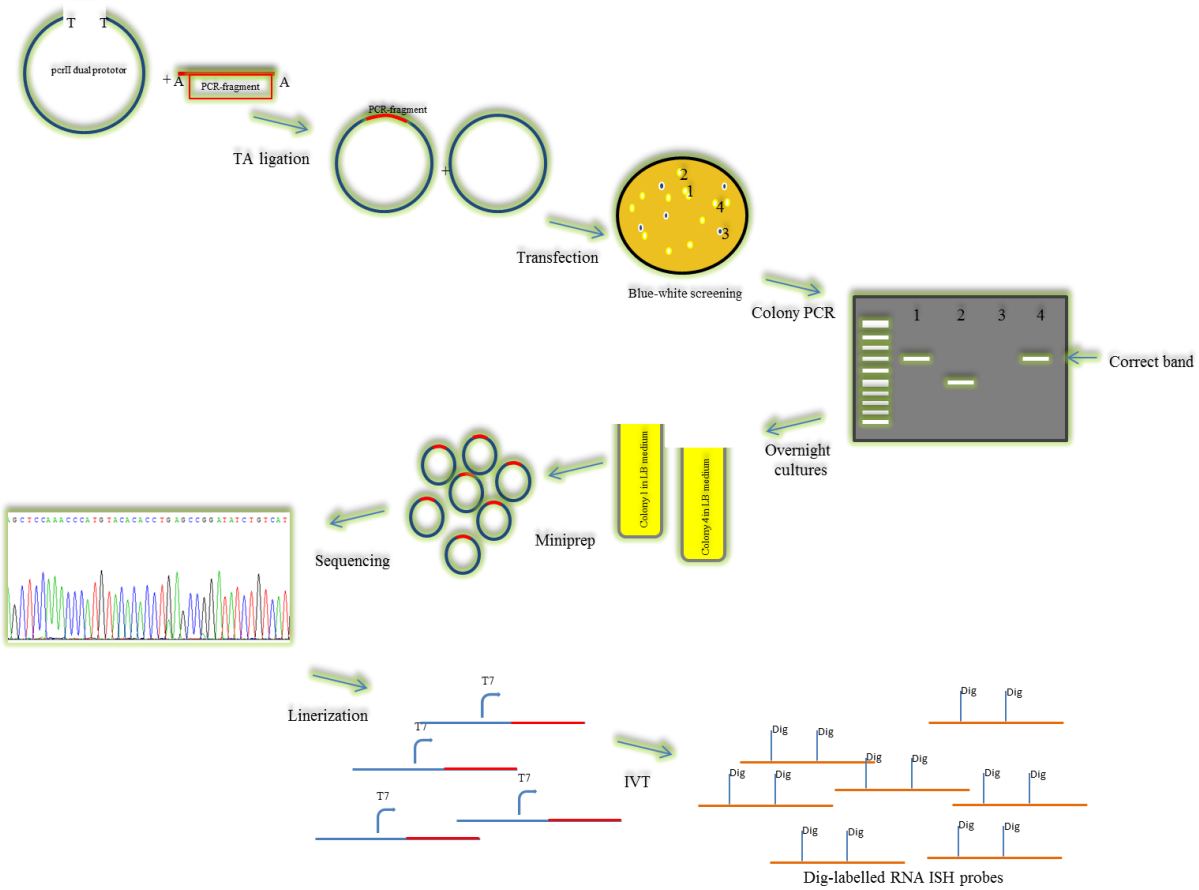

Figure 10. Overview of cloning strategy during *in situ* probe synthesis

Graphical step wise overview of *in situ* probe synthesis from PCR, to ligation and IVT

2.3.1 RNA isolation

RNA was isolated from embryos of the required stages. Embryos were washed in dH_2O to remove leftover medium and placed on ice. Embryos were then lysed in 1ml of TRIzol (Sigma) and protocol run in accordance to manufacturer's instructions.

2.3.2 Polymerase chain reaction

Polymerase chain reaction (PCR) was used to amplify the target sequences for both *in situ* probes, rescue mRNA and qPCR fragments. Specific primers (see tables in supplemental C), which were used to bind to the target and amplify it, were designed with PrimerBlast (Ye et al., 2012). For *in situ* probes and colony PCR's, the HS Red Mix (Qiagen) was used, for reduced errors, e.g. for rescue sequences, a Q5 polymerase (Thermo) was used. For complex sequences, the One-Step RT-PCR Kit (Qiagen) was used. A general protocol was as followed:

Table 8. PCR protocol

Step	Temperature	Time
1. Initial denaturation	95 °C	3 min
2. Denaturation	95 °C	30 sec
3. Annealing	50-72 °C	30 sec
4. Elongation	72 °C	1-3 min (1 min / kb)
		x34 cycles Step 2-4
5. Final elongation	72 °C	10 min
6. Storage	4 °C	∞

2.3.3 Agarose gel electrophoresis

Agarose gel electrophoresis takes advantage of the negative charge of DNA or RNA to separate different size fragments of PCR amplified sequences in a 1-2% gel. Agarose is dissolved in 1X TAE and 0,5 µg/ml ETBR final concentration added for DNA or RNA visualization under UV light. The liquid agarose is poured into a model form with wells and left to polymerize. The gel can then be used for DNA separation and run in 1X TAE.

2.3.4 Gel purification

PCR was analyzed on 1% agarose gels run at 120V for 45 min in 1X TAE Buffer. Bands were then visualized under UV light and respective bands cut out of the gel. Gel pieces were then purified using GenElute Kit (Thermo Scientific) according to manufactures' instructions.

2.3.5 Ligation

For ligation of rescue sequences, equimolar amounts of linearized plasmid and fragment were used in each ligation reaction. T4 Ligase (ThermoFisher) reaction was according to manufacturer's instructions. Both plasmid and fragment were digested with the respective restriction enzyme at 37 °C for 10 min, previous to ligation.

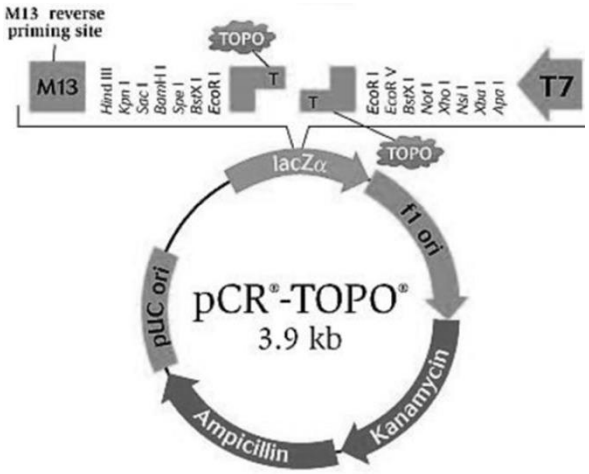

Figure 11. Plasmid map of pCRII TOPO dual promotor

Map taken from ThermoFisher pcrII dual promotor manual

For DNA fragments created for ISH probes, TA cloning into dual promotor pcrII vector, which allows for expression from T7 and SP6 promotor, (Fig.11) was done. A 6 µl ligation setup with 4 µl PCR fragment, 1µl salt solution and 1 µl TA plasmid stock was done.

2.3.6 Transfections

For transfections, 5µl of the respective ligation setup or plasmid was added to 25µl DH5-α *E.coli* (NEB) and placed on ice for 30 min, a 30 sec heat shock was done by 42 °C, with following cooling on ice for 2 min. 250 µl SOC Medium was added to the bacteria and allowed to recover at 37 °C at 300rpm for 1 hour. 100 µl of the culture was streaked onto LB agar plates with antibiotic and grown overnight at 37 °C.

2.3.7 Bacterial selection

LB Agar plates were poured by adding 15g/l bacterial agar to 1X LB medium and autoclaving the solution. After cooling to 55 °C the selected antibiotic, either Ampicillin (100 µg/ml) or Kanamycin (50 µg/ml) was added, and 25 ml each poured into petri dishes. After cooling, the plates were coated with X-Gal and IPTG for blue white screening. Since the pcrII vector contains the lacZ operon one can screen for colonies that contain plasmids with DNA insert and ones without. If the lac operon is intact, the operon will be activated by IPTG and the X-gal sugar broken down to a blue compound. If the operon is disturbed by the DNA insert, it cannot break down the sugar. Therefore, colonies with plasmid and DNA insert remain white and without insert turn blue (Juers et al., 2012).

2.3.8 Colony PCR

Colony PCR was performed by the previously mentioned protocol (2.3.2) by using HS Red Mix. Instead of a template, half of a picked colony was added to the reaction. Initial denaturation was increased to 5 min to fully lyse the cells. Primers were matching the insert only. Samples were run on a 1% gel and positive colonies identified by showing the insert band.

2.3.9 Miniprep

For plasmid isolations, miniprep cultures of 3 ml were grown overnight in LB medium with antibiotic, of the respective positive identified colonies. The Gold MiniPrep kit (PeqLab) was used to manufacturer's instructions to isolate the plasmid DNA.

2.3.10 Plasmid quality control

To determine plasmid quality and concentration, we used a Nanodrop. Concentration was determined by absorbance at 260 nm with the equation of the Beer-Lambert Law:

$$[DNA] = Absorbance_{260} \times 50ug.$$

Quality was determined by 260 nm: 280 nm ratios and 260 nm: 230 nm ratios. A pure DNA sample has a 260:280 ratio of 1.8 and a change can indicate protein contamination. In case of 260:230 a ratio of 2.0 is expected and a change may be caused by phenol contamination.

2.3.11 Sequencing

Isolated plasmids were sent for sequencing to SeqLab (Göttingen). Sequences showed both the sequence and orientation, which is required for determining sense and antisense of the *in situ* probes or producing the correct rescue mRNA.

2.4 Sequence analysis

The sequences obtained for the generated plasmids were analyzed via "Blastn" (Altschul et al., 1990) and "Expasy translate tool" (Gasteiger et al., 2003). The sequence was compared to the database of NCBI in Blastn, to determine the sequence homology. Deleted bases were shown as Gaps, while incorrect bases are shown as mismatch. Furthermore, the location of the sequence is shown graphically. For *in situ* probes only sequences with 99% identity (maximum of 5 mismatches) and 0 Gaps were used. In case of rescue sequences of *qdprb1* mRNA, the sequence was additionally tested in ExPASy, to determine if the sequence generates the correct amino acid sequence and no frameshifts or deletions.

2.5 *In vitro* transcription (IVT)

IVT allows for the synthetic generation of mRNA. It uses the linearized plasmid and a promotor sequence form which it generates the complementary mRNA and adds a polyA with a 5'-methylcap for stability. This mRNA can then be purified and injected into the zebrafish embryo to induce an overexpression or in case of a knockdown replenish the mRNA pool.

2.5.1 IVT

The IVT was done as shown in the following pipetting scheme:

Table 9. IVT

Ingredient	Volume
DEPC-H_2O	To final volume of 20 µl
Transcription buffer 10X	2 µl
Dig-RNA labeling Mix	2 µl
Linearized Plasmid (1µg)	—
RNAse inhibitor	1 µl
RNA polymerase (SP6 or T7)	1 µl

- Incubate at 37ºC overnight
- Add 1ul RNAse free DNAse 1 (Roche) and incubate at 37 °C for 15 min
- Stop reaction by heating to 65°C for 10 min

2.5.2 Lithium chloride precipitation

To isolate the generated RNA, we used lithium chloride (LiCl) precipitation, which uses high concentration LiCl and Ethanol to saturate the RNA out of solution:

- To 20 µl of IVT Mix (2.5.1)
- 3 µl LiCl (4M)
- 80 µl Ethanol (-20 °C)
- Place in -20 °C for 30 minutes
- Centrifuge frozen sample at 13000rpm for 10 minutes at 4 °C
- Remove supernatant
- Wash pellet with 100 µl Ethanol 70% in DEPC-H_2O
- Vortex
- Centrifuge 13000 rpm for 10 min at 4 °C
- Remove supernatant

- Let pellet dry in hood
- Resuspend carefully in 20-80 µl DEPC-H_2O
- Aliquot and store at -80°C

2.6 WISH

WISH is the main method for analyzing gene expression in whole mount embryos. It uses the complementarity of the generated ISH RNA probes against the mRNA produced *in vivo*. As control we use RNA probes identical to the mRNA, which therefore will not bind. It then takes advantage of the Dig-incorporation in the probes, which serves as target for an antibody staining, which is then visualized via alkaline phosphatase linked secondary antibody and the NBT/BCIP reaction, which finally develops a dark blue dye near the bound antibody (Fig 11.). The reaction has to be performed RNAse free, to avoid digestion of the mRNA and/or the probes and unspecific results.

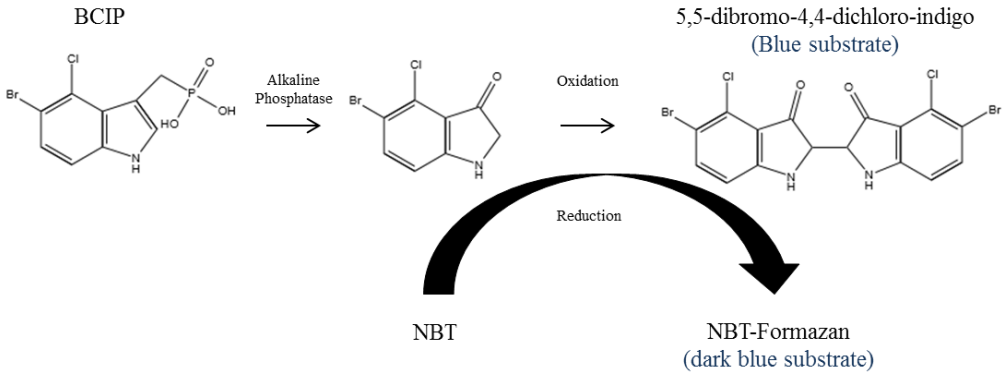

Figure 12. NBT/BCIP reaction with alkaline phosphatase

The 3-day protocol is as follows:

Post development

- Embryos fixed in 4% PFA
- Dechorionate under microscope with sterile tweezers in PBS-DEPC
- Fix in 4% PFA for 20 min
- Incubate in 50% methanol for 5 min
- Incubate in 100% methanol for 5 min
- (Possible storage in -20 °C for months, at least overnight

Day 1

- Incubate in 75% methanol (in PBST) 1x times for 5 min
- Incubate in 50% methanol (in PBST) 1x times for 5 min
- Incubate in 25% methanol (in PBST) 1 times for 5 min
- Incubate in PBST 5x times for 5 min
- Digest with 1X Proteinase K: 10 µg/ml in PBST (depending on stage: 24hpf 10 min /48hpf up to 1 hour/72hpf with 2X Proteinase K for 1 hour)
- Wash 3x in PBST for 3 min
- Refix in 4% PFA/PBST for 20 min
- Wash in PBST 3x times for 5 min
- Prehybridze in hybridization buffer at 70 °C for 3-4 h
- Hybridize in hybridization buffer with tRNA (250 mg/50 ml) and
- Heparin (2,5 mg/50 ml) at 70 ^{o}C + 1 µl Probe overnight

Day 2

- Wash with 75% hybridization mix and 25% 2xSSC
- 1x times for 10 min at 70 °C
- Wash with 50% hybridization mix and 50% 2xSSC
- 1x times for 10 min at 70 °C
- Wash with 25% hybridization mix and 75% 2xSSC
- 1x times for 10 min at 70 °C
- Wash with 100% 2x SSC for 10 min at 70 °C
- Wash with 0.2x SSC 2x times for 30 min at 70 °C
- Step: 75% 0,2x SSC + 25% PBST for 5 min
- Step: 50% 0,2x SSC + 50% PBST for 5 min
- Step: 25% 0,2x SSC + 75% PBST for 5 min
- Step: 100% PBST for 5 min
- Place in Blocking Solution (2% Sheep Serum 2mg/ml BSA) for at least 4 h
- Add Ab in Blocking solution at 1:7500 overnight at 4 °C

Day 3

- Wash with PBST 4x times for 25 min
- Wash with Alkaline Phosphatase buffer (AP buffer) 3x times for 5 min

- Stain with NBT/BCIP in AP buffer in dark until stained (observe under microscope)
- Fix by washing in PBS 3x times for 10 min
- Place in 70% Glyercol in PBS and store in dark in fridge

Embryos were mounted in 100% glycerol and oriented between slide and coverslip, which allows for accurately orienting the specimen. For this setup, 4 small coverslips were stacked on each side of the slide to generate a space for the embryo to be completely coated in glycerol for imaging (Fig 12.). Embryos were imaged using a Leica light microscope.

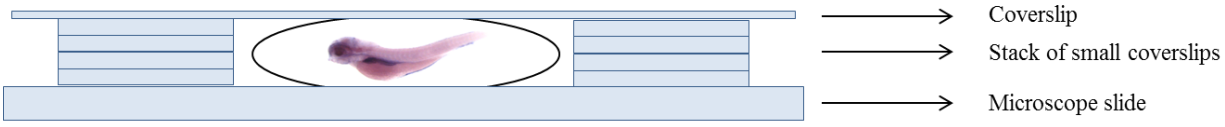

Figure 13. Embryo mounting setup

Sketch presentation of mounting setup used for light microscopy of stained embryos

2.7 Chemical exposure

To determine phenotypic effects of chemicals and inhibitors in the developing embryo, fish can be simply exposed to the effector. The embryos were dechorionated (after gastrulation) and the respective inhibitor or chemical added to the medium. Embryos were placed in 6 well dishes and 3 ml of medium used per well per 20 embryos. Comparisons between control (unexposed) and exposure where from embryos of the same clutch and experiments done in duplicate each time.

We used inhibitors LMSO and DHKA, as well as compounds L-glutamine and BH_2. Concentrations for the inhibitors were previously published (Cox et al., 2016; McKeown et al., 2012) and compounds were tested in a toxicity screen where exposure levels between 1 µM to 50 mM were tested. Medium and effector were changed daily and dead embryos removed to avoid secondary effects.

2.8 Biochemical analysis

For biochemical analysis samples were processed as whole embryo lysates. Embryos were sedated on ice previous to reaction preparation.

2.8.1 Amino acids

For amino acid analysis a lysate from approximately 15 embryos was generated in dH_2O. The lysate was passed 30 times through a 27G gauge needles and furthermore 3x10 pulses by Branson Sonifier, 50% duty opened the cells. The lysates were used for deproteinization by precipitation with 20% sulfosalicylic acid. Samples were spun at 13'000rpm for 10 minutes and supernatant used to load into a "Biochrom 30+" for cation exchange chromatography. Detected levels were normalized to total protein concentration determined by Lowry assay.

2.8.2 Pterins

For pterins, samples were treated identical to amino acid tests, but placed in a DTE/DETAPAC buffer for lysis. Samples were then treated with trichloracetic acid (10% total volume) for 1 hour on ice to precipitate proteins. Then 45 min, 13000 rpm centrifugation pelleted the proteins and the supernatant was filtered through centrifuge filer at 8000 rpm for 5 min. Treated sample was then run on HPLC to detect BH_4, BH_2 and biopterin.

2.8.3 Melanin content

Melanin content was determined by previously published method of Shin et al., 2013 and Wu et al., 2015. Exactly 50 embryos were lysed in 2N NaOH and boiled at 95 °C for 1 h. The sample was then centrifuged at 13000 rpm for 10 min to remove sediment. The samples were then measured at 495 nm to determine melanin level.

2.8.4 Protein determination

Protein levels were determined by the method of Lowry for biochemical measurements and Bradford for RNA binding experiments. The lowry kit from BioRad involves Reagent A and B mixed at a ratio of 8:1 and added sample which was diluted 1:1 in 1% SDS. All samples were measured at 750 nm. For Bradford 1 µl of lysate was mixed with 100 µl of water and 900µl of 1:5 diluted Bradford reagent (BioRad) and incubated 10 min in the dark. Wavelength at 595 nm was measured. All samples were run in duplicates. Concentration was then calculated by measuring a set of BSA standards and generating a regression curve.

2.9. Whole mount antibody stainings

For analysis of proliferation and differentiation, whole mount antibody stainings, will give insight into the pattern change and expression of certain proteins. Markers such as pH3 show mitotic cells. Protocol was established as previously shown by Verduzco et al. (2011).

2.9.1 Protocol

Day 1

- Embryos at their respective stages are stopped in 4% PFA overnight
- Wash in PBST 5x for 5 min
- Digest in proteinase K 10µg/ml in PBST(for 24hpf 10min, 3dpf 1 hour)
- Stop by 3 washes in PBST
- Refix in 4% PFA for 20 min
- Wash in PB-Tr 3x for 5 min
- Incubate in Blocking buffer for at least 2 h
  Add Primary antibody in Blocking buffer (concentrations!) at 4 °C overnight in the dark

Day 2

- The next day wash embryos 6x in PB-Tr for 30 min
- Incubate in Blocking buffer for at least 2 h
- Add secondary antibody to blocking buffer (concentration) at 4 °C overnight in the dark (at this stage also add DAPI (1/1000) solution to the buffer)

Day 3

- The next day wash embryos 6x in PB-Tr for 30 min
- Embryos can now be imaged. Store embryos in the dark for up to one week in PB-T. Afterwards the staining can lose strength.

The stained embryos were mounted in low melting agarose and oriented as required. Embryos were imaged using a 2-photon microscope with 64x magnification. Z-stacks of half the retina for the eye and the PTR of the midbrain were generated and the positive cells counted in comparison to control embryos.

2.10 Quantitative RT –PCR (qRT-PCR)

We performed qRT-PCR for quantitative analysis of gene expression levels by determining the mRNA levels in comparison to a housekeeping gene (in this case Elf1-alpha). Then the relative expression is determined by comparison to the expression of the same gene in a control. In the experiment a Ct value is determined, which identifies at which amplification cycle the mRNA level reached a previously determined threshold. The data is then calculated to identify the fold change of expression by the equation:

$$\Delta\Delta CT = (Ct_{\text{target gene}} - Ct_{\text{reference gene}})_{\text{sample}} - (Ct_{\text{target gene}} - Ct_{\text{reference gene}})_{\text{control}}$$

$$\text{Fold change} = 2^{-\Delta\Delta CT}$$

To determine specific results, individual qPCR primers were designed which had a size between 150 and 250 bp. Additionally, at least one of the primers had to cover an exon/exon boundary, if possible. Primers were tested in by PCR before running a qRT-PCR. At the end of each run a melting curve or dissociation curve, was determined and analyzed for secondary peaks that could identify unspecific amplification or primer dimers.

The reaction mix was set up as follows:

Table 10. qRT-PCR reaction mix

Ingredient	Amount
2x SensiFast SYBR Mix	10 µl
Fwd Primer	1 µl
Rev Primer	1 µl
Water	7 µl
cDNA	1 µl

The running protocol for qRT-PCR was as follows:

Table 11. qRT-PCR protocol

	Step	°C	Time
1.	Initial Denaturing	95 °C	25sec
2.	Denature	95 °C	3 sec
3.	Elongation	60 °C	30sec
			40x Step 2-3
4.	Initial Denaturing	95 °C	15sec
5.	Melt Curve	65-95 °C	1min / + 1degree each cycle
6.	Final elongation	60 °C	15sec

The experiment was run on a BioRad CFX Connect® qRT-PCR cycler.

2.11 Cryosections

Cryosections allow for a closer more detailed visualization of the respective tissues. In this study Cryosections were used to analyze which tissues or cell clusters were expressing the targeted RNAs after *in situ* hybridization. The embryos were treated in with sucrose as cryoprotectant after *in situ* hybridization and then frozen in mounting medium and sectioned.

2.11.1 Protocol

- If embryos stored in 4% PFA: Wash embryos twice in PBS
- Add embryos to tube containing 15% sucrose in dH_2O and wait until sunk to bottom (often overnight)
- Add embryos to 30% sucrose until sunk to bottom
- Place embryos in prepared blocks out of aluminum foil and fill with TissueTec® media.
- Freeze carefully on dry ice or liquid nitrogen
- Blocks can be stored at -20 °C for months
- Retain cryostat at -20 °C
- Cut sections at 10-20 µm of the sample
- Mount section immediately onto a “superfrost” cover slide and air dry
- Cover sections in mounting medium (Eukitt) and place coverslip on top. Let dry before imaging

2.12 RNA binding studies

2.12.1 FLAG-Tag

Proteins can be tagged with specific amino acid sequences, which in turn can be targeted by specific antibodies. This study used the FLAG-Tag to "tag" the Protein DHPR and test the protein for its RNA binding properties. The assay associated uses beads that are linked to FLAG-Ab to pull only the tagged protein out of a lysate.

We added the FLAG tag by PCR extension. First the open reading frame of the mRNA of interest is amplified via PCR. Then a second PCR involves primers that bind to the N or C terminus and add the FLAG sequence. It is important that either the start codon is moved before the FLAG, or the stop codon after the FLAG.

2.12.2 Cell culture of Huh7 cells

Huh7 cells were used for the study, as a screen detected RNA binding of DHPR in these cells (Castello 2012). All work was performed sterile in a laminar hood. Huh7 cells were seeded in and passaged in T75 flasks and kept at 37 °C with 5% CO_2 and 100% humidity. Cells were maintained in DMEM medium containing 10% FCS, penicillin/streptomycin, and 10mM L-glutamine. Stocks of early passaged were frozen in liquid nitrogen for long term storage. Cells were treated with trypsin at 37°C for 5 min until loose from the flask. Medium was added to stop the reaction. The samples were then centrifuged 10 min at 8000 rpm and washed with DPBS. Cells were then resuspended in 45% FCS/45%DMEM/10%DMSO medium and gradually frozen and stored in liquid nitrogen.

2.12.3 Transfection

Plasmids containing the FLAG-tagged DHPR, and siRNA against DHPR were transfected into the cells via Lipofectamin 3000 (Invitrogen) according to manufacturer's protocol. The plasmid or siRNA was incubated with lipofectamine (1:1 ratio) for 5 min and then added to the cell flask. Cells were grown for 24-48 h and then harvested. Harvest was done by direct removal of the cells with cell scratcher in 500P lysis buffer. As control cells were transfected without plasmid added to the lipofectamin.

2.12.4 Crosslinking

To study the interaction between protein and RNA, we cross-linked cells with UV light. Cells were grown in 15 cm petri dishes until 90% confluent. The petri dishes were placed on ice and crosslinked at 0.15 J/cm2. Cells were harvested immediately for further experiments.

2.12.5 Immunoprecipitation (IP) of DHPR

For immunoprecipitation, magnetic beads (ThermoFisher) were used. The beads were washed 5 times with 500P buffer and rotated 1 min each time. Magnetic beads were then incubated with primary DHPR antibody (ProteinTech) and rotated for 1 hour. The cell lysate was added to the beads and rotated overnight in 4 °C. For PNK assay the sample was then processed. In case of western blot analysis, the sample was boiled at 95 °C to remove the sample from the beads and then run on a gel.

2.12.6 SDS-PAGE

To analyze protein expression we ran protein lysates on an SDS-PAGE. The proteins were separated based on their size. Lysates were boiled at 95 °C in 1x Laemmli Buffer for 5 min to denature. Samples were then loaded into the wells of a 4-15% precast gel. Gels were run in 1X MOPS buffer for 1 hour at 140V.

2.12.7 Westernblot

SDS-PAGE gels were placed onto a PVDF mini membrane and sandwiched between Whatman paper layers. Blots were then run in a TurboBlotter at 14V for 7 min. Blots were washed twice in PBST and then blocked for 1 h in 15% Milk powder in PBST. Primary antibody was added to the blot in milk and the blot rotated at 4 °C overnight. The second day primary antibody was washed off with PBST 5 times for 30 min. Secondary antibody was added to the blot in milk and the blot rotated at 4 °C overnight. The next day secondary antibody was washed off with PBST 5times for 30 min. The blot was dried on Whatman paper and 3 ml ECL solution were used to cover the blot for 2 min. The blot was then exposed to X-Ray film in darkness for various times and then developed.

2.12.8 Polynucleotide Kinase (PNK) assay

The PNK assay is used to determine RNA bound to proteins. It radioactively labels the RNA with ^{32}P, which can then be visualized by X-ray films. The experiments are performed in special “hot labs”, which are especially equipped for radioactivity experiments.

The protocol was as follows:

A. Crosslinking and cell lysis

- Place the (induced) cells on ice. Cells should be at 90% Confluency
- Wash the cells 2x with ice cold PBS
- Completely remove PBS
- Place the cells in UV cross-linker and crosslink 0,15 J/cm2 (= 1500 Energy on crosslinker)
  Lyse cells immediately on plate with 1 ml 500P lysis buffer
- Scrape down cells
- Sonify on ice. Use 3 cycles of 10 pulses, level 4 each, with 15 sec pause in between. Check if the lysate is still viscous, if so apply one/two more cycles.
- Centrifuge the lysate 10 min at 13'000 rpm at 4 °C.
- Measure Concentration using Bradford assay (see 2.8.5)
- Adjust input material for IPs to 1,5-2 mg per aliquot.
- Continue with IP or snap freeze aliquots and store in -80 °C.

B. Clearing, RNAse treatment and IP

- Thaw lysates on ice
- Save some of the input for later analysis
- Prepare antibody containing beads. For FLAG M2 beads, use 15 µl/ml of lysate. Wash beads 3x 1ml with 500P lysis buffer -
  Resuspend the beads after last wash with 50% of initial volume of slurry with lysis buffer
- Add DNAse Takara to new tube, use 50U per ml lysate final concentration
- Dilute the RNAse A in water. For QDPR screen with 8 ng/ul, 2 ng/ul, 0,5 ng/ul and 0 ng/ul RNAse A/lysate.
- Add the lysates to the DNAse/RNase and mix by pipetting.
- Incubate 15 min at 37 °C shaking at 1100 rpm
- Place immediately on ice and cool for 5 min
- Add the beads to the lysate and incubate 2 h with 13 rpm at 4 °C on orbital shaker

C. IP washes

- Collect the beads on magnet after short spin on bench. Wash beads with 1ml of buffer and rotate 3 min with 13 rpm on orbital shaker at RT. Repeat washes as follow:
  - 500P 3x1ml
  - 100N 3x1ml
  - 100N 1x150 µl without rotation (to collect beads on bottom of tube)

D. y-32-ATP labeling (in hot lab!)

- Resuspend beads in 30 µl hot PNK mix
- Incubate 15 min at 850 rpm at 37 °C (Carry eppis behind plexiglas to shaker and back)
- Remove hot PNK mix
- Wash with 4x 1ml PNK buffer
- Check if the last flow through is hot, in case yes, continue washing (30-50cpm of wash is OK).
- Do last wash with 150 µl PNK buffer to collect beads on the bottom.
- Elute: FLAG M2 beads use 3x Flag peptide at 2 mg/ml concentration. The volume is the same as beads slurry 15 µl/ml. Resuspend the beads and incubate 45 min on ice.
- Throw out hot beads!
- Mix supernatant with 4x sample buffer and incubate 10 min at 70 °C
- Measure the CPM of eluates on small Geiger counter and record values.
- Samples were run in an SDS-PAGE and Western blot as described before. Films were developed in various times to detect the best signal.

2.13 Statistics

Statistical analysis was done either by t-test for simple comparison and one-way ANOVA when comparing multiple variables with Bonferroni and Holm post hoc test to determine significance. Significance levels were set as follows: significant (*) = $p<0.05$; very significant (**) = $p<0.01$; extremely significant (***) = $p<0.001$). Every experiment was repeated a minimum of three times.

3. Results

3.1 *De novo* pathway in *D.rerio*

The BH_4 pathway has been shown multiple times to be conserved in zebrafish and other species (Ziegler et al., 2000; Kim et al., 2013; Xu et al., 2013). Yet a full characterization of it in teleosts, with specific focus on BH_4 recycling, has not been previously done. We analyzed both *de novo* synthesis and recycling in the whole developing embryo. Using an RT-PCR screen we could detect mRNA expression for the correlating homologs (Fig 14.).

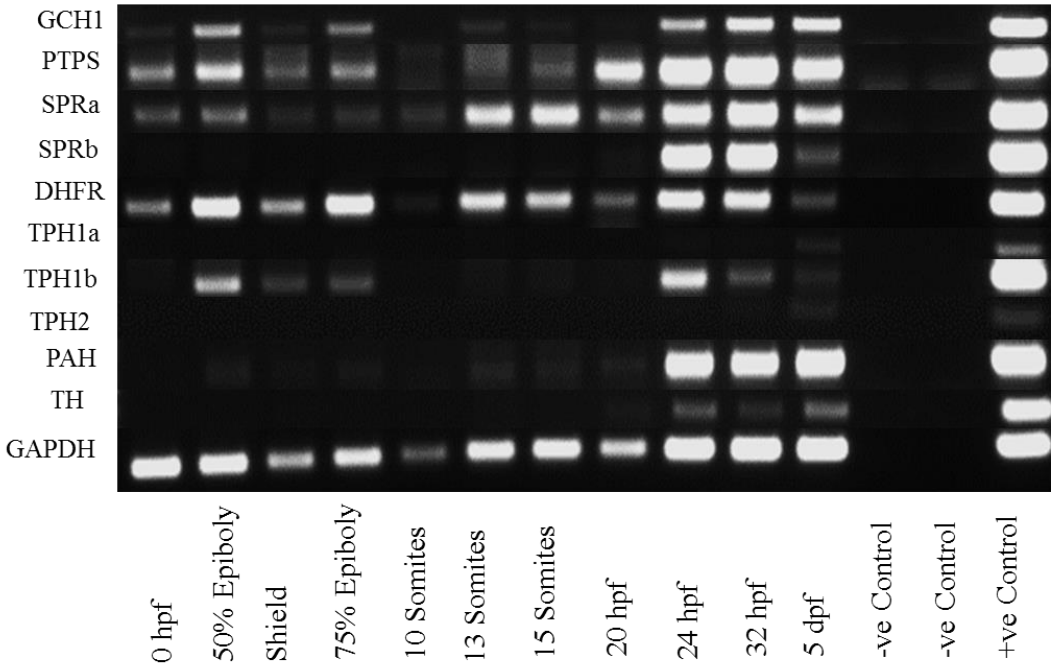

Figure 14. RT-PCR screen of BH_4 pathway members

RT-PCR Screen of BH_4 *de novo* pathway, BH_4 dependent enzymes. Each RT-PCR was run on a single gel in comparison to housekeeping gene *gapdh* and imaged at same UV intensity and focus. –ve controls are no reverse transcription and no template RT, +ve control is a mixture of all cDNAs used.

The *de novo* pathway initiator *gch1* was expressed during gastrulation and later reappears at 24 hpf. At 24 hpf it is expressed in early dopaminergic neurons of the midbrain, in direct link to *th*. *Th* on the other hand was not expressed during gastrulation and is exclusively in dopaminergic neurons (Filippi et al., 2010). *Ptps* and *spra* have similar expression to *gch1* starting maternally and then increasing at 13 somites. *Sprb*, shows the same expression pattern as *th*. Similarly, *pah* is expressed from 24 hpf. The *tph* parologs, show a previously established pattern, with *tph1b* being expressed during gastrula and late, while t*ph2* had low expression in later stages. The BH_4 related enzyme *dhfr* was expressed throughout development. These

expression patterns show that not all members of the pathway correlate directly to dopaminergic neurons and liver expression, which should arise from 24 hpf. Most members are expressed before that time, maybe linking a role to BH_4 metabolism before neuronal and hepatic development. Overall the analysis shows a conservation of expression of these homologs in the developing embryo.

As the focus of this study is the recycling enzyme DHPR and since it is the member of the BH_4 pathway that results in the most severe phenotype in patients, we extensively characterized all DHPR homologs.

3.2 Homology

The human DHPR protein is highly conserved and is present in most species from invertebrates to mammals. While it is extremely well conserved among mammals with 95% and 94% in rat and mouse, respectively, it is still highly conserved among vertebrates and teleost fish with 74% and 72% in medaka and zebrafish, respectively. Still in invertebrates such as drosophila and worms the conservation is above 50%.

Table 12. Homology of protein sequence among species

Species	Homology to Human DHPR (Amino acids)
Mus musclus (Qdpr)	94%
Rattus norvegicus (Qdpr)	95%
Oryzias latipes (Qdpra)	74%
Danio rerio (Qdpra)	72%
Danio rerio (Qdprb1)	72%
Danio rerio (Qdprb2)	62%
Drosophila melanogaster (DHPR-RA)	59%
Caenorhabditis elegans (qdpr)	51%

3.3 Qdpra

The first homolog in zebrafish we characterized was Qdpra. Compared to human, it has a conservation of 72% in the amino acid sequence (Table 12). The common domains for short chain dehydrogenases are conserved in this homolog. Further characterization of expression via WISH shows a very distinct expression pattern (Fig. 15). At 18 somites the expression locates to 3 major clusters, at the developing eye, neural crest cells (NCC) at the midbrain and back, which are likely melanophore precursors. We also observe expression near the Kupffer's vesicle at the tailbud. At 24 hpf the expression is located to migrating cells of the neural crest along the body axis of the embryo and in the eye towards the arising pigment retinal epithelium. This is seen even more accurately in cryosections of 24 hpf embryos (Supplemental A. Fig 1), showing staining exclusively in the retinal pigment epithelium and NCC, without showing expression near neuronal regions. Continuing during development, at 48 hpf the expression remains in the neural crest pigment cells and the pigment retinal epithelium, with additional expression in the choroid fissure of the eye. At 72 hpf the first developing liver cells show expression. Besides the developing liver, expression remains in the retinal pigment epithelium and melanophores. At 4dpf the expression pattern remains, while the pigment cells have now migrated along the outer edges of the developing fins. At 5 dpf the liver is the strongest expression cell type for *qdpra* and the expression in pigments and retinal pigment epithelium is now lost. In agreement with this expression pattern, the relative mRNA expression levels during zebrafish development show very low expression during somitogenesis but a rapid increase in expression after 20 hpf, reaching over 3-fold the expression level detected during gastrulation (Fig. 16). This is in agreement with the mentioned expression pattern expression increasing with the number neural crest cells and again at the beginning of liver development.

It is to note that we could not detect any expression of *qdpra* in dopaminergic or serotonergic neurons, nor in any other major neuronal population during the first 5 days of development.

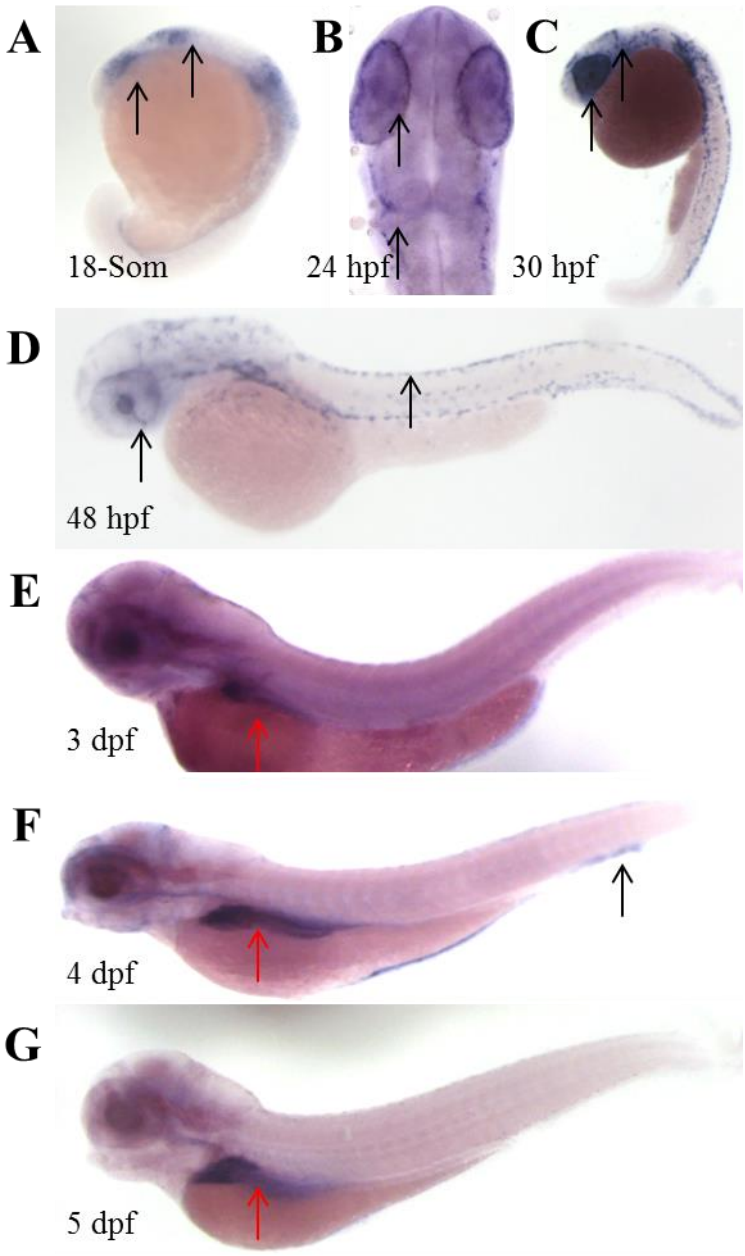

Figure 15. *qdpra* expression pattern

WISH of *qdpra* at various developmental stages. (A) WISH at 18-somites, lateral view, shows expression in eye, NCC and Kupffer's vesicle, (B) 24 hpf, dorsal view, shows expression in NCC and eye (black arrows), (C) 30 hpf, lateral view, shows expression in eye and NCC along the body axis (black arrows), (D) 48 hpf, lateral view, shows expression in retinal pigment epithelium and NCC (black arrows), (E) 3 dpf, lateral view, shows expression in liver (red arrow), (F) 4 dpf, lateral view, shows expression in liver (red arrow) and pigments (black arrow), (G) 5 dpf, lateral view, shows only expression in liver (red arrow)

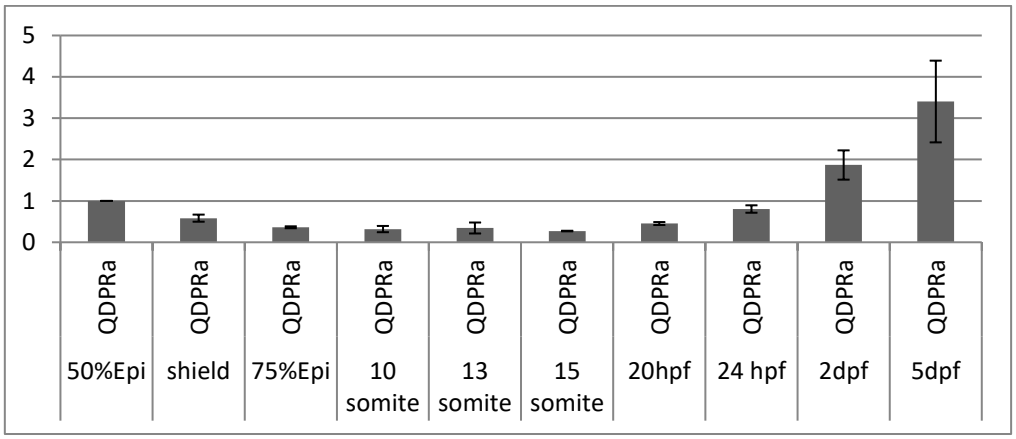

Figure 16. Relative mRNA expression of qdpra during development

Relative mRNA levels of *qdpra* determined by qRT-PCR of different developmental key stages in AB/AB wildtype embryos. Expression is relative to mRNA levels of 50% epiboly and y-axis shows fold change.

This expression pattern in WISH that we see in *qdpra* is almost identical to the one we observe for *pah*. At 24 hpf *pah* is expressed in the NCC along the body axis. At 3 dpf *pah* is expressed in the retinal pigment epithelium, the fin buds and the liver (Fig 17). *pah* is also not detected in any neurons of the midbrain and remains colocalized with *qdpra*. As Qdpr and Pah are directly required for the production of melanin, the neural crest cells are likely melanophores.

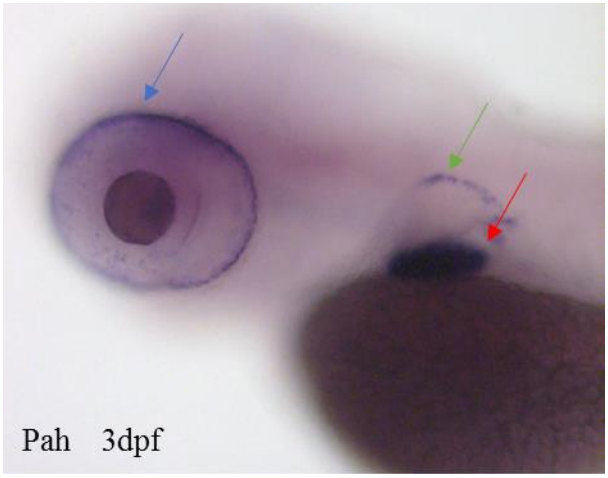

Figure 17. WISH of *pah* at 3 dpf

Lateral view of WISH for *pah* at 3 dpf. Expression is seen in retinal pigment epithelium (blue arrow), fin bud (green arrow) and liver (red arrow).

3.4 Qdpra knockdown

3.4.1 Qdpra - Morphology

Since protein sequence and mRNA expression analysis let strongly assume that qdpra displays the homolog of human DHPR, we further attempted to mimic DHPR deficiency, we used morpholinos to knockdown the protein level of Qdpra. Injection with a splice targeting morpholino (MO Qdpra 2; 2.6.1) resulted in a specific exclusion of exon 3 which was shown by RT-PCR (Fig. 18).

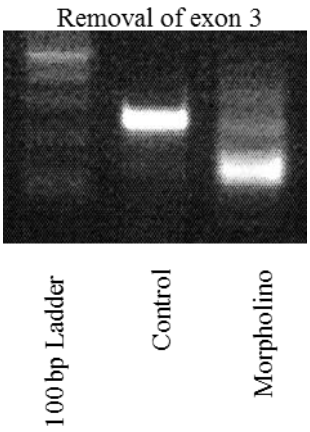

Figure 18. RT-PCR control for Qdpra knockdown

RT-PCR Control of Qdpra splice MO targeting exon 3. 100bp Ladder in lane 1, control injected embryos lane 2 and MO injected lane 3, shows removal of exon 3 in MO injected embryos. Only a faint band of wildtype mRNA remains.

In correlation with the expression pattern observed in WISH, the knockdown phenotype did not influence the overall development of the embryo at the effectively used concentration of 0,3mM. There were no morphological changes observed in the knockdown. The knockdown did however affect the melanophore intensity and melanin production. Already at the onset of pigmentation around 24 hpf we can detect less melanin in the eye and no dark melanophores along the body axis (Fig. 19). At 3 dpf we observed a significant reduction in size of the pigments located in the head region. These are likely the cells that previously were *qdpra* positive in WISH experiments. Furthermore, we were able to determine the melanin content of 3 dpf zebrafish which was significantly reduced by 20 % (Fig. 19). Control injections with 5bp-mismatch MO showed no pigment related phenotype. All controls assist to confirm the specificity of the effect.

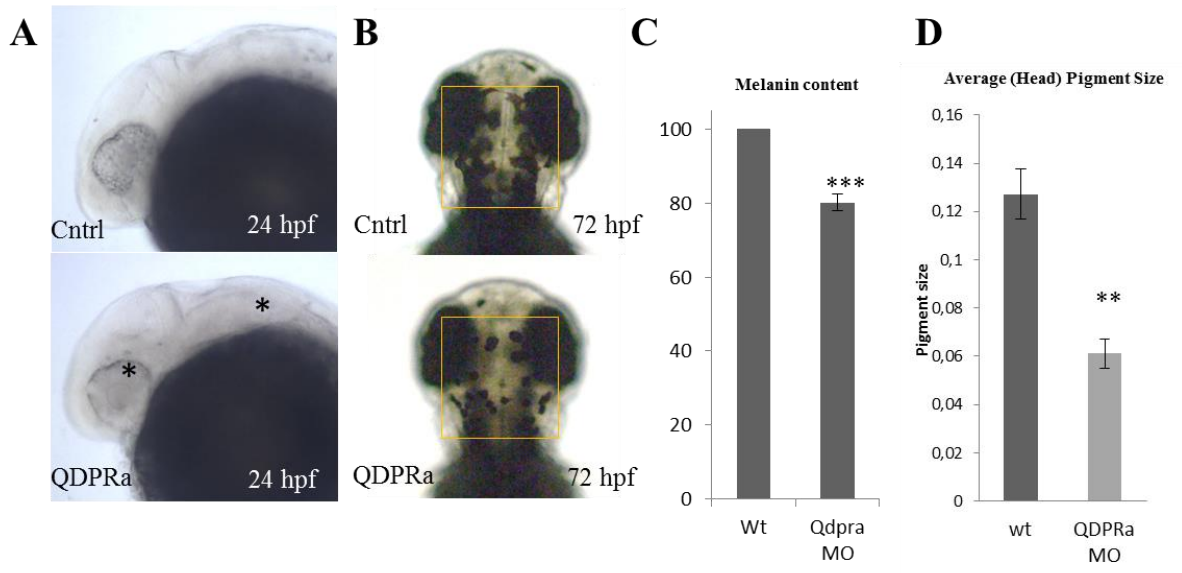

Figure 19. Qdpra knockdown morphology and pigment pattern

(A)Melanin dispersion and content in Qdpra knockdown is obersved at 24 hpf with reduced melanin content in the eye and melanophores arising from the neural crest (asterix), while morphology is unaffected (lateral view). (B) At 3dpf (dorsal view) the melanophores of the head (orange box) are smaller in appearance. (C) Melanin content in Qdpra knockdown embryos is significantly lower by 20% (D) The average head pigment size is significantly reduced in head pigments (same as (B)) by ½. Units are arbitrary and measured via ImageJ.

Co-injection of the embryos with 80 pg mouse *Qdpr* mRNA rescued the pigment size reduction and melanophores appeared normal in development (Fig. 20). This indicates that the function for BH_4 recycling in melanophores is conserved in mice.

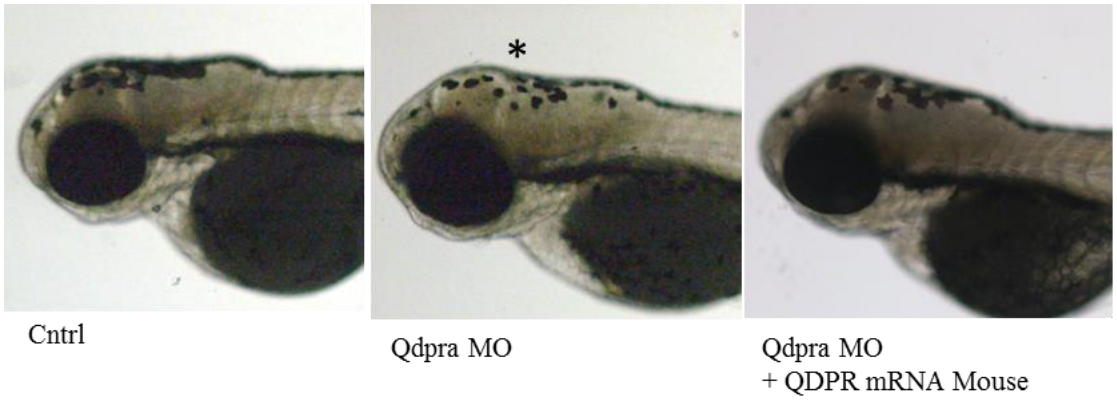

Figure 20. Qdpra knockdown and rescue

The figure shows the knockdown in lateral view of 3dpf Qdpra knockdown of Control MO injected (left), Qdpra knockdown (middle) and Qdpra knockdown with co-injected 80pg of mouse mRNA (right). Co-injection rescued the pigment depletion in the head.

3.4.2 Qdpra - Biochemistry

Furthermore, to further characterize the knockdown we determined the biochemistry of amino acids and BH_4 related neurotransmitters. Just like patients, the Qdpra morphants have a HPA i.e. significantly increased phenylalanine (wt: 34,05 +/- 3,92 µmol/mg; Qdpra MO: 47,48 +/- 3,36 µmol/mg; p*=0.036). No significant decrease in tyrosine (wt: 31,47 +/- 1,23 µmol/mg; Qdpra MO: 31,38 +/- 4,68 µmol/mg) is also observed.

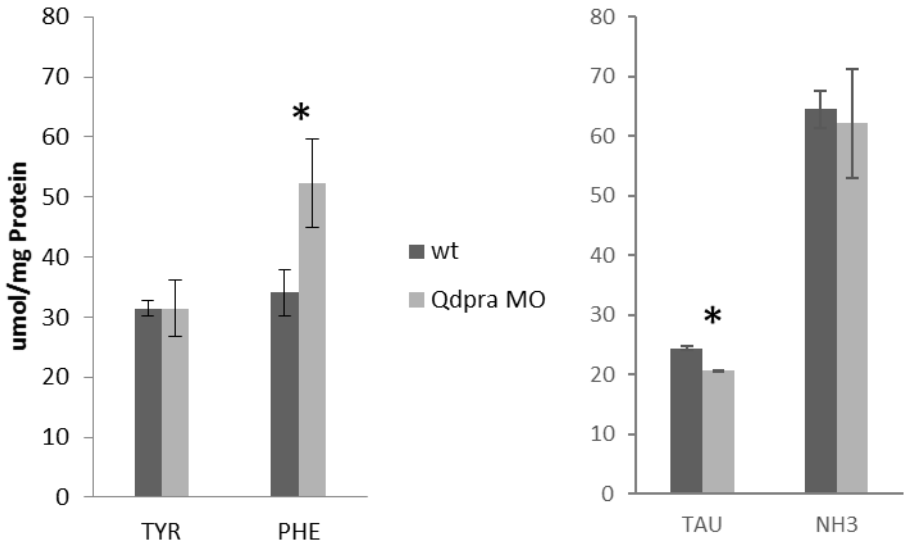

Figure 21. BH_4 related amino acids in Qdpra knockdown

Total amount of amino acids (µmol/mg Protein) in 3 dpf zebrafish of wildtype (dark grey) and Qdpra knockdown embryos (light grey). Left: directly BH_4 dependent amino acids tyrosine and phenylalanine, with significant HPA and no significant depletion of tyrosine, Right: In mice and Qdpra knockdown depleted taurine and unchanged NH_3

Just like the knockout mouse (Xu et al. 2011) we detected a significant decrease in taurine (wt: 24,39 +/- 0,35 µmol/mg; Qdpra MO: 20,67 +/- 0,16 µmol/mg; p**<0,01)). Furthermore, we did not detect any increase in NH_3 (Fig. 21). Other amino acids were not affected, which includes the BCAA. Also, other BH_4 related amino acids such as arginine of the urea cycle were unchanged. Since the expression and knockdown link the function to melanin synthesis and later BH_4 supplementation for Pah function in the liver, no relevance for neurotransmitter synthesis is likely during early development.

Overall the knockdown of Qdpra showed an evolutionary conserved role for BH_4 recycling for early melanin synthesis and later Pah related BH_4 recycling in the liver.

3.5 Qdprb2

The homolog Qdprb2 was characterized in analogy Qdpra. Qdprb2 has 62% homology with human on protein level (Table. 12), which is the lowest homology of all three homologs. An expression screen for *qdprb2* showed low levels of mRNA supplied maternally to the embryo but full depletion of expression after gastrulation (Fig. 22). On top of that we were not able to detect any expression via WISH in the developing embryo. Finally, knockdown with a specific ATG MO showed no effect on development and no morphological changes (data not shown).

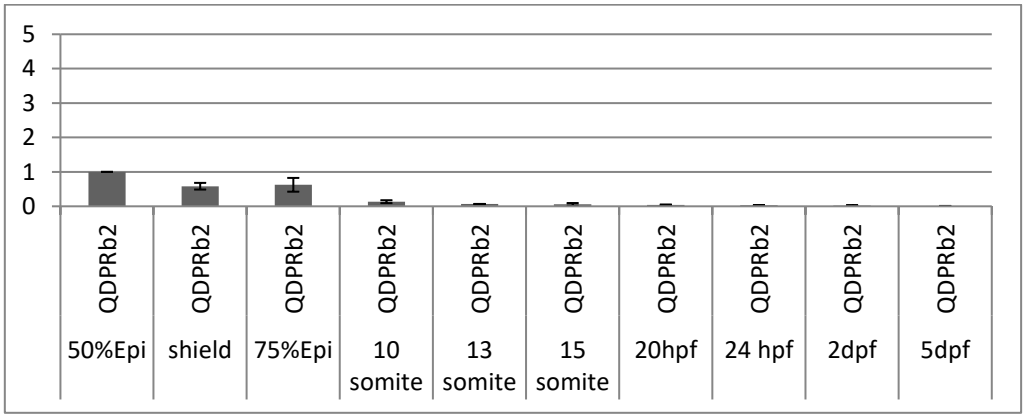

Figure 22. Relative mRNA expression of *qdprb2* during development

Relative mRNA levels of *qdprb2* determined by qRT-PCR of different developmental key stages in AB/AB wildtype embryos. Expression is relative to mRNA levels of 50% epiboly and y-axis shows fold change.

3.6 Qdprb1

Qdprb1 is conserved 72% to human on protein level, just as Qdpra, yet only contains 73% identity to Qdpra in amino acid sequence. Sequence analysis shows a lack of a "short chain dehydrogenase conserved sequence" which was conserved in Qdpra (Sigrist et al., 2012). In WISH experiments we determined a specific *qdprb1* expression pattern (Fig. 23). It is expressed ubiquitously already before gastrulation. After gastrulation, at 18 somite stage the expression is still very broad but with a trend towards proliferative regions of the embryo. At this stage, already midbrain and eye show stronger expression. At 24 hpf the staining strongly localizes to the proliferative region of the developing midbrain, the MHB. Also, a defined expression in the rapidly proliferating eye is observed. At more developed stages around 48 hpf the expression localizes to the proliferative regions of the eye, midbrain and habenula region. The expression becomes more clustered toward the arising CMZ and more distinct to the PTR. It appears that cells migrating outwards from the midbrain are also *qdprb1* positive. While at this stage distinct dopaminergic neuron clusters are present, the expression does not overlap with these clusters. At 72 hpf the expression is localized at the proliferation region of both midbrain and cerebellum, some expression is also seen along the hindbrain. Additionally, the staining is localized to the proliferation region of the eye in the CMZ and faint expression is seen in the glia rich inner nuclear layer (INL). At 4 dpf, also cells of the INL in the eye are *qdprb1* positive. At 5 dpf the CMZ and inner retinal layer and the proliferative tectum region are the only defined expression regions (Supplemental A, Fig. 2). Yet again, even at 5dpf we could not observe any expression in dopaminergic or serotonergic neurons. Furthermore, *qdprb1* is not localized to any other BH_4 dependent regions such as melanophores and liver, as was seen for *qdpra*.

Expression screens for *qdprb1* show a steady expression from early stages on throughout development, with a tendency to increase after 15 somites. Expression levels seem to vary more at later stages, as seen by the larger standard deviations (Fig. 24).

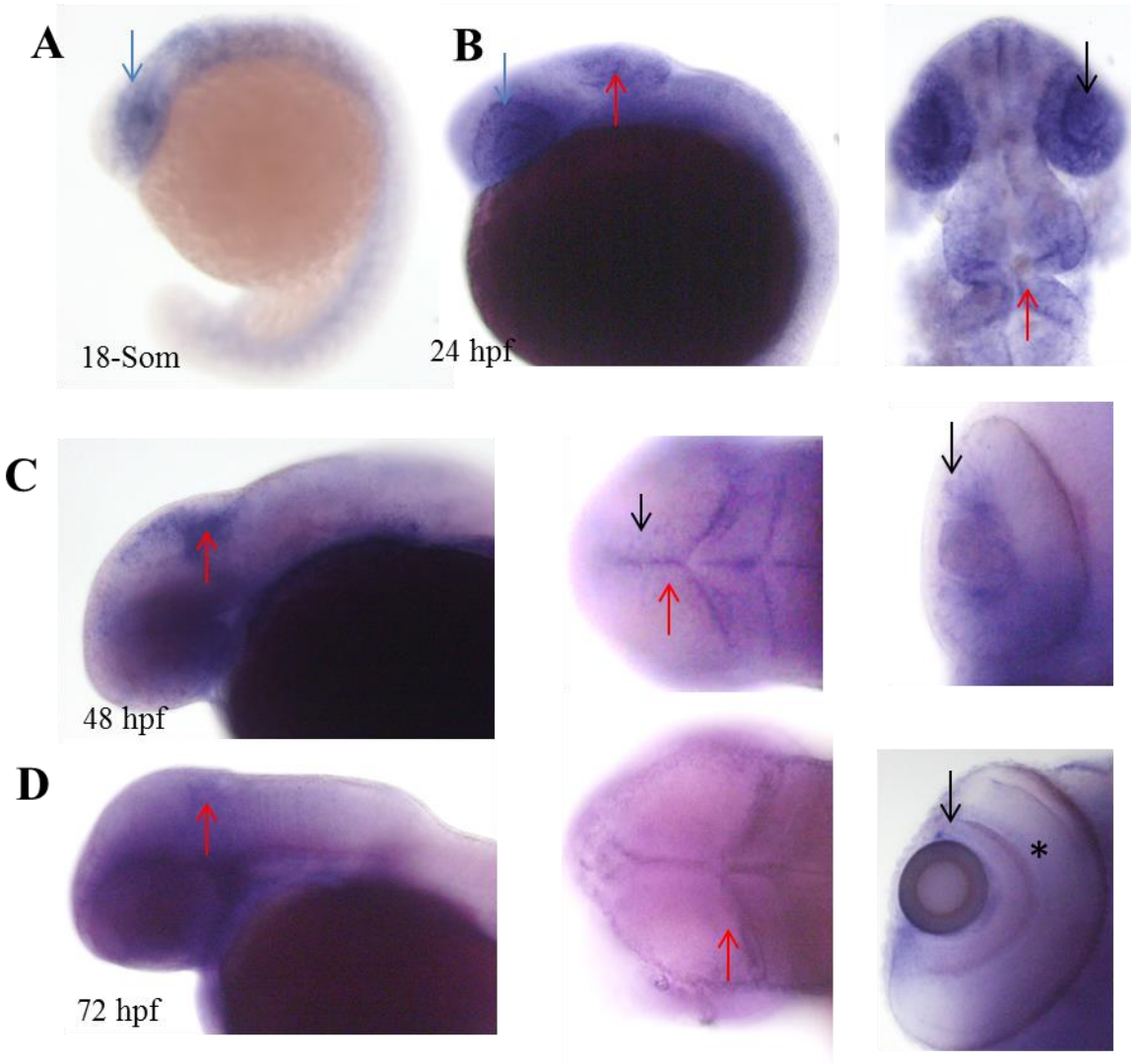

Figure 23. *qdprb1* expression pattern

WISH of *qdprb1* at various developmental stages (A) 18 somites, lateral view, shows expression in eye and along body axis, (B) 24 hpf (left) lateral view, shows expression in proliferative tectum (red arrow) and eye (blue arrow), (right), dorsal view of same proliferative regions, (C) 48 hpf (left) lateral view, shows expression proliferative midbrain (red arrow), and habenula, (middle), dorsal view shows expression in proliferative tectum (red arrow) and in migrating cells in the tectum (black arrow), (right), dorsal view, shows expression in eye around the lense in the developing CMZ, (D) 72 hpf (left) lateral view, shows expression in midbrain (red arrow), (middle) dorsal view, expression in PTR (red arrow), (right) shows expression in CMZ (black arrow) and in INL (asterisk)

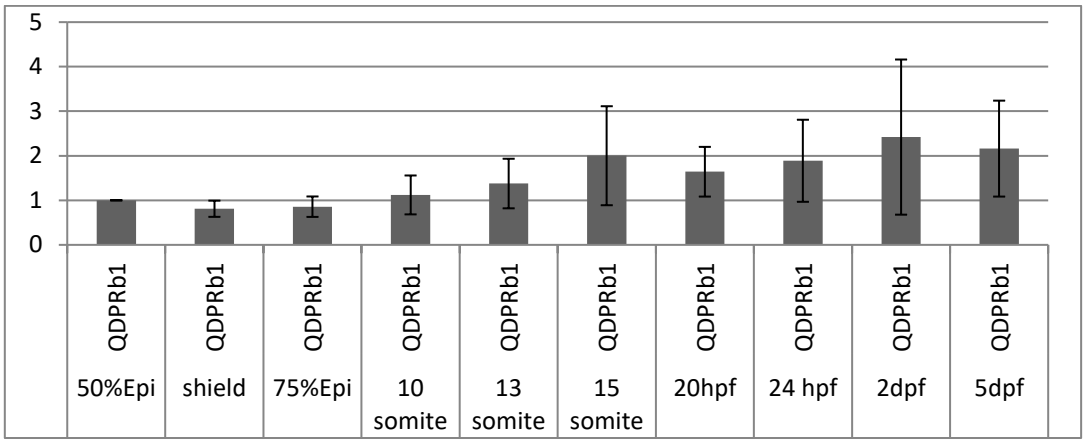

Figure 24. Relative mRNA expression of *qdprb*1 during development

Relative mRNA levels of *qdprb1* determined by qRT-PCR of different developmental key stages in AB/AB wildtype embryos. Expression is relative to mRNA levels of 50% epiboly and y-axis shows fold change.

3.6.1 Qdprb1 - Morphology

Knockdown of Qdprb1 was done by both splice targeting and ATG targeting morpholinos. The majority of experiments were done with splice MO and confirmed with the secondary ATG MO. Targeted knockdown showed an inclusion of intron 3 upon splice MO injection. In addition, qRT-PCR experiments showed an almost complete depletion of correctly spliced Qdprb1 mRNA, confirming a specific knockdown of Qdprb1 (Fig. 25). While injection of 5-bp mismatch MO led to a normal development of the embryo (Fig. 26).

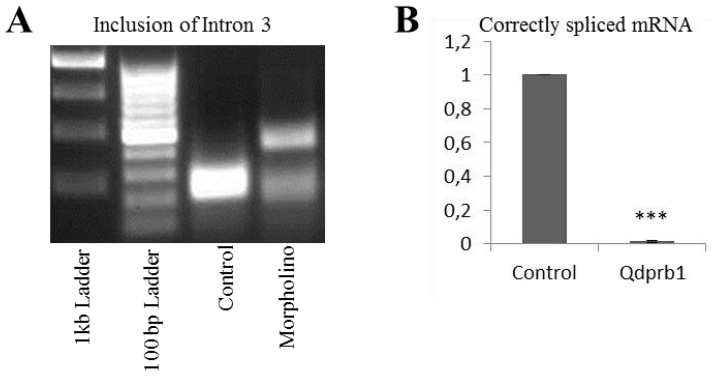

Figure 25. RT-PCR and qRT-PCR controls of Qdprb1 knockdown

RT-PCR of Qdprb1 Splice MO injected mRNA, A: Lane 1 1kb ladder, Lane 2: 100bp ladder, Lane 3: control injected embryos, Lane 4: Qdprb1 Splice MO injected, shows inclusion if intron 3 and little wildtype mRNA remaining. B: qRT-PCR shows extremely significant depletion of correctly spliced mRNA in Qdprb1 MO injected embryos.

Qdprb1 knockdown resulted in a head specific phenotype (Fig 26). Already at early neuronal development at 17 somites we observed a smaller midbrain region and a “snubnose” phenotype, with distinctively smaller anterior region (Fig. 26). The other structures of the embryo along the body axis appear unaffected. During continuing development at 30 hpf we detect a now severely decreased midbrain size, but notably no effect on the tail or body axis development of the embryo. Overall the head and eyes appear smaller. At this stage the eyes are smaller, albeit no structure appears missing. At 72 hpf the embryo shows a smaller and flattened head, smaller tectum region, smaller eye, but notably no effect on the tail or body axis development.

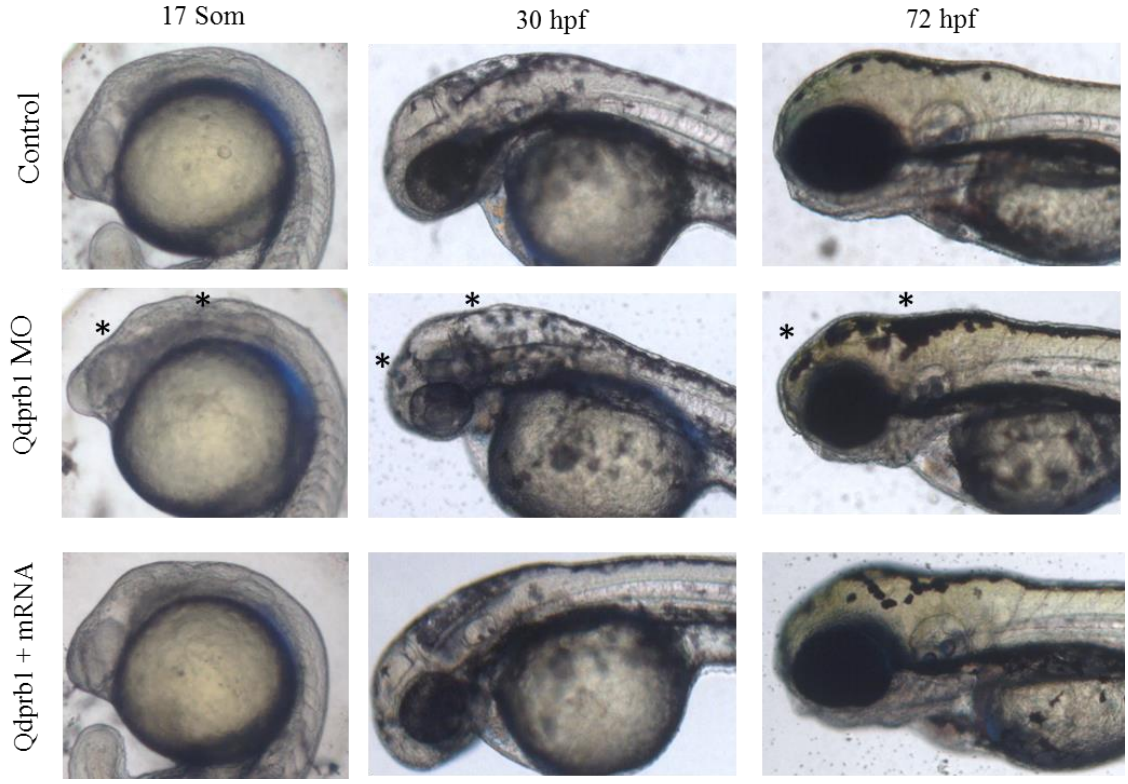

Figure 26. Qdprb1 knockdown morphology and rescue

Top row shows control MO injected embryos at the key developmental stages of 17 somites, 30 hpf and 72 hpf. Middle rows present Qdprb1 splice MO knockdown at the onset of phenotype at 17 somites, with depleted midbrain and hindbrain (asterisk), at 30 hpf with depleted midbrain and constricted MHB (asterisk), and 72 hpf with flattened midbrain and depleted brain size (asterisk), as well as smaller eyes. Bottom row shows Qdprb1 splice knockdowns co-injected with 80 pg of *qdprb1* mRNA. Embryos of the stages are fully rescued and structure identical to control-injected embryos.

Additionally, co-injection with 80 pg of zebrafish qdprb1-mRNA fully rescued the phenotype, whereas co-injection with 500 pg mouse Qdpr-mRNA at least partially normalized the morphological phenotype (Supplemental A, Fig. 3). This shows again the specificity of the knockdown effect and a partial species conservation of function between zebrafish and mouse. Co-injections with 500 pg of a mouse Qdpr splice variant without amino acid 1-48, did not rescue the phenotype.

Injections using the Qdprb1 morpholino targeting the ATG resulted in a generally more severe phenotype, showing the same phenotype when using the splice morpholino. At 26 hpf the injected embryos show a collapsed and smaller brain region. Subsequently, the brain remains small and at 72 hpf embryos have a smaller head, smaller eyes and little effect on tail and body axis (Fig. 27).

Both morpholinos can be co-injected at low concentrations that show no phenotype and together result in the observed characteristic phenotype. This suggests a synergistic effect of the two morpholinos to interfere with Qdprb1. To assess whether the phenotype was caused by p53 mediated apoptosis we co-injected the embryos with p53 MO (Robu et al., 2007). For both the ATG and splice MO, it did not rescue nor improve the phenotype (Fig. 27).

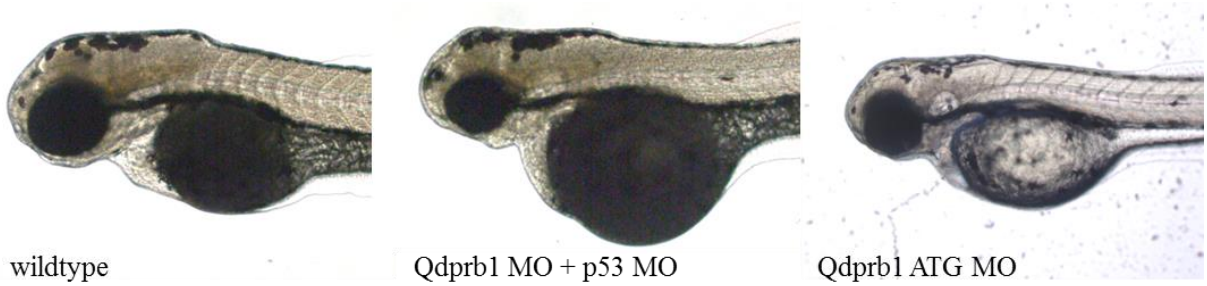

Figure 27. Qdprb1 knockdown with p53 MO co-injection and ATG MO knockdown

Morphology of wildtype, Qdprb1 splice MO + p53 MO and Qdprb1 ATG shows comparable phenotype as observed for Qdprb1 splice knockdown.

3.6.2 Qdprb1 - Biochemistry

In analogy to Qdpra, we determined the amino acid pattern of Qdprb1 morphant embryos at 72 hpf generated using the splice morpholino (Fig. 28) and the ATG morpholino (Fig.29), respectively. Contrary to Qdpra knockdown, we could not detect any changes in the typical DHPR related amino acids phenylalanine (wt: 34,05 +/- 3,92 µmol/mg; Qdprb1 MO: 35,46 +/- 3,099 µmol/mg) and tyrosine (wt: 31,47 +/- 1,22 µmol/mg; Qdprb1 MO: 34,59 +/- 2,56 µmol/mg) (Fig. 28). Furthermore, no change in arginine (wt: 15,52 +/- 0,41 µmol/mg; Qdprb1 MO: 15,68 +/- 3,30 µmol/mg) or ornithine (wt: 9,22 +/- 1,47 µmol/mg; Qdprb1 MO: 6,74 +/- 0,60 µmol/mg) as detected. Additionally, we did not observe the depletion of taurine (wt: 24,39 +/- 0,35 µmol/mg; Qdprb1 MO: 20,04 +/- 2,63 µmol/mg; p=0,081) as was seen in Qdpra knockdown and mouse knockouts (Xu et al. 2011) (Fig. 28).

We could also detect a general increase in BCAA, of which only valine (wt: 20,97 +/- 2,29 µmol/mg; Qdprb1 MO: 30,45 +/- 0,48 µmol/mg; p**<0,01) was significantly increased in splice MO injected (Fig. 28). In ATG injected embryos leucine was significantly increased (wt: 28,62 +/- 2,90 µmol/mg; Qdprb1 MO: 54,49 +/- 7,02 µmol/mg; p**<0,01) (Fig. 26). All other BCAA showed an increasing trend. This pattern was also observed in p53 co-injected embryos (Fig. 29). Along with the increase in BCAA we detected a significant depletion of the cytosolic *bcat1* mRNA in qRT-PCR. *bcat1* is the key mediator in the breakdown of BCAA. The mitochondrial homolog *bcat2* was unaffected, and co-injection with Qdprb1-mRNA rescued the *bcat1* expression level (Fig. 28). This shows that BCAA increase when *bcat1* is depleted.

Notably, we detected no change in NH_3 (wt: 64,44 +/- 3,17 µmol/mg; Qdprb1 MO: 61,81 +/- 6,32 µmol/mg) or glutamate (wt: 57,27 +/- 7,62 µmol/mg; Qdprb1 MO: 54,29 +/- 11,35 µmol/mg) hinting at no neuronal toxicity via ammonia in the developing brain (Albrecht and Norenberg, 2007) (Fig. 28). This result indicates that Qdprb1 does not induce neural toxicity nor toxic hyperammonemia.

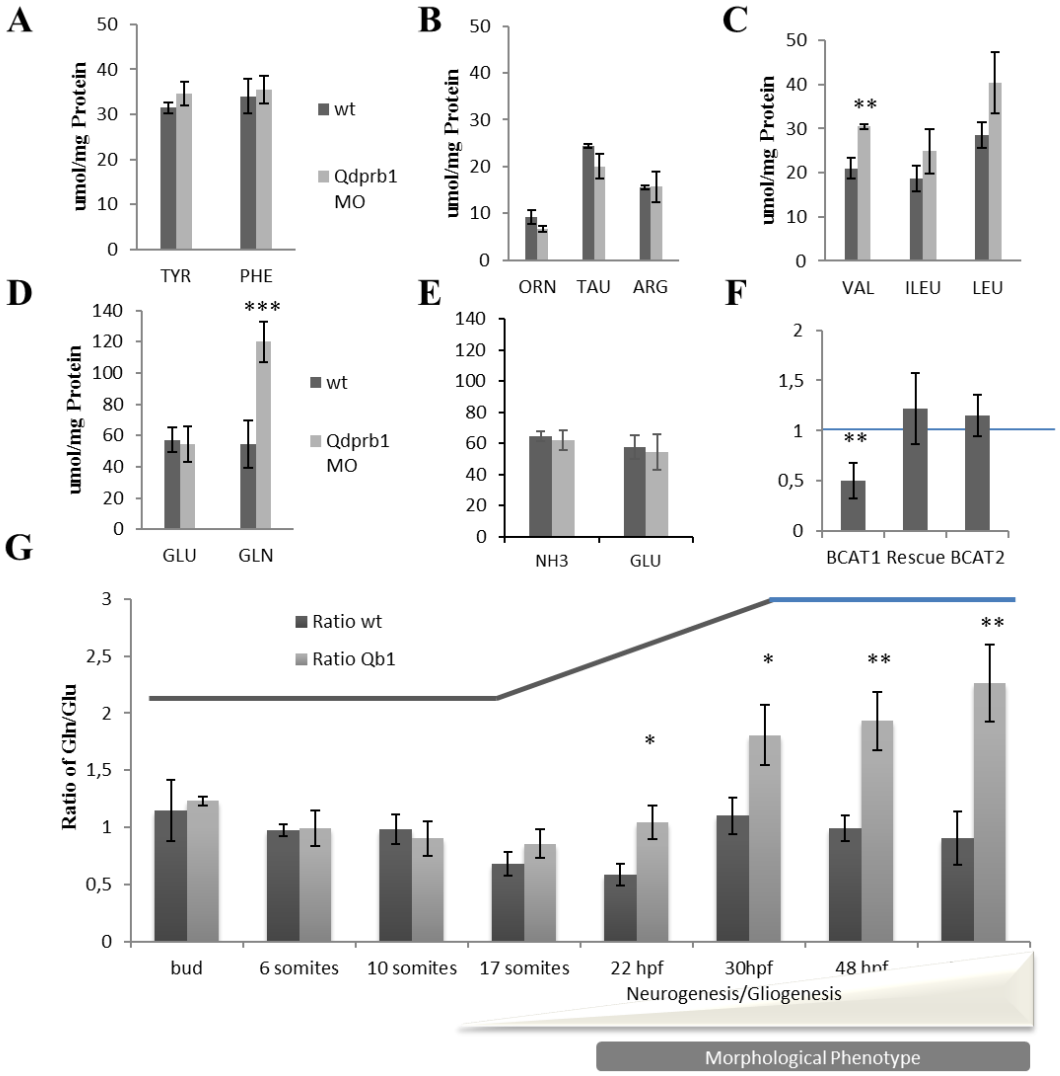

Figure 28. Amino acid analysis of Qdprb1 knockdown

(A) Wildtype in dark grey and Qdprb1 splice knockdown in light grey at 3dpf; top: BH_4 dependent amino acids tyrosine and phenylalanine are unchanged; (B) BH_4 related amino acids ornithine, taurine and arginine all normal (C) Increased BCAA, with significant increase in valine and not significant increase in isoleucine and leucine, (D) significant increase of glutamine levels in morphant embryos at 3 dpf (E) Normal NH_3 and glutamate levels in morphant embryos at 3 dpf (F) bottom: relative mRNA down regulation of *bcat1* which is restored after *qdprb1* mRNA injection and unchanged *bcat2* (G) glutamine to glutamate ratio at significant developmental stages starting after gastrulation up to 3dpf, shows significant increase after 17 somites of development and in relation to neurogenesis

Most surprisingly we detected a significant increase in glutamine (Fig. 28). Glutamine concentrations doubled in comparison to wildtypes at 72 hpf, with 119,88 µmol/mg (+/- 13,22 µmol/mg) protein in comparison to 54,57 µmol/mg (+/- 15,03 µmol/mg), respectively. In ATG injected embryos we observed levels at 162,85 µmol/mg (+/- 22,46 µmol/mg) protein (Fig 29). At the same time, we could not detect any significant change in glutamate (wt: 57,27 +/- 7,62 µmol/mg; Qdprb1 MO: 51,44 +/- 30,08 µmol/mg), the directly with glutamine associated amino acid and neurotransmitter.

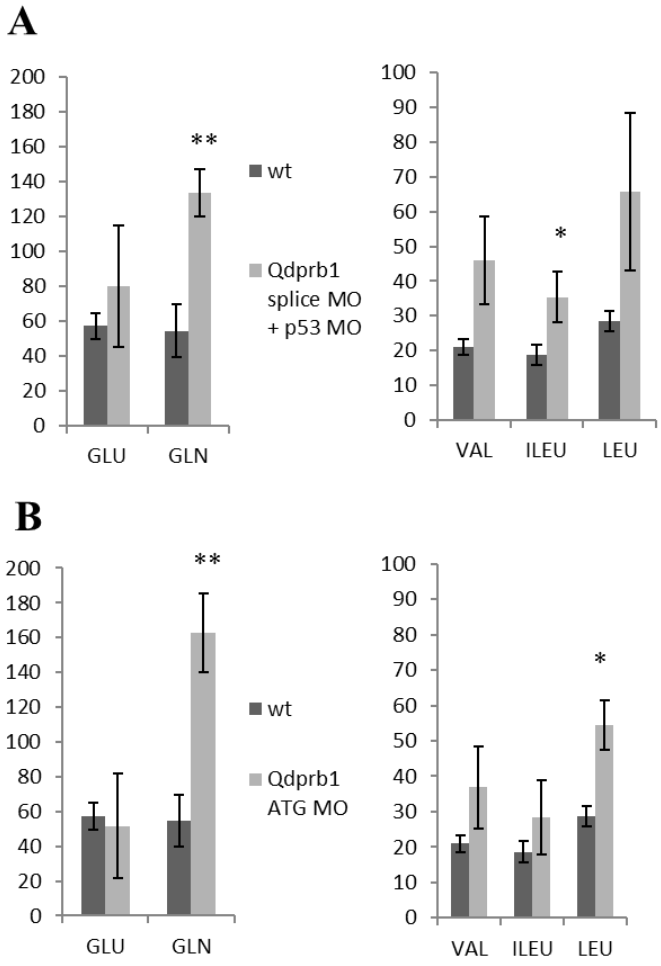

Figure 29. Biochemical analysis of Qdprb1 ATG MO and p53 MO co-injected embryos

Biochemical analysis of p53co-injected and Qdprb1 ATG injections, A: Biochemical screen for Qdprb1 MO + p53 MO injected embryos, shows very significant peak in glutamine and significant increase in isoleucine, B: Biochemical analysis for Qdprb1 ATG MO injected embryos, shows very significant glutamine peak and increased BCAA.

To detect the onset of the glutamine increase, we analyzed multiple key developmental stages for glutamine and glutamate (Fig. 28). Glutamine to glutamate ratio remains relatively stable at 1:1 during development, with the exception of a rise in glutamate at 17 somites to 22 hpf, slightly reducing the ratio. During late gastrulation and onset of somitogenesis, where no phenotype is observed, no change in glutamine to glutamate ratios was detected in the knockdowns. Interestingly, the first trend towards an increase in glutamine is at 17 somites (Ratio Gln/Glu: wt: 0,68 +/- 0,10; Qdprb1 MO: 0,86 +/- 0,13; p=0,197), where we also detected the first onset of the phenotype. Glutamine then is steadily increased significantly at 22 hpf (Ratio Gln/Glu: wt: 0,58 +/- 0,14; Qdprb1 MO: 1,04 +/- 0,15; p*=0,02), 30 hpf (Ratio Gln/Glu: wt: 1,10 +/- 0,16; Qdprb1 MO: 1,81 +/- 0,26; p*=0,03), 48 hpf (Ratio Gln/Glu: wt: 0,99 +/- 0,11; Qdprb1 MO: 1,93 +/- 0,25; p**<0,01 and 3 dpf (Ratio Gln/Glu: wt: 0,91 +/- 0,24; Qdprb1 MO: 2,27 +/- 0,34; p**<0,01) reaching its maximum at 3 dpf. Therefore, the levels of glutamine temporally correlate to the onset and development of the knockdown phenotype. Yet again upon co-injection of *qdprb1*-mRNA we could rescue the biochemical phenotype and reduce the glutamine peak back to normal levels at 72 hpf.

In this fundamental characterization of the three homologs Qdpra, Qdprb1 and Qdprb2 we were able to focus the following studies in zebrafish on a single gene. Firstly, Qdpra was characterized as the functional homolog to DHPR, with expression in melanophores and liver and with direct link to Pah and secondly, *qdprb2* was not linked to any phenotype by the used methods, we thirdly found Qdprb1 morphants to develop a brain specific phenotype during early development without close link to BH_4, but rather connected to glutamine metabolism. As this morphology closely resembled the morphological phenotype of patients and the biochemical data suggested a novel role for Qdprb1, further studies were focused exclusively on Qdprb1 morphants.

3.7 Neuron development in Qdprb1 knockdown embryos

3.7.1 Qdprb1 - Neuronal development

Along with the biochemical pattern, the severe phenotype of patients presents with severe brain atrophy and infantile parkinsonism, as well as dystonia and epilepsy (Opladen et al., 2012). This shifted our focus towards neuronal development of the embryo. Since Qdpra was likely to function in melanophores and possibly liver development we shifted our attention to the proliferative regions of eye and midbrain that showed *qdprb1* expression.

Analysis of neurons in morphants of transgenic lines and expression levels via qRT-PCR showed that Qdprb1 knockdown had no major effect on neuronal development. The transgenic lines that marks differentiated neurons, (tg(HuC/D:GFP)), showed no loss of neuronal layers or patterning (Fig. 30). It did however corroborate the strong microcephaly, with 15% reduction to the wildtype brain size that could be fully restored by co-injection with *qdprb1* mRNA. Finally, expression of the GFP in tg(HuC/D:GFP) in the eye confirms that retinal layering occurs, even though the eye is overall smaller. Screening for other neuronal systems in the embryo confirmed the specific effect to the head region (Fig. 31). Expression of neurons in the spinal cord and neuromast cells of the lateral line organ in tg(NBT/lyn:GFP) transgenic morphant embryos, remain their normal patterning. This suggests that neuronal patterning was overall unaffected.

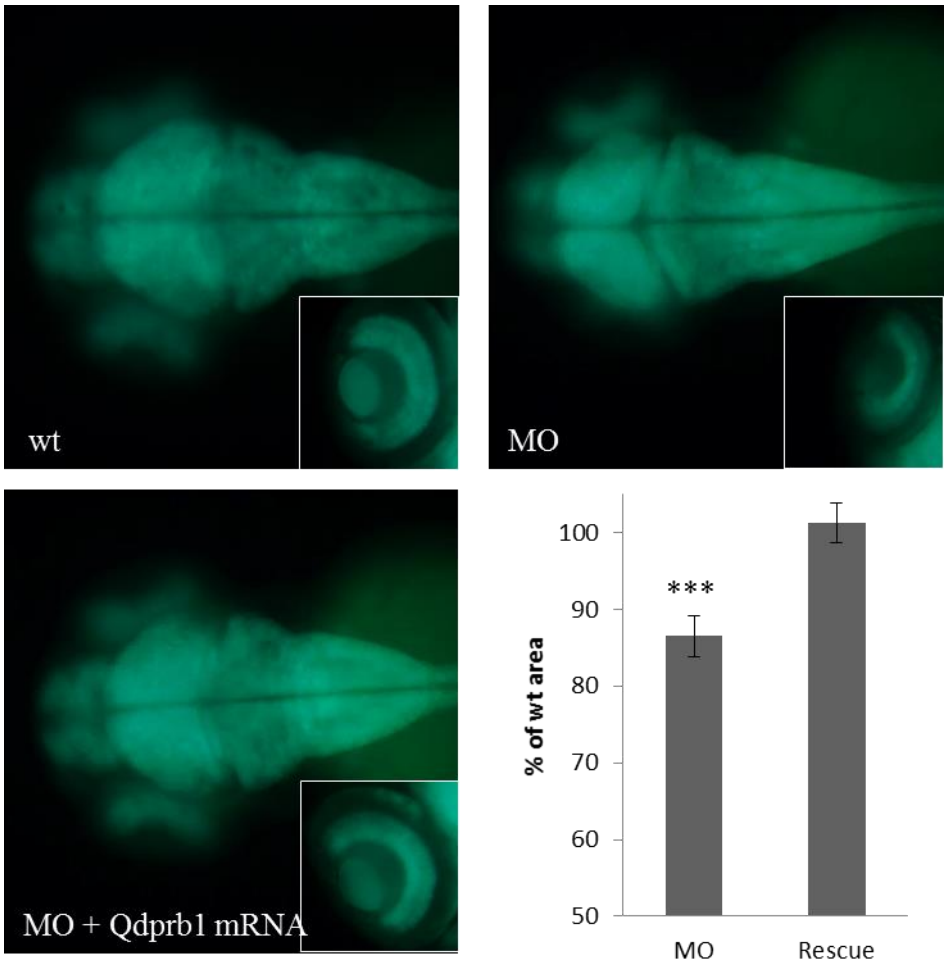

Figure 30. Neuronal brain expression and microcephaly in Qdprb1 knockdown embryos

Expression pattern of the midbrain and eye in tg(HuC/D:GFP) embryos (dorsal view) of wildtype (top left) show broad expression in the optic tectum and hindbrain. In the eye (magnified in right corner of each image) expression in the middle layers is detected. In Qdprb1 splice MO knockdowns (top right) the area of the optic tectum is smaller and constricted, as is the region of the hindbrain. Rescued embryos with *qdprb1* mRNA (bottom left) show fully recovered brain area and strong GFP signal in midbrain and eye. Statistical analysis of the brain area (bottom right) show significant reduced brain size by 15% in the Qdprb1 knockdown and fully recovered brain area in rescued embryos.

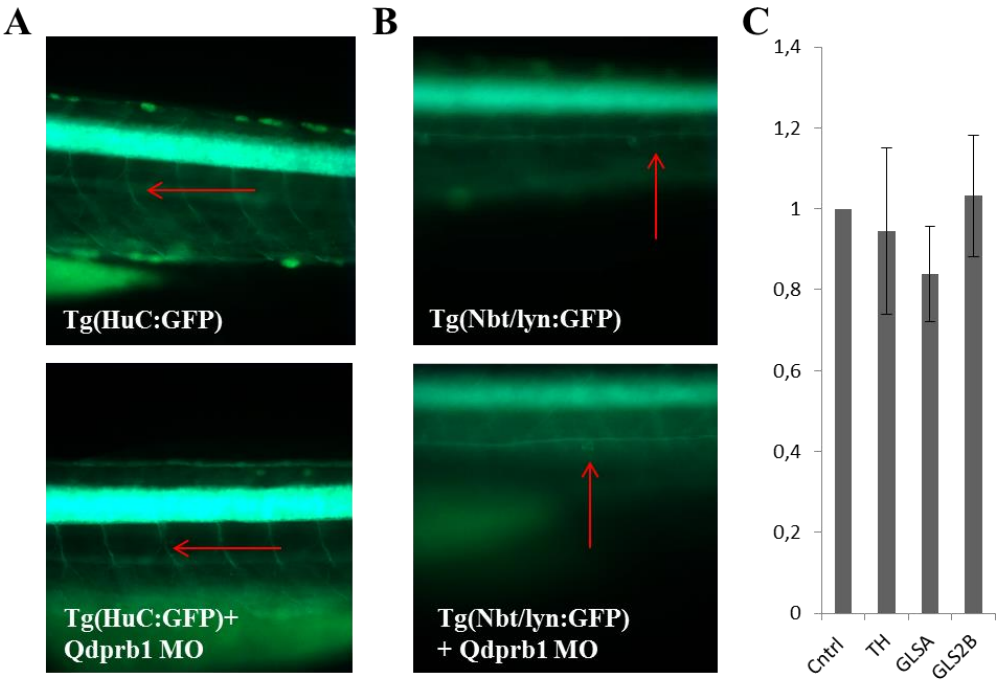

Figure 31. Neuronal networks in transgenic lines of Qdprb1 knockdown embryos

(A) Neuronal networks in tg(HuC/D:GFP) zebrafish (lateral view) of non-injected (top row) and Qdprb1 splice knockdowns (bottom row) show intact motor neurons of the tail (first column, red arrows) and (B) intact neuromasts of the lateral line organ (red arrows) in tg(NBT/lyn:GFP). (C) qRT-PCR expression levels of key neuronal markers: th (in dopaminergic neurons), glsa and glsb (in glutamatergic neurons) are unchanged.

To further investigate a potential impact of Qdprb1 loss on neuronal networks, we analyzed the expression of dopaminergic and glutamatergic markers (Fig. 31). Strikingly, the key dopaminergic markers *th* remained unchanged in expression at 3 dpf, as are the markers for glutamatergic neurons *glsa* and *glsb*. Qdpr is shown to be required for the production of precursors for dopamine and serotonin. qRT-PCR data, however, shows no change in expression levels of BH_4 pathway initiator *gch1*, which we detected in dopaminergic neurons. In WISH experiments we could show that *gch1* remains unchanged in expression and pattern despite the morphological defect of the head region (Fig. 32). Not only is *gch1* unaffected, but the homolog Qdpra remains also unchanged in expression levels. This shows that the embryo neither compensates the lost function with increased *de novo* mRNA synthesis nor by overexpressing another homolog. This supports the idea of a BH_4 pathway independent function of Qdprb1.

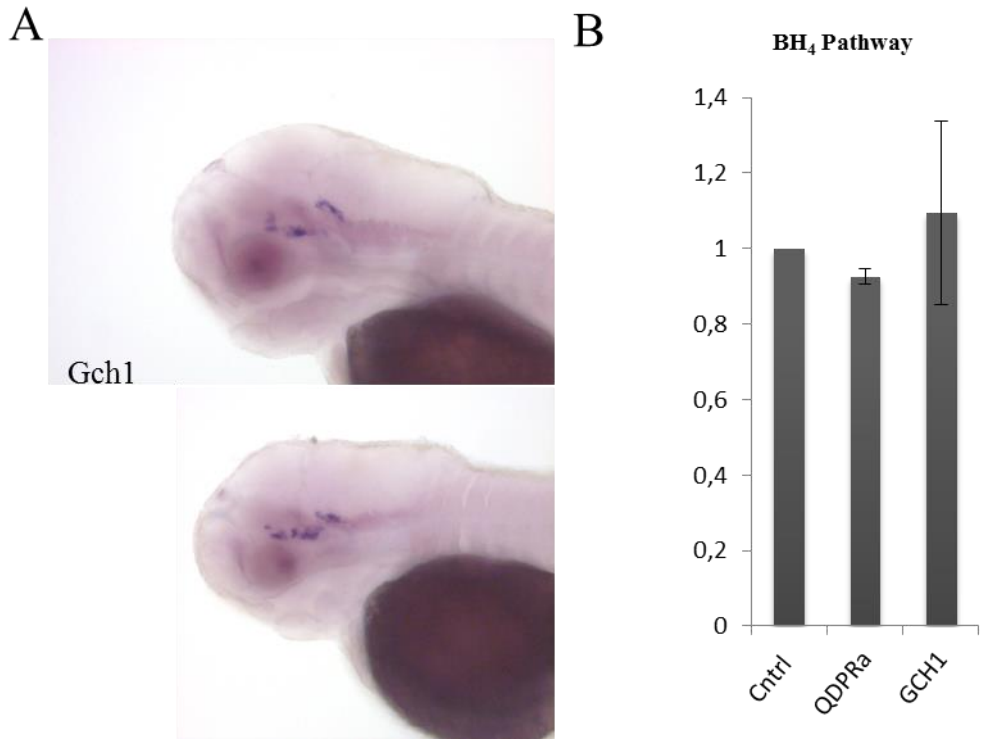

Figure 32. WISH and qRT-PCR of BH4 pathway genes in Qdprb1 knockdown

Analysis of BH_4 pathway in Qdprb1 knockdown embryos. A: WISH of de novo initiator *gch1*, shows patterning identical in wildtype (top) and knockdown (bottom) in dopaminergic neurons of the midbrain, B: qRT-PCR of *qdpra* and *gch1* show no significant change in relative expression.

3.7.2 BH_2 Toxicity

To assess whether BH_2 may act as neurotoxic agent, as proposed may be the cause in patients (Opladen et al., 2012), we injected and exposed embryos with high concentration of BH_2 (Table 13). Even at high concentrations of 10 mM BH_2, it was not lethal, nor did it affect development based on survival, motility and developmental stage in comparison to wildtypes. We therefore excluded BH_2 as neurotoxic agent in early zebrafish development.

Table 13. BH_2 Exposure and injection

Test	Non-exposed	Exposure 10mM BH_2	Control-injected (H_2O)	Injected 10mM BH_2
# of unaffected embryos	50/50	50/50	45/50	45/50

3.7.3 Microglia

Microglia arise from a different lineage than macroglia and act as macrophages of the brain (Chan et al., 2007). Microglia have a BH_4 dependency due to NOS expression (Liu et al., 2002). From 60 hpf the macrophages of the embryo differentiate to microglia of the brain (Herbomel et al., 2001). The transgenic line tg(mpeg:GFP), displays a readout for macrophages and microglia. Interestingly, the knockdown of Qdprb1 in tg(mpeg:GFP) revealed a control-like microglia GFP expression at 72 hpf (Fig. 33). As the microglia specific transporter *slc1a3a* was also unchanged in qRT-PCR tests (Fig. 39), we excluded microglia from our focus.

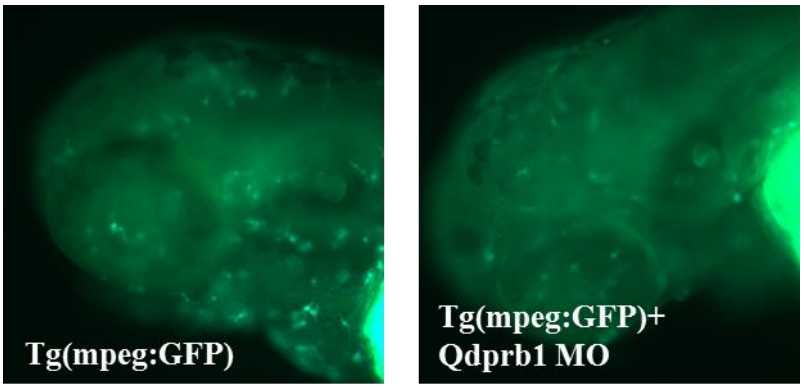

Figure 33. Tg(mpeg:GFP) microglial expression

Microglial expression in 3dpf tg(mpeg:GFP) (lateral view), which marks macrophages and microglia cells shows no change in number or localization in Qdprb1 knockdowns

3.7.4 Qdprb1 – proliferative regions

When we analyzed the eyes of Qdprb1 morphants by immunofluorescence at 3 dpf, the DAPI staining indicated that they are smaller in size but had normally differentiated layers such as GCL, INL, IPL and ONL. Furthermore, it appears that the proliferative CMZ region was broadened due to the knockdown (Fig. 35). To investigate if this effect was due to differentiation or proliferation problems of cells from the proliferative regions, we next analyzed the mitosis specific marker phospho-histone 3 (pH3) (Fig. 35 and Fig. 36).

Antibody staining with pH3 showed a 4-fold, significant increase in pH3 positive cells (wt: 46,71 +/- 13,38 pH3 positive cells/half retina; n=7; Qdprb1 MO: 153,67 +/- 27,82 pH3 positive cells/half retina; n=6; p***<0.001). Rescue experiments also confirmed this effect to be specific, by reducing the number of pH3 positive cells to control-like levels (avg: 14,75 +/- 5,89 pH3 positive cells/half retina; n=4) (Fig. 35 and Fig. 36). Unlike the wildtype, most of these cells in the eye are located outside the CMZ (Fig. 35 and Fig. 36) with a high number of positive

cells in the ONL. The 4-fold increase in pH3 positive cells is also seen in the second expression region of Qdprb1, the PTR (wt: 28,33 +/- 5,24 pH3 positive cells; n=3; Qdprb1 MO: 74,33 +/- 17,46; n=3; p*=0,023) (Fig. 37). As control and to account if apoptosis plays a role in the observed phenotype we tested if co-injection of a p53 MO affected the phenotype. A similar increase in pH3 positive cells was observed in p53 co-injected embryos (Supplemental A, Fig. 4) It is to note that no other region in the embryo showed a change in pH3 positive cells. In line with the increased pH3 positive cells we analyzed cell cycle markers of the retina via qRT-PCR. We detected an increase in the proliferative cell cycle marker *ccnd1*(fold change: 1.62, SD +/- 0,27) (Das et al., 2009; Cerveny et al., 2010) and in the proliferation maker *myca* (fold change: 1,41, SD +/- 0,23) (Stephens et al., 2010) of the retina, while stem cell marker mz98 remained unchanged (fold change: 1,14 SD +/- 0,37) (Cerveny et al., 2010). Two key eye development genes, *rx1* (fold change: 0,50 +/- 0,24) and *rx2* (fold change: 0,71 +/- 0,05) were also decreased. To analyze if an activation of the proliferative pathway causes increased proliferation we screened for purine and pyrimidine, which commonly increase, if more proliferative cells arise (Lane et al., 2015). As these patterns were unchanged, (Fig. 34) we deduced these additional cells are not proliferating, rather failing to differentiate and are arrested in the cell cycle.

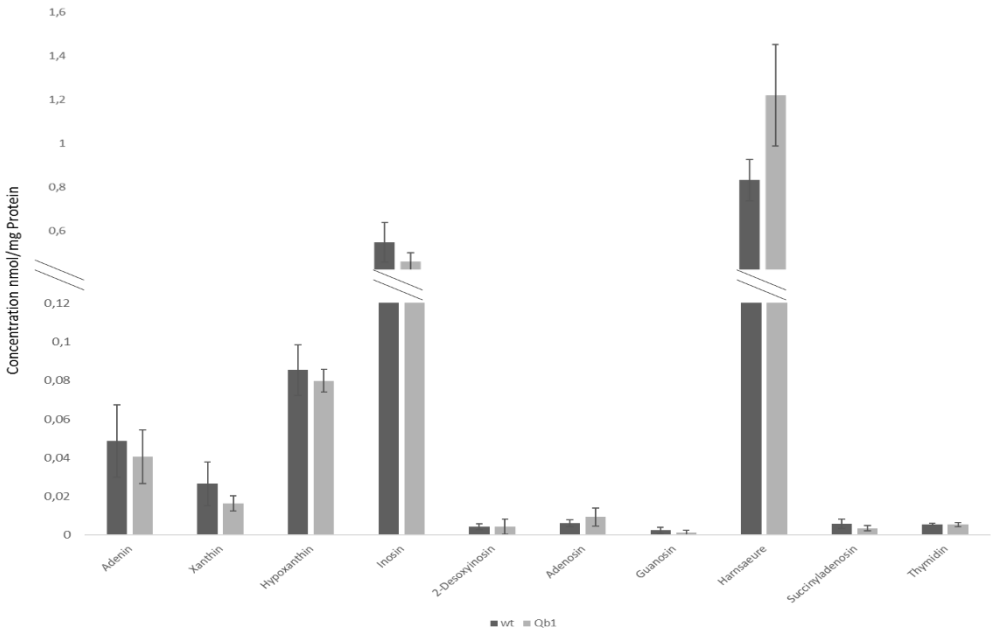

Figure 34. Purine and Pyrimidine levels in Qdprb1 morphants

Purine and Pyrimidine measurements show no significant change in any measurement of adenine, xanthine, hypoxanthine, inosine, 2-deoxyinosin, adenosine, guanosine, uric acid, succinyladenosine and thymidine.

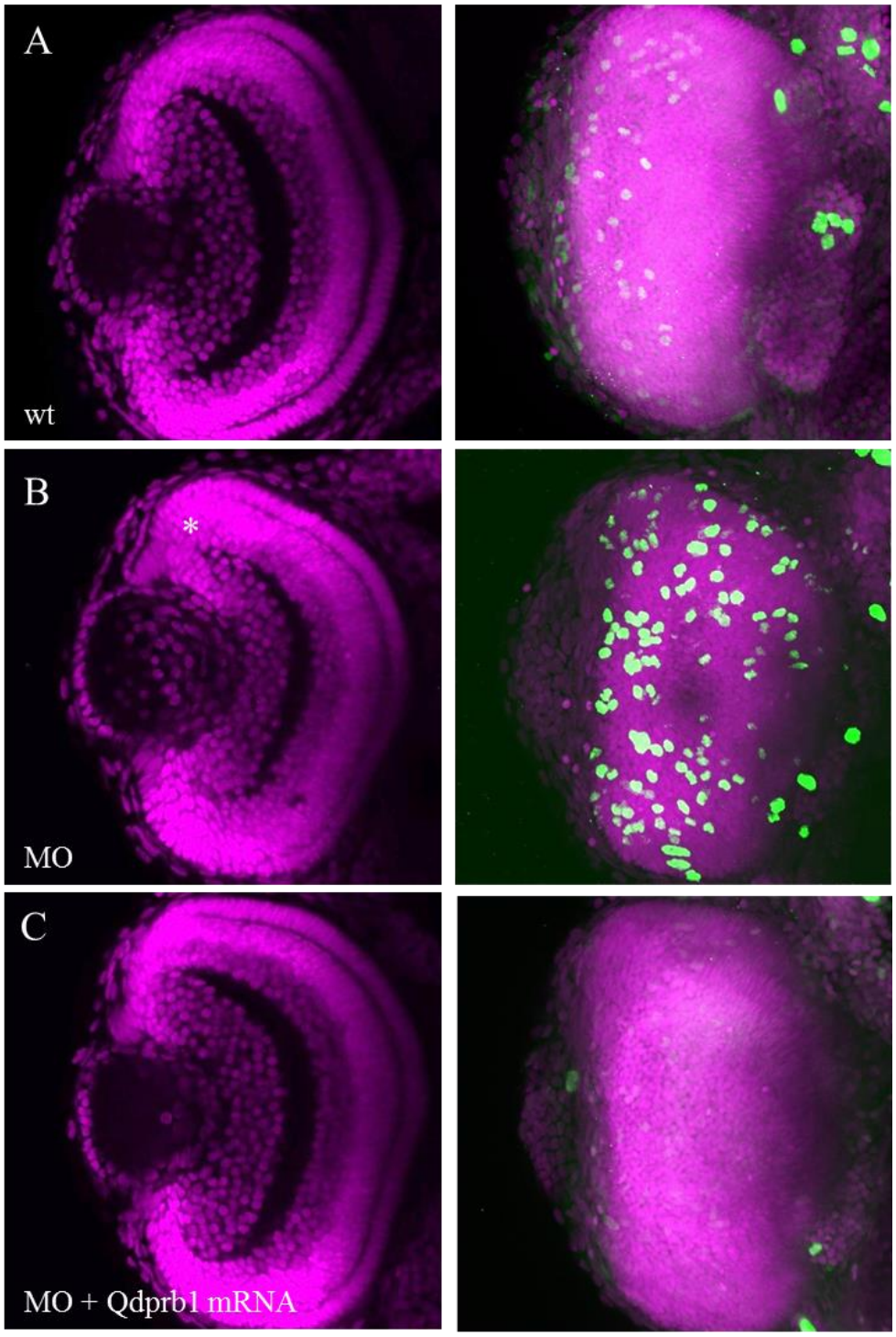

Figure 35. DAPI and pH3 antibody staining of Qdprb1 knockdown and rescue in the retina at 3 dpf

Proliferation and structural analysis of the 3 dpf retina, (A) (left), wildtype structure of the retina stained with DAPI, (pink, left) pH3 antibody staining (green, right) and Z-stack of one half retina shows pH3 positive cells in the CMZ, (B) (left) Qdprb1 MO knockdown retinal structure, shows smaller retina and enlarged CMZ (asterisk), (right) pH3 antibody staining and z-stack of one half retina shows significant increase in pH3 positive cells over the retina, (C) (left) Rescue of Qdprb1 knockdown with *qdprb1* mRNA retinal structure is wildtype-like, (right) pH3 antibody staining and z-stack of one half retina

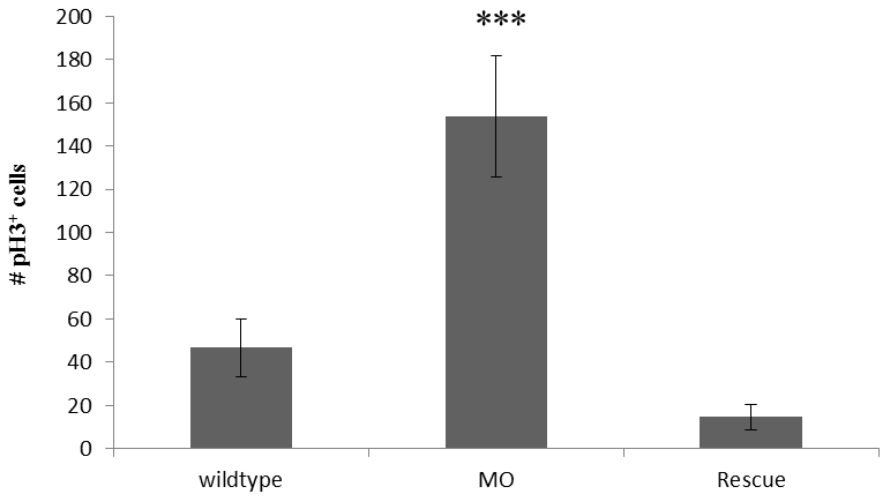

Figure 36. pH3 positive cells in Qdprb1 morphant retina

Statistical analysis of pH3 positive cells in the retina of wildtype (n=7), qdprb1 MO (n=6) and qdprb1 MO+ qdprb1 mRNA (n=4) injected embryos at 3dpf. MO has 4-fold highly significant increase. Statistical analysis via one-way ANOVA and Bonferroni and Holm test shows significance between wildtype and MO, MO and rescue, but not wildtype and rescue.

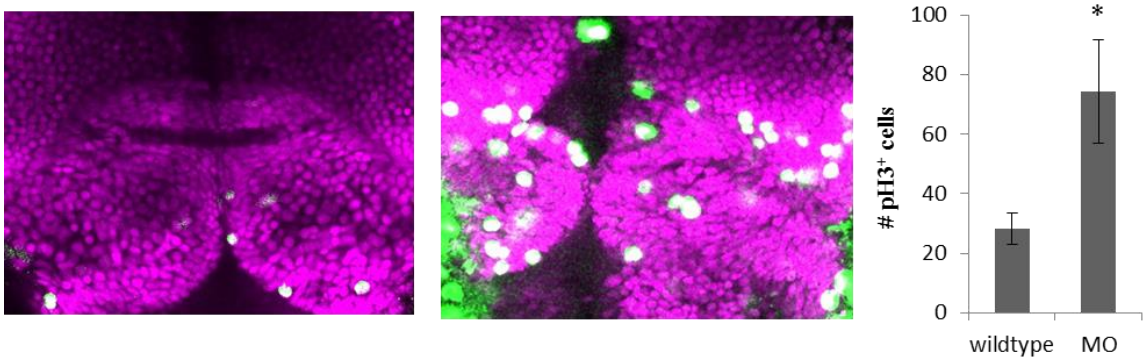

Figure 37. pH3 antibody staining in tectum of 3dpf Qdprb1 knockdown embryos

Magnification of tectum proliferation region (dorsal view), (left) wildtype PTR with few pH3 positive cells, (middle) Qdprb1 knockdown PTR with many pH3 positive cells, (right) statistical analysis of pH3 positive cells shows significant increase in number (n=3).

3.8 Glial development in Qdprb1 knockdown embryos

3.8.1 Qdprb1 - glial development

Since we detected no effect on neuronal and microglial development we continued to analyze the second major cell type in brain networks: Glial cells. Glial cells in zebrafish are mainly present as radial glia and are present in midbrain and eye (Barresi et al. 2010; Bernardos et al., 2007). Glial cells in the eye are termed “Müller glia”. The key markers for glia cells are glutamine synthetase (Glula and Glulb) and glial fibrillary acidic protein (Gfap).

qRT-PCR shows a significant reduction of glial specific marker *glula* (fold change: 0,39 +/- 0,04) and *gfap* (fold change: 0,47 +/- 0,03*)* in the developing brain (Fig. 38). As internal control we also checked *glulb*, which is only expressed in the periphery. Here a control-like expression was found in the morphants. WISH experiments show the specific affect in the eye and midbrain glia. *Glula* is lost in the Müller glia of the eye, while the midbrain shows very little remaining expression (Fig. 38). qRT-PCR shows a twofold reduction in mRNA level. Little expression remains in the hindbrain glia. This matches the expression of Qdprb1 in the midbrain region and eye, where the strongest effect is seen. The second key marker *gfap* is also reduced two-fold in qRT-PCR and is lost in the midbrain expression. The expression in the spinal cord for *gfap* remains unaffected, which again confirms the specific effect in the midbrain region and the areas corresponding with *qdprb1*.

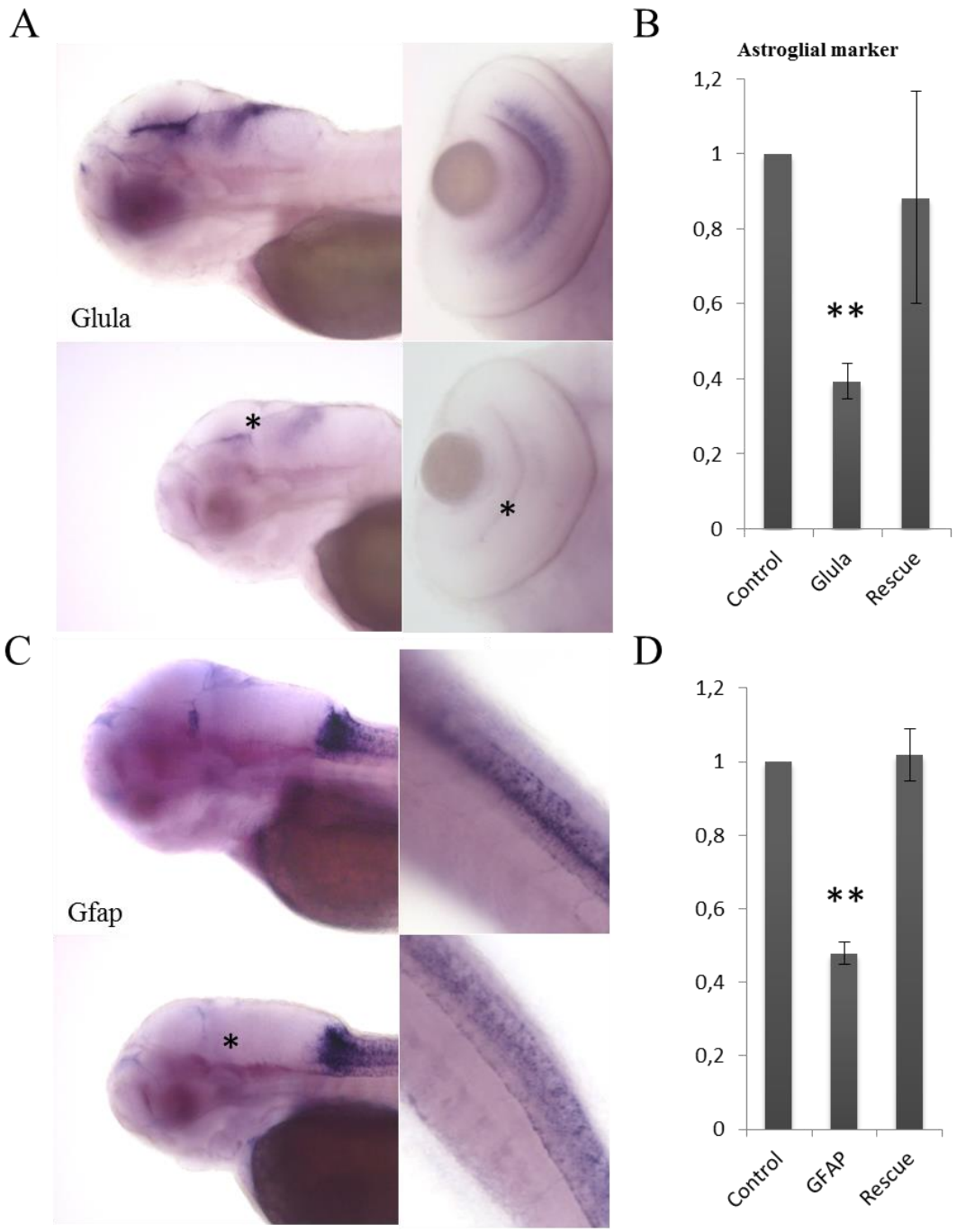

Figure 38. WISH and qRT-PCR of glial markers *glula, gfap* at 3dpf

(A) WISH of glial marker *glula*, expressed in midbrain proliferative region and in dorsal view of eye in inner retinal layer (dorsal view), Qdprb1 knockdown shows depletion of signal in midbrain and loss in inner retinal layer (asterisk) (B) qRT-PCR of *glula* shows highly significant depletion and return to normal levels upon rescue with Qdprb1 mRNA (C) WISH of glial marker *gfap*, expressed in midbrain proliferative region and in dorsal view of spinal cord, Qdprb1 knockdown shows loss of signal in midbrain (asterisk) and no change in spinal cord signal (D) qRT-PCR of *gfap* shows very significant depletion and return to normal levels upon rescue with *qdprb1* mRNA

We also evaluated earlier stages of development in qRT-PCR and found that the expression levels for *glula* and *gfap* were already depleted at 26 hpf. Surprisingly only astroglial cells were affected by the Qdprb1 knockdown. qRT-PCR analysis for the oligodendrocyte specific marker *olig2* showed a significant increase in expression. This indicates that precursors fail to differentiate into astroglia rather than oligodendrocytes.

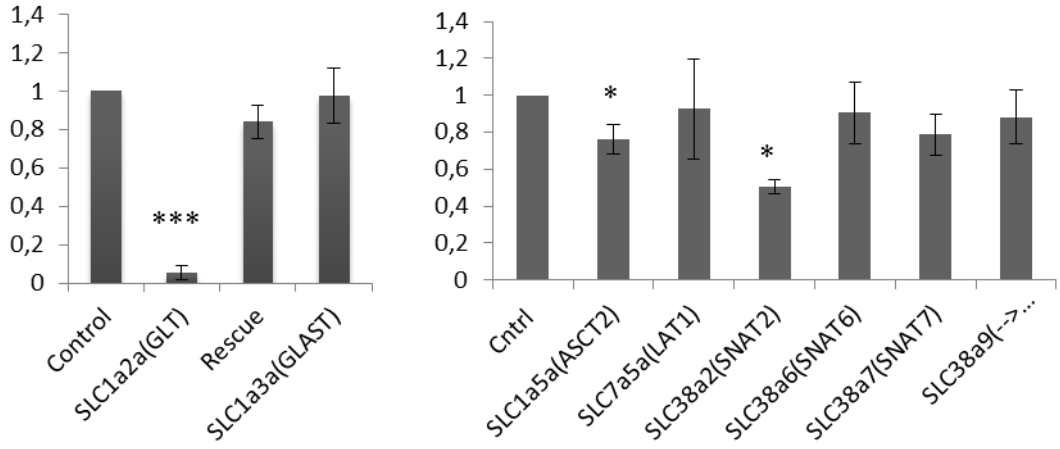

Figure 39. qRT-PCR of amino acid transporters

Relative mRNA expression levels amino acid transporters, (left) significant depletion of *slc1a2a* with rescue to normal levels and *slc1a3a* expression, (right) Relative transporter expression shows significant depletion for *slc1a5a* and *slc38a2*

To find the link between glia and glutamine we screened for alternative amino acid transporters in zebrafish (Fig. 39). We detected that most transporters are uninfluenced by the knockdown, which include *slca7a* (LAT1), the major amino acid transporter and Slc38a9 the activator of mTOR affected by glutamine levels (Lipton and Sahin 2014). The transporters *slc38a2* (SNAT2) and *slc1a5a* (ASCT2), were significantly depleted.

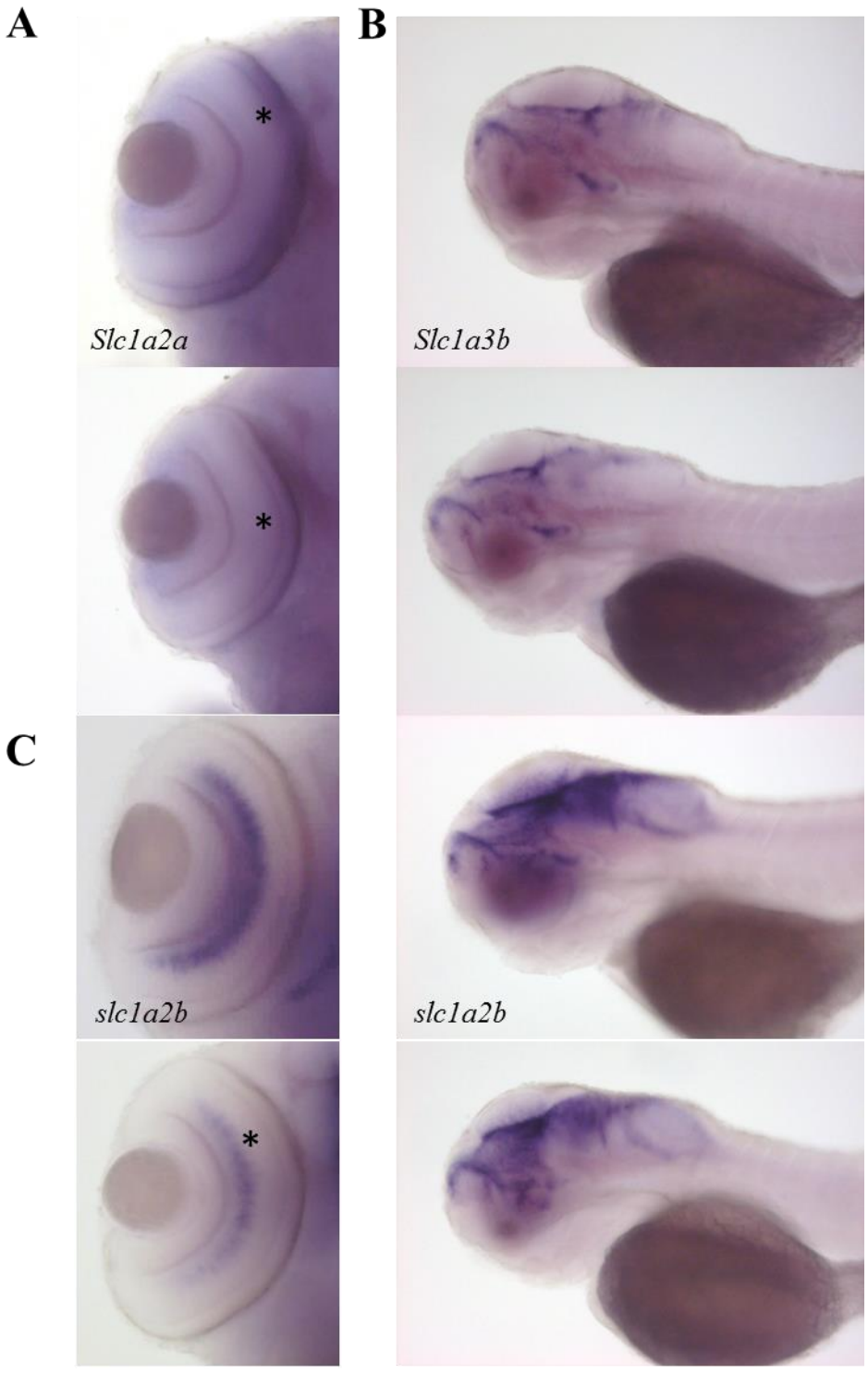

Figure 40. WISH of glutamate transporters *slc1a2a, slc1a2b* and *slc1a3b*

Expression analysis of transporters, (A) (top) wildtype *slc1a2a* expression in ONL and (bottom) loss of *slc1a2a* expression in ONL, (B) (top) wildtype expression in midbrain and hindbrain and (bottom) remaining expression of *slc1a3b* in these region, (C) (top) wildtype expression of *slc1a2b* in midbrain/hindbrain and eye INL, (bottom) depletion of expression in midbrain and strongly reduced in INL (asterisk)

Upon investigation of amino acid transports, most notably the family of glutamate transporters *slc1a2* and *slc1a3* were affected by the knockdown. In qRT-PCR the expression of *slc1a2a* was abolished, while the homolog *slc1a2b* remains stable (Fig. 40). In WISH experiments we detected that *slc1a2a* in the rod and cone rich ONL of the eye was entirely lost, matching the qRT-PCR results (Fig. 40). *slc1a2b* expression was slightly affected in the midbrain, but was depleted in the eye. The marker *slc1a3b* is expressed in multiple brain regions and possible neurons remained stable in WISH experiments. s*lc1a3a* on the other hand is expressed in microglia, which we have previously shown not to be affected by the knockdown (3.7.3).

It is to note that the used nomenclature reverses the letter use of “a” and “b” for each gene *slc1a2* and *slc1a3* annotated in Gesemann et al 2010 vs the NCBI RefSeq database. This result is due to the contradictory nomenclature used in the Genbank used by Gesemann et al. (ID HM138691.1 for *slc1a2a*) and the RefSeq database used in this study (NM_001190305.1 for *slc1a2a*). The naming of *slc1a2a* in Genbank refers to the sequence of *slc1a2b* in the Refseq Database, and vice versa. The same is the case for *slc1a3* (Data accessed 10.9.2017).

With extensive analysis of the glia markers we could show a specific loss of these gene expressions in the midbrain and retina of the developing embryo, spatially linked to *qdprb1*. Although the link between increased glutamine levels and depletion of glia markers remains to be identified.

3.8.2 Qdprb1 – glutamine relation to gliogenesis

In an attempt to determine if the loss of Qdprb1 directly caused increased glutamine which in turn affects gliogenesis, or if altered gliogenesis causes increased glutamine, we tested the effect on embryological development by direct exposure to glutamine. We tested expression levels of markers that were affected by Qdprb1 knockdown, and Qdprb1 itself, by treating embryos with different concentrations (Fig. 41). Chronic exposure at low concentrations of 1mM L-glutamine caused no noticeable morphological effect. Under chronic exposure to extremely high concentration of 20mM L-glutamine we observed global development retardation and a similar phenotype observed in the Qdprb1 knockdown with smaller head and eye size. The analysis of mRNA expression levels revealed that low concentration of L-glutamine had little influence on glia markers. 20mM on the other hand did reveal a similar pattern observed in Qdprb1 knockdown, including that *gfap* (fold change: 0,54 +/- 0,05, ***p<0,001) was significantly reduced and the transporter *slc1a2a* expression was nearly abolished (fold change: 0,27 +/- 0,23, **p=0,003). However, we did not observe any effect on the glutamine synthetase

homologs *glula*, and *glulb*. Surprisingly also *qdprb1*(fold change: 0,65 +/-0,21, **p=0,004) was significantly depleted by the high levels of L-glutamine. Exposure to L-Glutamine to embryos injected with Qdprb1 MO showed a similar phenotype with smaller head and eyes and had no increased severity of the morphological effect. To test if this mRNA level is a direct response to the increase in L-glutamine or a developmental effect we tested acute exposure. Acute exposure starting at 48 hpf development showed normal development and morphology. Furthermore, the acute exposure did not affect mRNA levels of the selected markers. Even though this dataset has to interpreted carefully due to the extremely high concentrations and additional effects on the whole embryo due to the method, it implicates that high glutamine levels can interfere with gliogenesis in the early embryo and that it can deplete not only *qdprb1*, but also the glia marker *gfap*.

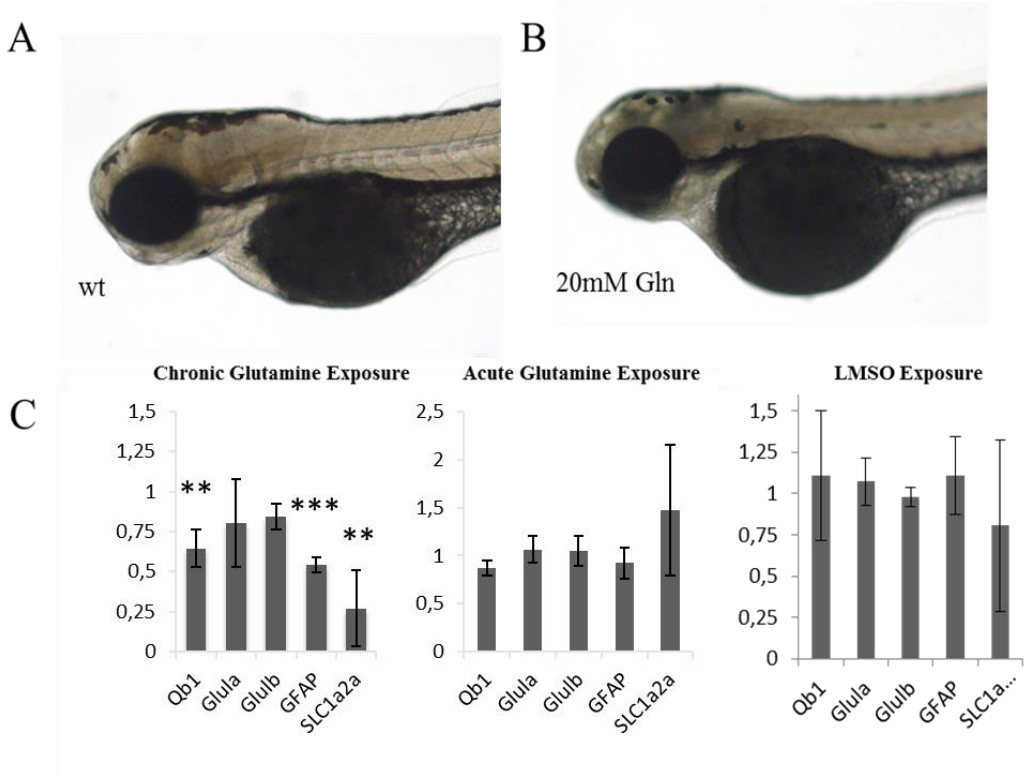

Figure 41. Glutamine exposure morphology and qRT-PCR analysis of chronic glutamine, acute glutamine, LMSO exposure

Exposure experiments and analysis, (A) wildtype morphology at 3 dpf (lateral view), (B) morphology after chronic exposure to 20mM L-glutamine shows smaller head and eye, (C) qRT-PCR analysis of early developmental (chronic) L-glutamine exposure shows relative expression change to control level at 1, with significant depletion in *qdprb1*, *gfap* and *slc1a2a*, as well as no change in *glula* and *glulb*; (middle, right) late developmental (acute) exposure to L-glutamine and *glula* inhibition did not affect relative mRNA levels.

3.8.3 Qdprb1 – glutamate transporter inhibition

To further deduce the chain of events, we inhibited the activity of both the Glul and the Slc1a2 transporter via LMSO and DHKA, respectively (Cox et al., 2016; McKeown et al., 2012). Both inhibitors showed no effect on developmental morphology at the previously published concentrations. We also detected no change in mRNA expression levels. We hypothesized that inhibition of Glula could deplete the glutamine pool and rescue the phenotype. Inhibition in Qdprb1 morphant embryos were not rescued by the inhibitors at any developmental stage. Control experiments with only LMSO did not deplete glutamine levels in wildtypes, therefore efficiency of the inhibitor must be confirmed before concluding these results. Although these results are intriguingly suggesting that Glula inhibition rescues the glutamine accumulation and in turn does not rescue the morphological changes therefore challenging the glutamine exposure experiments, it has to be confirmed by further experiments.

3.9 Patient biochemistry

We next assessed the translatability of the observed effects in zebrafish to the severe phenotype seen in patients. While traditionally patients are diagnosed based on HPA, pterin pattern change and DHPR enzyme activity test, we also looked for the amino acid pattern we observed in zebrafish.

We were able to obtain data from two DHPR deficient patients for amino acids in both plasma and CSF before treatment. Table 14 summarizes the amino acids, with high levels shaded in red and low levels shaded in blue. Patient 1 presents with a very mild HPA and has very mild symptoms. Glutamine levels measured in liquor are normal and so are the BCAA levels, except for reduced valine. Patient 2 presents with HPA detected in plasma and CSF and has a severe phenotype with brain atrophy, dystonia and epilepsy. Patient 2 has normal glutamine in plasma, but has very high glutamine levels in CSF. Contrary to our data in zebrafish the BCAA levels were lower than normal. After treatment with neurotransmitters, folates and a phenylalanine restricted diet, the glutamine levels normalized. We could not observe any glutamine accumulation in other BH_4 deficiency patients (GTPCH and PTS).

The finding of a patient with highly increased glutamine in the CSF of a DHPR patient, suggests that our hypothesis may be connected to the patient's phenotype.

Table 14. Amino acid analysis in plasma and CSF of two DHPR patients before treatment

	Patient 1	Patient 2
Phenylalanine (plasma)	N.A.	861 µmol/l
[normal-range]		[23-75 µmol/l]
Phenylalanine (CSF)	34.0 µmol/l	287.2 µmol/l
[normal-range]	[3.2-14.0µmol/l]	[7.0-12.3 µmol/l]
Glutamine (plasma)	N.A.	499 µmol/l
[normal-range]		[247-900 µmol/l]
Glutamine (CSF)	509.22µmol/l	759.7 µmol/l
[normal-range]	[231.00-765.00 µmol/l]	[373.3-556.3µmol/l]
Valine (CSF)	7.4µmol/l	11.4 µmol/l
[normal-range]	[11.9-29.4 µmol/l]	[14.8-22.5µmol/l]
Leucine (CSF)	10.7 µmol/l	9.9 µmol/l
[normal-range]	[3.5-18.9 µmol/l]	[11.0-18.7µmol/l]
Isoleucine (CSF)	5.2 µmol/l	2.3 µmol/l
[normal-range]	[1.7-8.9 µmol/l]	[14.8-22.5 µmol/l]

3.10 Species conservation

In consideration that we were able to hypothesize a link of qdprb1 to glutamine metabolism, as well as glia development, we analyzed expression data for human, mice and medaka to test possible conservation across species.

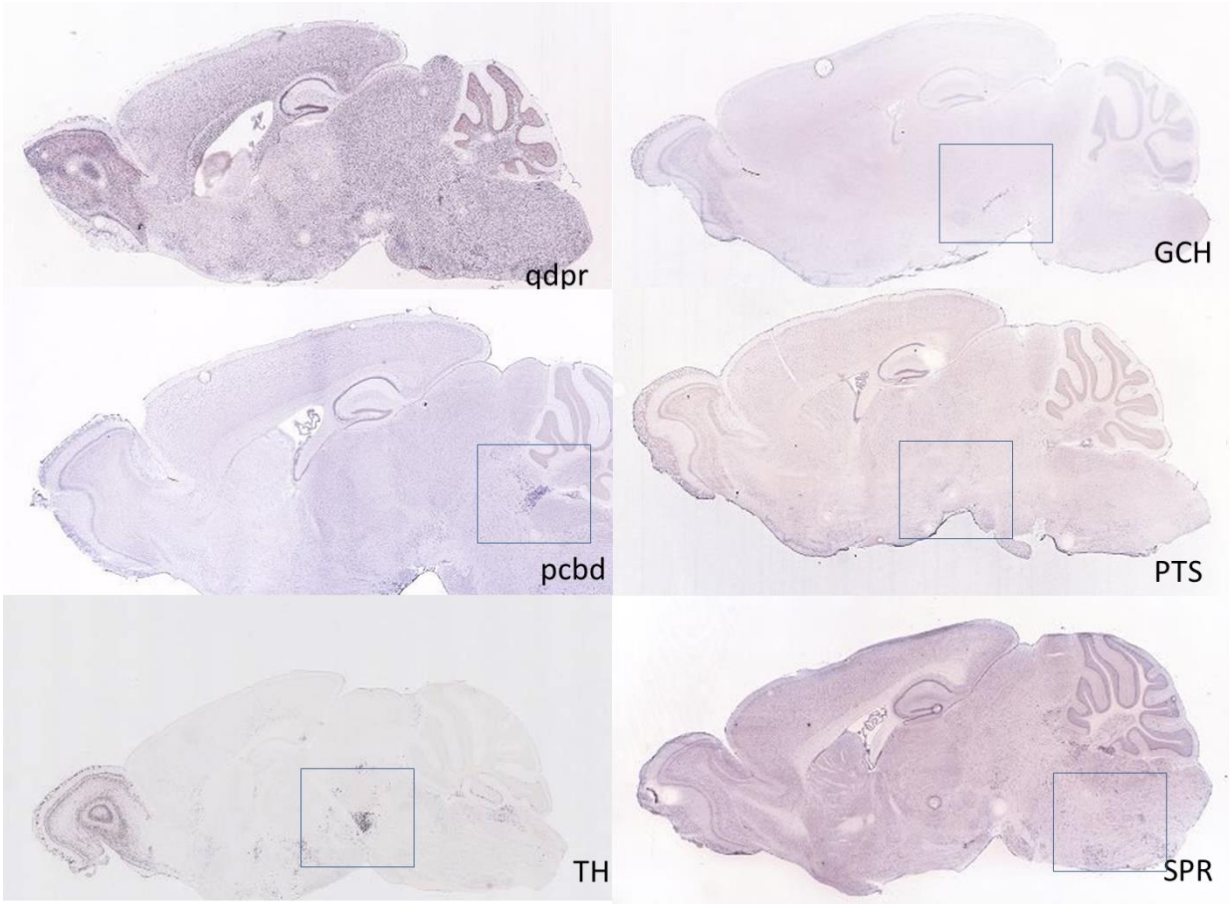

Figure 42. ISH data of BH_4 related genes in the P56 adult mouse brain

Data and images taken from Allen Mouse brain atlas (Lein et al., 2007). ISH of mouse brain (P56) sections for the BH_4 relevant genes, *Gch, pts, spr, qdpr, pcbd and th*. Strongest expressions are marked by blue box and qdpr shows ubiquitous expression

Comparison of expression patterns retrieved from expression databases (Allen Brain Atlas << accessed February 17th, 2017>>; Lein et al., 2007) show a strong overall expression of qdpr throughout the adult mouse brain (Fig. 42). This holds true for human tissue (databases show cerebral cortex and visual cortex). The antibody staining of DHPR in human brain tissue (Protein Atlas << accessed February 17th, 2017>>; Uhlen et al., 2015) shows expression exclusively in glial cells and not neurons. Additionally, RNA-Seq data in the cerebral cortex of adult mice show intense levels of Qdpr in oligodendrocytes and oligodendrocyte precursor (OPC) (Zhang et al., 2014).

Furthermore, when comparing the expression patterns of Qdpr in mouse to the *de novo* pathway and BH_4 dependent enzymes, we observed a lack of overlap in both *in situ* and microarray data (Fig 39). In direct comparison there seemed to be an expression overlap of *Spr* to *Dhfr*, as well as *Gch1* to *Pts* (Lein et al., 2007). There was a lack of overlap to *Qdpr*. In fact, *Dhfr* and *Qdpr* hardly overlap at all.

While the genes are distinctly expressed and confined to specific brain regions in ISH analysis, *qdpr* expression is not confined to a region. Although present in every region, qdpr is not expressed in every cell. The stained cells we can assume to be glial cells, as shown by Protein atlas (Uhlen et al., 2015). The lack of overlap is constant for the dopaminergic marker *Th*, serotonergic marker *Tph* and NOS marker *nNOS1*.

As expected, the database for medaka expression (MEPD: Medaka Expression Pattern Database <<accessed February 17th,2017>>), show a conservation of the here identified pattern, with expression on CMZ, proliferative region of hind and midbrain, as well as liver expression. Mouse embryonic *in situ* hybridization also shows expression of *Qdpr* in the ventricular zones of the developing brain (Allen Brain Atlas << accessed February 17th, 2017>>; Lein et al., 2007).

We were able to find indications that qdpr is expressed separately from other BH_4 pathway enzymes and that expression in glia cells rather than dopaminergic neurons is conserved across species.

3.11 RNA Binding of DHPR

To determine the possible mechanisms of DHPR function that involve more than the enzymatic function in BH_4 recycling, we tested the capability of DHPR to bind RNA. A previous screen by Castello et al., 2012, detected DHPR as an RNA binder in Huh7 cells. We first overexpressed FLAG-tagged DHPR of wildtype sequence and of a patient sequence. As control overexpression of p62, a proven RNA binder, was done (Castello et al., 2012). IP of p62 showed a stable band at 62 kDa. IP of DHPR showed a band 26kDA and roughly 55 kDa. Since the samples were crosslinked by UV, which also interlinks protein-protein interaction, we assumed the higher band to be a DHPR dimer. The loading control confirmed the presence of these band before IP in widltypes but not in an overexpression of a patient DHPR (Fig. 43).

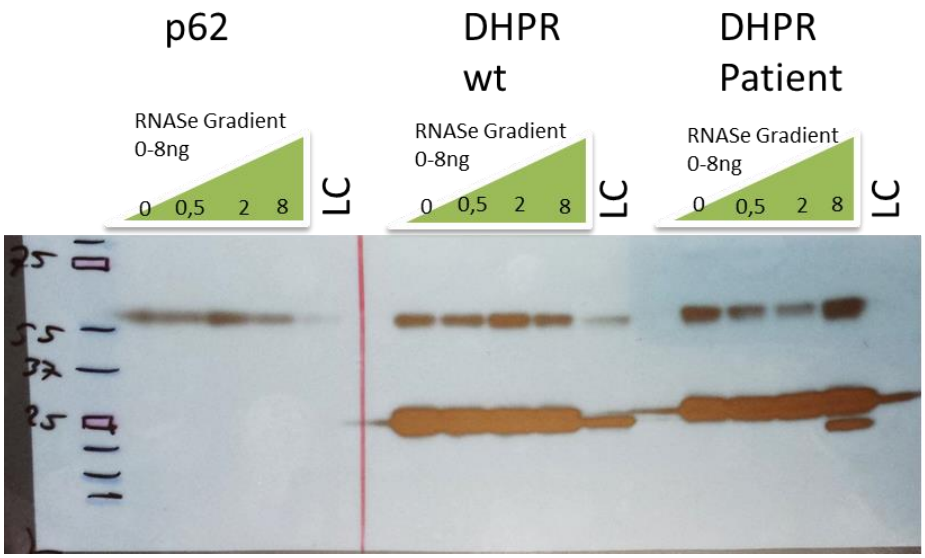

Figure 43. IP of FLAG-tagged p62 and DHPR

FLAG-IP for p62, DHPR wt and DHPR patient transfected Huh7 cells. 2mg/ml sample were loaded into each well. Bands were detected with anti-Flag antibody. p62 shows a band at 62kDa, DHPR show a band at 26kDa and 55kDa. Loading control (LC) are lysates previous to IP. Samples were digested with increasing RNAse concentrations for PNK.

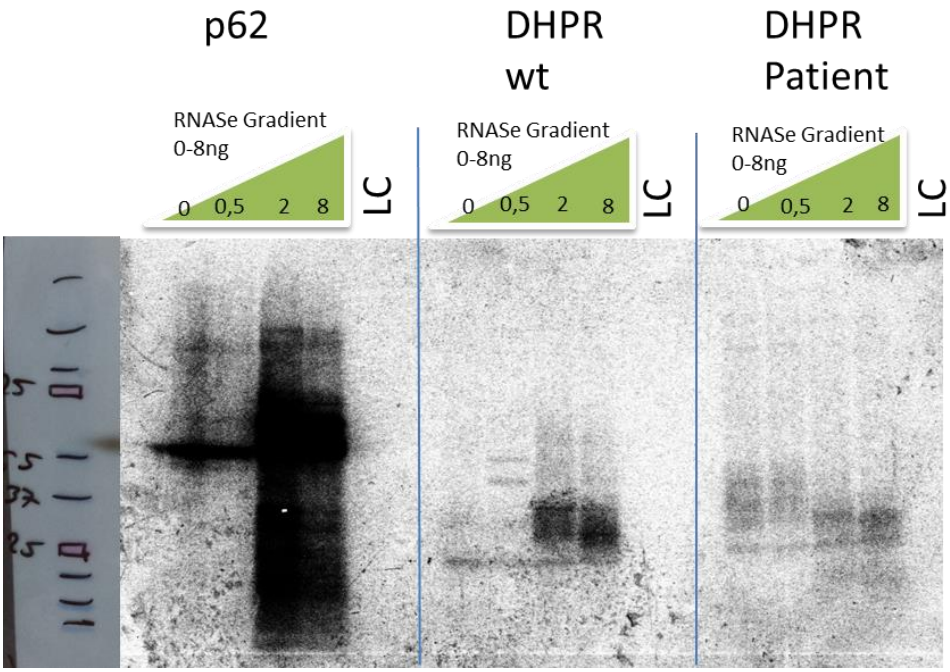

Figure 44. PNK assay of wildtype and patient DHPR

Radioactive western blot shows ladder of blot (left), and radioactive signal of p62, DHPR wt and DHPR patient. Strong signal shown for p62, with increasing intensity related to increasing RNAse. Clear signal for DHPR wt at 26kDA once digested with more than 2 ng RNAse. DHPR patient shows same pattern with reduced intensity. LC are not treated.

PNK assays determine the capability of binding RNA by radioactively labeling the RNA. We used p62 as confirmed RNA binder (Fig. 44). We observe a strong radioactive smear around 62kDA at low RNAse concentrations and a signal along the whole lane once digested with more than 2ng RNAse. For DHPR, we observed a radioactive smear at the size of 26kDa, which becomes more discrete with increased RNAse digest and is more intense for the wildtype than the patient DHPR. This may indicate that the patient DHPR has reduced capability of binding RNA. The RNAs are too bulky to enter the gel and once digested with more than 2ng RNAse are capable to enter the gel and result in the radioactive smear at and above the protein band. The protein band we observe for DHPR is specific as is lost when the protein is knocked down via siRNA, confirming that we detect the correct protein.

Although this is a conclusive result, further experiments such as iCliP (Huppertz et al., 2014) are necessary to determine the bound RNA and its possible function. We concluded from these results that DHPR contains in deed a function that goes beyond its generic enzymatic function and is capable of RNA binding. Even though the role of this function remains unclear in this study it implies an intriguing mechanism for the severe phenotype associated with DHPR deficiency.

4. Discussion

The thesis presents a detailed analysis of the expression pattern as well as, biochemical, genetic and developmental functions of the DHPR homologs in zebrafish. Our findings place the enzyme in a novel pathway for gliogenesis and glutamine household, sheds light on the mechanism underlying gliogenesis and may contribute to a better understanding and future therapeutic approaches for the treatment of human DHPR deficiencies.

4.1 BH_4 pathway in zebrafish

The BH_4 pathway was previously characterized for pigment synthesis in multiple model organisms (Ziegler et al. 2000; Kim et al., 2013; Xu et al., 2013). We identified all homologous members of the pathway in zebrafish, for an overall characterization with focus on the recycling pathway and more specifically the DHPR homologs.

In an RT-PCR screen we could observe the expression of all genes and design expression clusters. A set of *de novo* pathway expression was seen during gastrulation for *gch1*, *ptps* and *spra*. These also cluster after 24 hpf. The second homolog *sprb* was only expressed with onset of neuronal expression at 24 hpf. This is the same pattern observed for *pah* and *th*. *tph* expression was unique and previously described with an arisal of *tph1b* during gastrulation and later in serotonergic neurons, while *tph2* expression is only in late serotonergic neurons. This dataset links an early *de novo* expression to be required during gastrulation while the major hydroxylases are only expressed once the required neurons arise in the embryo after 24 hpf.

In case of the recycling pathway we could show in more specific qRT-PCR screens that *qdpra* and *qdprb1* are expressed upon melanin development and during entire development, respectively. *Qdprb2* was not expressed after gastrulation. Along with this dhfr, was expressed during the entire development, similar to *qdprb1*. One can assume that the expression of *qdprb1* is necessary during development as the later data confirms, and *qdpra* only in pigment and liver expression.

This pattern screen shows that not all BH_4 pathway members are expressed at the same timelines. But we are able to cluster the expression of all *de novo* members and later all members required for dopamine or serotonin production. Overall the pathway homologs are conserved and expressed in the developing embryo as previously shown (Ziegler et al. 2000). The conservation is the basis for the zebrafish as model organism in our study.

4.2 DHPR homology

As zebrafish had a "whole genome duplication" throughout development, many genes are present in multiple versions (Postlethwait et al., 1998). After this time, some genes perform the same function, others have developed unique functions and expression pattern, while yet others are just present as genome duplication leftovers that are without function (Kassahn et al., 2009). It therefore takes careful evaluation to determine the role of a homolog detected in fish.

The high conservation of DHPR throughout species/phyla indicates an important function. While the mouse and rat protein homologs show the highest conservation, the teleost homologs are still highly conserved with around 72%. Qdpra shows conservation of all major domains, while Qdprb1 and Qdprb2 lack the short chain dehydrogenase conserved sequence (PROSITE; Sigrist et al., 2012). This genome duplication along with the variation in sequence conservation and exclusive expression patterns, subsequently led to the rare advantage to study the sub-functionalization of the DHPR homologs in zebrafish.

4.3 Morpholino knockdown approach

MOs have been widely used to phenocopy diseases in zebrafish and frog (Brown et al., 2005; Himmelreich et al., 2015; Santorellio and Zon, 2012). In recent years, morpholinos have become questioned in their specificity and accuracy, since toxicity and off target effects were detected (Eisen et al., 2008). This must be countered by numerous controls and rescue experiments, which were performed in this study. Furthermore, morpholinos are of great advantage for disease model studies that involve reduced protein level and function and no complete loss-of-function or loss-of-protein diseases. In the case for DHPR most patients present with little leftover enzyme function (Arai et al., 1982; Smooker and Cotton, 1995, Zhang et al., 1996). Additionally, in DHPR deficiency, a genotype-phenotype correlation between the severities of phenotype to enzyme activity seems to apparent (Dianzani et al., 1998; Smooker et al., 1999). As complete knockouts may evoke other pathways that may compensate for the lost function, a reduction of Protein level by MOs, may reflect certain diseases more accurately than knockouts (Rossi et al., 2015; El-Brosoly and Stanier 2017). This also offers a possible interpretation for the Qdpr $^{-/-}$ mouse that has a complete loss of protein but no morphological phenotype (Xu et al., 2013). It is unclear if this loss of mRNA and Protein may evoke alternative salvage pathways or just abolish the signaling cascade and the effect that may be observed by reduced levels. Since DHPR patients have such a great variety of phenotypes, which possibly result from differently severe DHPR hypomorphic conditions, the morpholino

approach may be a promising approach to reflect this (Arai et al., 1982; Smooker and Cotton, 1995, Zhang et al., 1996).

4.4 Qdpra function

We collected strong evidences for Qdpra being the homolog connected to BH_4 dependent mechanisms, implying the expected BH_4 recycling function. Firstly, the expression pattern shows *qdpra* in the BH_4 dependent melanophores that require sufficient levels for the activity of Pah and therefore the production of melanin. Other pigments are not BH_4, but *de novo* synthesis dependent and therefore lack Qdpra (Ziegler 2003). The retinal pigment epithelium is also rich in melanophores (Burgoyne et al., 2015). All pterin dependent cells, including melanophores, express *gch2* the second homolog of the pathway initiator (TeSlaa et al., 2013). If Qdpra is reduced there is insufficient BH_4 and less melanin is produced, as observed by the 20% reduction in melanin content. Furthermore, the significantly reduced melanophore size confirms this role. The observed effect is also a symptom in patients, which when untreated, present with lighter hair due to lack of pigments (Blau et al., 2005). This is also the case in classical PKU patients, that lack pigments due to impaired PAH function (Blau et al., 2005). The role for Qdpra is therefore required for the sufficient production of melanin in early melanophores, most likely involving its traditional enzymatic function in BH_4 recycling.

At later stages, at 5 dpf of development, the *qdpra* expression in melanophores is lost, hinting at BH_4 or melanin being sufficient in later developmental stages and that *qdpra* expression is not required in maintenance. This difference of genetic requirement for early pigment development and later maintenance is known for numerous genes (Odenthal et al., 1996).

Secondly, the expression of *qdpra* in the liver, similar to Pah and its activity, which exhibits the same expression pattern. Pah mainly functions in the liver and requires BH_4 as a cofactor (Flydal and Martinez, 2013). The epistatic relation between Qdpra and Pah becomes apparent in the classical PKU amino acid pattern in Qdpra morphant embryos. The increased phenylalanine results due to reduced activity of Pah. The decrease in taurine however, that has also been observed in the knockout mouse (Xu et al., 2013), remains unexplained.

The lack of expression of *qdpra* in dopaminergic or serotonergic neurons suggests no requirement for BH_4 in early neurotransmitter synthesis. There is no overlap with *gch1* and *th*, which are distinctively expressed in dopaminergic neurons (Yamamoto et al., 2010). It remains unclear if the observed effect at 72 hpf arises additionally from the increasing number of liver cells and early liver function of Pah or exclusively from the pigments requiring melanin.

However, as liver activity increases only after 72 hpf (Chu and Sadler, 2009; Tao and Peng, 2009), the hyperphenylalaninemia is expected to become even more intensive during development.

Overall this leads to the conclusion that Qdpra function as BH_4 recycling enzyme for the cofactor supplementation in the production of melanin and Pah activity is conserved in teleosts and restricted to the Qdpra homolog. Yet our data confirms that it does not affect neurotransmitter production in the early developing embryo.

4.5 Qdprb2 function

Qdprb2 has the least homology to human DHPR and is the only homolog we could not link to a function. It has no detectable expression post gastrulation and MO knockdown generated no phenotype. Also WISH showed no expression during development. We therefore excluded Qdprb2 from further analysis. This does however not eliminate that Qdprb2 may function during maternal stages before zygotic expression, where we could detect mRNA levels, or be expressed after some stress event that we were not able to determine.

4.6 Qdprb1 function

Our findings represent a novel, previously unknown function of Qdprb1 in the regulation of glutamine during astrogliogenesis in the developing embryo independent of the BH_4 pathway. Additional preliminary data obtained from DHPR patients, may imply that this Qdprb1 mediated mechanism could be conserved from fish to man.

4.6.1 Qdprb1 function

The *qdprb1* expression pattern we observe does not overlap with the expected BH_4 dependent region of the dopaminergic and serotonergic regions, NOS in microglia and the liver. In fact, the expression of these markers such as *th*, *gch1*, *pah* are entirely unaffected by the knockdown of Qdprb1. Instead we observe the expression in proliferative rich regions of the developing embryo. These include the eye and the proliferative midbrain. While during early development the expression is broad in the regions i.e. the entire eye, it becomes more distinct after 48 hpf localizing to the CMZ and the PTR. In later stages we also observed expression in the inner retinal layer which is rich in Müller-glia cells. The Qdprb1 morphant phenotype becomes first visible at the onset of major neuro- and therewith gliogenesis (Schmidt et al., 2013). At 17 somites we can already observe a smaller midbrain and affected hindbrain. At 30 hpf the midbrain and eye are considerably flattened. This phenotype is restricted to the regions where *qdprb1* is expressed.

A moonlighting function for members of the BH_4 pathway has been previously described. *Gch1* knockout mice are embryonically lethal and cannot be rescued with BH_4 supplementation, while not having a morphological phenotype. This may link Gch1 independent of BH_4 synthesis, to early embryogenesis (Douglas et al. 2015). Similarly the Pts knockout mouse dies after 48 hours post birth (Sumi-Ichinose et al., 2001). The most detailed study was shown for the second recycling enzyme Pcbd, which was identified to play a keyrole as cofactor in the dimerization of hepatic nuclear factor 1 (HNF-1) and was therefore renamed: dimerization cofactor of HNF-1 (DcoH) (Ficner et al. 1995, Lei et al. 1999). Like Qdpra in this study, it was also shown to play a keyrole in early pigmentation in *Xenopus* (Pogge v. Strandmann et al. 2000). It may therefore not be farfetched that yet another member of the BH_4 pathway may have a moonlighting function.

4.6.2 Biochemistry

In the classical diagnostic approach for BH_4 deficiencies we determined the amino acid patterns. Amino acid measurements were intended to detect the hyperphenylalaninemia that is present in BH_4 deficient patients, due to the lower function of Pah, as shown in Qdpra and patients (Blau et al., 2005; Opladen et al., 2012). Unlike in the Qdpra morphants, we did not observe any effect on the BH_4 related amino acids phenylalanine and tyrosine. In fact, other related BH_4 amino acids such as ornithine, arginine, from the NOS and urea cycle respectively, were unaffected. Furthermore, the amino acid taurine, which was depleted in the Qdpr deficient mouse was also unchanged (Xu et al., 2011). The change in taurine may therefore be connected to the BH_4 recycling function seen in mice (Xu et al., 2011) and Qdpra in this study. This is the next piece of evidence that, unlike Qdpra, Qdprb1 may act BH_4 independent.

In Qdprb1 morphants, the amino acid pattern showed a general increase in BCAA. Increased BCAA was already detected in Bcat deficient mice and gliomas, since the breakdown of valine, isoleucine and leucine is inhibited (Tönjes et al., 2013; She et al., 2007). In the Qdprb1 knockdown, the cytosolic *bcat1* is in fact depleted in qRT-PCR and therefore may account for the increased BCAA. Furthermore, since Bcat1 is expressed in gliomas (Tönjes et al., 2013), a tumour arising from glia cells, the depleted *bcat1* expression may be caused by the depleted glia in Qdprb1 morphants. Finally, *bcat1* shows a similar expression pattern at 24 hpf and 3 dpf as *qdprb1*, possibly connecting the two enzymes (Thisse and Thisse, 2004). We could rescue the *bcat1* expression levels with *qdprb1*-mRNA. The second mitochondrial homolog *bcat2* is unaffected and may therefore be not required at these developmental times or expressed in other regions of the embryo.

Most surprisingly is the significant increase in glutamine we detected upon Qdprb1 knockdown. At 3 dpf the glutamine concentrations are doubled in comparison to controls. We compared the morphological phenotype to the glutamine peak by screening the ratio of glutamine/glutamate during development. With the onset of the phenotype at 17 somites the first increase is seen. At 22 hpf the increase is significant and rises continuously until 3 dpf. This occurrence is parallel to the increasing neuro- and gliogenesis in the developing embryo and the collectives of data spatially link the phenotype to the increased glutamine levels.

4.6.3 BH_4 and Qdprb1

The data we obtained does not infer any link between Qdprb1 and the BH_4 pathway. Firstly, our knockdown did not generate a DHPR deficiency typical HPA (Flydal and Martinez et al., 2013). Secondly, *qpdrb1* is not expressed in any BH_4 dependent regions such as the dopaminergic or serotonergic neurons, Liver or melanophores. We also could not link the knockdown to any changes in NOS expression which is mostly present in microglia (Minghetti and Levi, 1998).

Unfortunately, we failed to consistently measure BH_4 and BH_2 via HPLC. Although we could detect peaks at the expected times, there was an overlay of a major peak masking the result. When we treated the embryos with PTU, we were able to remove the covering peak. We therefore deduce the covering peak to be melanin or a compound after the tyrosinase step which is inhibited by PTU (Karlsson et al., 2001). Although this initially solved the readout problem, it induces the problem that PTU indirectly affects the BH_4 pathway. Since it causes increased L-Dopa by blocking tyrosinase activity, it may therefore increase 3-OMD and may backtrack to tyrosine and phenylalanine levels, which in turn affect BH_4 metabolism. Additionally, measurements of pteridines via HPLC identified multiple bands but lacked the direct correlation to the corresponding pteridines, as was previously attempted (Odenthal et al., 1996). These results could have further confirmed the moonlighting of *qdprb1*. Unfortunately, we could not underline our results with the evaluation of BH_4, BH_2, biopterin and neopterin levels in morphants, since the interpretability of these datasets was not ascertained.

In consideration of the proposed hypothesis that the accumulation of BH_2 acts toxic we studied the response of the developing embryo to BH_2 (Opladen et al., 2012). We did not however observe neurotoxicity of high levels of BH_2, nor did we detect any effect on the developing embryo. In zebrafish we therefore excluded BH_2 as pathomechanistic basis for the phenotype. Since we had no neurotoxicity and the uncertainty of pterin measurements, we decided to focus

on further advantages of the zebrafish embryo, including the developmental analysis of neuronal networks.

4.6.4 Proliferation of CMZ and PTR

As we expected Qdprb1 to influence proliferation based on expression and phenotype we looked for pH3 positive cells. In widltypes, at 72 hpf, few cells in the eye remain pH3 positive, of which most are confined to the CMZ. In contrast, we detected a massive increase in pH3 positive cells in Qdprb1 knockdown embryos. These cells were not restricted to the CMZ, with a portion of them in the ONL. As we lose the expression of the glutamate transporter *slc1a2a*, which is present in the ONL (Gesemann et al., 2010), we propose that these cells stuck in mitosis in the ONL are the missing *slc1a2a* positive cells that fail to differentiate. The same pattern of increased mitotic cells is present in the PTR. This is consistent with qdprb1 expression in both proliferative regions and both regions are genetically considered "sister" niches of proliferation (Recher et al., 2013). Along these lines the increase in proliferative markers of the retina and PRT, *myca* and *ccnd1*, as well as unchanged stem cell marker *mz98* of the retina, support the observed results.

The DAPI staining shows a broadening of the CMZ, which may be induced by the misregulation in differentiation. We could rescue the phenotype by co-injection with *qdprb1* mRNA. Since pH3 marks the cells in mitosis we concluded that these cells are slowed down in their cell cycle progression and indicate non- or delayed differentiating cells. This proposes a function for Qdprb1 as cell cycle/differentiation signal.

4.6.5 Neuronal involvement

The transgenic line for differentiated neurons, tg(HuC/D:GFP), showed no loss of signal in the brain and eye. We were however able to detect a microcephaly, which is a symptom of DHPR deficient patients and gives us a possible phenotype correlation to DHPR deficiency patients. Additionally, DHPR patients with severe symptoms do not present with a loss of dopaminergic neurons (Sedel et al. 2006; Furujo et al. 2014), therefore implying a different cell population to be affected. Tg(NBT/lyn:GFP) showed no effect on spinal cord neurons or lateral line neuromasts. Along with neurons we managed to exclude microglia cells from the focus as tg(mpeg:GFP) showed no change in number or localization of these cells. With these neuronal screens we excluded an effect on neurons by the knockdown. Contradictory to the exclusion, we detected a significant depletion of the neuronal differentiation maker *neurod1* (fold change: 0,47, SD +/- 0,12) in primary neurons (Lee et al., 1995; Lee et al., 1997). Neurod1 is believed

to regulate neuronal differentiation by promoting cell cycle exit of neuronal precursors, while inhibiting gliogenesis (Yan et al., 2005). It remains to be determined if this marker is indirectly affected due to the misregulated gliogenesis, since all neuronal networks we tested appear to develop normally. However, since gliogenesis and neurogenesis are tightly linked an overlap of effect appears likely (Lyons and Talbot, 2015).

4.6.6 Astroglia involvement

As neurons were unaffected we screened for the second largest group of cells in the brain. In both qRT-PCR and WISH studies we could show a strong depletion of glial marker *glula* and *gfap,* specifically in the midbrain and eye and not the spinal cord. *Glula* was entirely lost in the eye, therefore suggesting that the mitotic cells that fail to differentiate are *glula* positive cells. Furthermore, these cells arise from the CMZ were *qdprb1* is expressed, therefore Qdprb1 may act as differentiating signal for glial cells. This data goes in concert with the pH3 antibody staining that shows cells failing to differentiate. The same holds true in the midbrain region. Most *glula* positive cells arise from the proliferative midbrain were *qdprb1* is expressed and the signal is almost entirely lost. *Gfap* positive cells in the midbrain are entirely depleted. Since *gfap* remains in the spinal cord, we conclusively located the knockdown effect to these two proliferative regions. The glutamate transporter GLAST (*slc1a3a*) which in mammals is expressed in neurons, is unaffected by the knockdown. On one hand, the EAAT2 homolog *slc1a2a* fully depleted in the ONL, (Gesemann et al. 2010). On the other hand, the *slc1a2b* glutamate transporter (Gesemann et al., 2010), which is mostly in astrocytes, is depleted in the eye but little in the midbrain. Even though *slc1a2b* is used as glia marker, it is not depleted in qRT-PCR levels. This gives a hint at the stage of differentiation. In mammals proliferating precursors that have become restricted to the glia lineage are already EEAT2b/*slc1a2b* positive (Maragakis et al., 2003). Should this apply to the cells we see as pH3 positive and those lacking *glula* and *gfap,* it would account for the comparably high *slc1a2b* expression, but the complete loss of glula. However, the depleted expression in the eye recommends that not all precursor cells have managed to become *slc1a2b* positive.

4.6.7 Glia and the role of glutamine

The similar gene expression pattern seen in Qdprb1 morphants and after exposure to glutamine, suggests the reduced glia marker expression to be followed by glutamine increase in Qdprb1 morphants. Furthermore, it suggests that high glutamine effects the development of glia cells in the zebrafish embryo, by the reduced levels of *glula* and *gfap*, as well as the depletion of *slc1a2a*. The effect of depleted S*lc1a2* mRNA levels has been previously shown in hepatocytes

exposed to high glutamine concentrations (Ferrara et al., 2008). Even though the exposure affects the entire embryo rather than specific cells, it gives an intriguing suggestion that high glutamine concentrations interfere with proper gliogenesis. Additional, more specific experimental approaches, may confirm or improve on the observed results.

Considering the very high concentrations of L-glutamine we must consider toxicity via the "Trojan horse" or hyperammonemia. The "trojan horse" theory hypothesizes that high glutamine results in high ammonia and glutamate in mitochondria and this in turn will act toxic, by interfering with mitochondrial functions due to swelling and increased permeability (Albrecht and Norenberg, 2007; Rao et al., 2003; Zieminska et al., 2000).). In L-glutamine exposed embryos we did observe an increase in NH_3, which is expected by hyperammonemia. This could be accounted for by the high levels of L-glutamine and effect on the whole embryo. Strikingly and importantly we did not observe any increased glutamate or NH_3 in Qdprb1 morphants. Therefore, we have no evidence for ammonia toxification such as in hyperammonemia and likely exclude the "Trojan Horse" theory to be causative for the phenotype. However, as only few specific cells may be exposed to this mitochondrial stress in Qdprb1 morphants, that are not apparent in the amino acid screen of the whole embryo, a possible follow up on mitochondria dysfunction in astroglia may be necessary to fully exclude the "Trojan Horse" theory.

A very recent publication manages to tie Qdpr function to mTor activity. Qdpr overexpression decreased mTOR expression and in turn the mutation of Qdpr function affects mTOR and results in dysregulation of autophagy (Si et al., 2017). Considering this fact, the dysregulation of autophagy and the misexpression of a master regulator of multiple pathways, mTOR, has been linked to neurological disorders including epilepsy and Parkinson's (Litpon and Sahini 2014). Furthermore, mTOR is highly regulated by amino acids including glutamine (Altman et al., 2016). Although we did not observe expression change in the transporters *lat1* and *slc38a9*, which are linked to mTOR, the increased glutamine may still affect the amino acid homeostasis and deregulate mTOR. We did observe reduction in the transporter levels of SNAT2 and ASCT1. This however has been shown already in intestinal epithelial cells exposed to high glutamine (Li et al. 2015). It remains therefore unclear how the knockdown regulates the glutamine levels. It may be a direct effect of the enzymatic activity of Glul.

Considering the role of mTOR could be an opening focus of future studies. Along with the amino acid homeostasis we also observed an increase in BCAA and depletion of *bcat1*. Proper

expression of *bcat1* is required for regulated proliferation to produce the molecules required for cell division (Tönjes et al., 2016). Since BCAT1 has previously been connected to mTOR (Zhang and Han, 2017), the lack of *bcat1* in zebrafish may inhibit the dividing cells during mitosis and play a significant role in the observed phenotype.

4.7 *Glula* vs Glutamine peak

One of the unknown mechanistic results in this study remains the link between the glutamine synthetase and the highly significant increase in glutamine. If we consider *glula* exclusively as a glia marker in the midbrain and eye the results can be implied as previously discussed. It remains, however, the question how reduced *glula* levels link to the increased glutamine in the whole embryo, considering Glul is the major source of glutamine and main protection against excitotoxicity of glutamate and ammonia (Suárez et al., 2002).

There are multiple considerations for this cause, which include overactivity of the enzyme, activity of the secondary homolog, failure to remove glutamine and an alternative pathway. In one scenario it may be that Qdprb1 is involved in activity of Glula and therefore on protein level induces production of glutamine. This can still be the case even when mRNA levels are reduced, possibly as compensatory effect. Another option is an activity of the secondary homolog Glulb, which is unchanged in qRT-PCR. Yet it is expressed in the periphery and may therefore be unlikely. Nonetheless, another option involves the fact that early glia precursors, that do express *glula*, produce glutamine at a high rate but fail to remove these high levels from the cell or break them down within it. This could account for low levels of *glula* and high levels of glutamine and may be most likely. We did screen for glutamate transporters of the *slc1a2* family and have shown a severe effect of *slc1a2a*, but not *slc1a2b*. Yet glutamine related transporters *snat2* and *asct1* have been significantly downregulated in the embryo and may leave early glia progenitors with high glutamine content.

Finally, there could be an alternative glutamine pathway that is involved in early embryogenesis that has not yet been shown. Since we have no evidence at this point, the mechanistic basis for this effect needs to be further unraveled in future studies. To this point the data however shows a temporal correlation between increasing glutamine and the onset of the phenotype, as well as intriguingly similar consequences of Qdprb1 knockdown and glutamine exposure.

4.8 Conservation in teleosts and mammals

Along with the roles determined for the Qdpr homologs in zebrafish, we were interested in the conservation of this glia specific role, using the databases for medaka, mice and human. During embryological development in teleosts, we see that medaka have conserved expression of *qdpra* in the proliferative regions of eye and midbrain (Medaka Database; Alonso-Barba et al., 2015). Also, mice show expression during E13, in proliferative regions of the midbrain (Allen mouse brain Atlas, Lein et al., 2007). In adult stages we see expression only in glia cells and expressed all over the adult brain. There is no clear localization to dopaminergic or serotonergic neurons as we see for other members of the BH_4 pathway. Additionally, RNA-Seq shows highest expression in glia cells (Zhang et al., 2014). Also in adult humans, the expression localizes to glia cells and not neurons (Protein Atlas; Uhlen et al., 2015).

This set of data connects DHPR strongly to a role in glial cells. If recycling were the key function, one would expect high levels of Qdpr to be found in BH_4 dependent neurons. While shuttling of BH_4/BH_2 between neurons and glia is unknown, we therefore propose a glia specific role for the glutamine household. Furthermore, the lack of BH_2 toxicity which was previously proposed (Opladen et al., 2012) could not be confirmed by our study in zebrafish and could be confirmed in human cells in future studies.

4.9 RNA binding

One mechanistic target for the function we determined may be the RNA binding capability of DHPR. Our study is the first to show that DHPR does in fact bind RNA in a close focus study and not in a large-scale screen as done by Castello et al., 2012. We analyzed both DHPR in its wildtype sequence and a patient mutation. The PNK assay showed that FLAG-DHPR transfected cells have the capability of RNA binding in Huh7 cells. Patients showed a lesser binding efficiency to RNA. Yet both are had very low efficiency than compared to the p62 control. This links DHPR as a weak RNA binder. In more recent experiments we could detect RNA binding of endogenous DHPR in an IP. In this case, radioactivity was much more intense, showing a more sensitive and specific detection mode than transfection based. Finally, the band at 25 kDa was knocked down with siRNA, showing that we are pulling down DHPR protein. As this confirms that DHPR binds RNA and patients may be affected by mutations one needs to continue experiments to determine which RNA is bound and which function is correlated with it. Additionally, we need to perform RNA binding experiments in cells that are more representative for the phenotype we observed. This data may provide the mechanistic basis for the severe phenotype and iPSC cells may be of great profit for this study in the future.

4.10 Translation

Considering the conservation of expression in glia cells, apart from dopaminergic and serotonergic neurons, as well as RNA binding capability, implies a moonlighting function of Qdpr in the metabolism of glia cells. The results we obtained may be translatable to the patient's phenotype. We detected an increase in the CSF of a severe DHPR patient with brain atrophy, dystonia and epilepsies. Matching we did not detect any increase in glutamine in the plasma of the patient. After treatment with neurotransmitter precursors and folates the glutamine peak depleted. This may have multiple reasons. First, the role of DHPR involves multiple pathways and secondly the next sample was measured after 2 years of age, in which the glutamine peak may already disappear due to advanced development. A link between improved development and treatment due to normalized glutamine may be proposed. Since we detect the glutamine peak during early gliogenesis in the embryo, it was fortunate to detect a change in the newborn patient. Furthermore, the glutamine peak may have a connection to the severity of symptoms, since a patient with mild DHPR phenotype i.e. no brain atrophy and only light dystonia in the hands, showed no increase in glutamine in the CSF. This however requires a larger cohort study. Considering the wide appearance of the phenotype, varying from extremely mild to extremely severe, as shown by genotype-phenotype correlation (de Sanctis et al., 2000), glutamine may be a focus in future studies as a potential biomarker.

If we attempt to translate our data to the patient, then we have to conclude that DHPR in human involves multiple roles and pathways. As we know DHPR affects BH_4 recycling, therefore affecting the activity of Pah and creating a hyperphenylalaninemia. This in turn affects the production neurotransmitters dopamine and serotonin (Blau et al., 2005). Furthermore, we know that DHPR affects the folate pathway in link to DHFR (Xu et al., 2013). Finally, we know that patients, even with severe phenotype, have no loss in dopaminergic neurons (Sedel et al. 2006; Furujo et al. 2014). We were able to show that the homolog Qdprb1 rapidly increases glutamine levels in the developing zebrafish embryo. This in turn affects the glia development in the midbrain and eye. In adult mice and adult humans, databases show that DHPR is expressed majorly in glia cells, which may indicate that the major role of DHPR lies within glia cells and not BH_4 related neurons.

Since many disorders that somewhat resemble DHPR deficiency, such as Parkinson's disease (Sofroniew et al., 2010) and Alexander's disease (*Orphanet* <<accessed 20.10.2017>>; Brenner et al., 2001), are caused by glia cell deficits or loss, we can link that the severe phenotype to a glia cell defect, more precisely to the lack of differentiation caused by high glutamine levels.

We were able to detect these high glutamine levels and brain atrophy in a DHPR patient. Targeting astrocytes has become a promising treatment option (Finsterwald et al., 2015) and future research may shift a focus on the astrocyte role in DHPR deficiency.

5. Future research

Our work is the first to show a novel function for Qdprb1 in zebrafish, which in the light of our patient studies may well hold true to function also in humans. We anticipate that the results we obtained help substantially to better understand the pathophysiology of DHPR. With the recent and rapid advances in Parkinson's and degenerative disorder and their focus on glia cells, DHPR studies will benefit greatly from it (Sofroniew et al., 2010). Induced pluripotent stem cells from patients that can be differentiated into neurons and glia cells, can be the basis for future studies in the role of DHPR. Possible focus on glia differentiation and the role of glutamine should be of great importance. Comparing our zebrafish findings with the data from the knockout mouse may help unravel, why the mouse does not develop a severe phenotype and in turn help developing therapeutic treatments for DHPR patients. Uncovering the glutamine development in severe and mild patient may help to diagnose severity of the phenotype. Further studies on the RNA binding capacity of DHPR will help understand the multiple functions of this enzyme. Finally, future studies focusing on the early development of glia cells in patients will fully unravel the pathophysiology of DHPR deficiency.

6. Conclusion

This thesis is the first detailed scientific study analyzing roles and functions of all zebrafish DHPR homologs Qdpra, Qdprb1 and Qdprb2. It is first to propose and support a novel function for the enzyme Qdpr, by showing a morphological, neurological and embryological phenotype in the zebrafish model organism.

Our data confirms Qdpra as the major BH_4 recycling enzyme in early melanophores and later liver cells in direct link to the BH_4 dependent enzyme Pah.

Qdprb2 appears not to play a major role during embryonic development and lacks expression after maternal expression.

Qdprb1 was identified with a previously unknown function, by regulating the glutamine household in astroglial cells of the developing eye and midbrain. Increased levels of glutamine altered proper gliogenesis, affecting glia specific markers *gfap*, *glula* and *slc1a2a*. The majority of glia precursors fails to exit mitosis in time and to differentiate into *glula* positive cells.

Additional to the zebrafish characterization, RNA binding studies imply a novel mechanism of DHPR and furthermore, analysis of a severe young DHPR patient with brain atrophy and epilepsy identified elevated levels of glutamine. This finding intriguingly connects our study to the severe patient phenotype and may therefore be an excellent entry point for the unraveling of the pathophysiology of human DHPR deficiency.

7. References

Albrecht, J. and Norenberg, M. D. (2006), Glutamine: A Trojan horse in ammonia neurotoxicity. Hepatology, 44: 788–794. doi:10.1002/hep.21357

Aldiri I, Moore KB, Hutcheson DA, Zhang J, Vetter ML. (2013), "Polycomb repressive complex PRC2 regulates Xenopus retina development downstream of Wnt/β-catenin signaling" Development 140: 2867-2878; doi: 10.1242/dev.088096

Alenina N, Bashammakh S, Bader M, (2006), "Specification and differentiation of serotonergic neurons" Stem Cell Reviews March, Volume 2, Issue 1, pp 5–10

Allen Mouse Brain Atlas: Lein, E.S. et al. (2007), Genome-wide atlas of gene expression in the adult mouse brain, Nature 445: 168-176. doi: 10.1038/nature05453; Available from: brain-map.org/api/index.html <<accessed 23.8.2017>>

Altman BJ, Stine ZE, Dang CV (2016), "From Krebs to clinic: glutamine metabolism to cancer therapy" Nature Reviews Cancer 16, 619–634 doi:10.1038/nrc.2016.71 Published online 29 July 2016

Altschul, S.F., Gish, W., Miller, W., Myers, E.W. & Lipman, D.J. (1990) "Basic local alignment search tool." J. Mol. Biol. 215:403-410.

Alunni, A., Hermel, J.-M., Heuzé, A., Bourrat, F., Jamen, F. and Joly, J.-S. (2010), Evidence for neural stem cells in the medaka optic tectum proliferation zones. Devel Neurobio, 70: 693–713

Arai N, Narisawa K, Hayakawa H, Tada K. (1982) Hyperphenylalaninemia due to dihydropteridine reductase deficiency: diagnosis by enzyme assays on dried blood spots. Pediatrics. Sep;70(3):426-30.

Avanesov, A., & Malicki, J. (2010). Analysis of the Retina in the Zebrafish Model. Methods in Cell Biology, 100, 153–204. http://doi.org/10.1016/B978-0-12-384892-5.00006-2

Bacci, A., Verderio, C., Pravettoni, E., & Matteoli, M. (1999). The role of glial cells in synaptic function. Philosophical Transactions of the Royal Society B: Biological Sciences, 354(1381), 403–409.

Barresi MJF, Burton S, DiPietrantonio K, Amsterdam A, Hopkins N, Karlstrom RO. (2010) Essential genes for astroglial development and axon pathfinding during zebrafish embryogenesis. Developmental dynamics : an official publication of the American Association of Anatomists. 239(10):2603-2618. doi:10.1002/dvdy.22393.

Beckmann BM, Horos R, Fischer B, et al. The RNA-binding proteomes from yeast to man harbour conserved enigmRBPs. (2015) Nature Communications. 6:10127. doi:10.1038/ncomms10127.

Bendall JK, Douglas G, McNeill E, Channon KM, Crabtree MJ. (2014) Tetrahydrobiopterin in Cardiovascular Health and Disease. Antioxidants & Redox Signaling. 20(18):3040-3077. doi:10.1089/ars.2013.5566.

7. References

Beretta, C.A., Dross, N., Guglielmi, L., Bankhead, P., Soulika, M., Gutierrez-Triana, J.A., Paolini, A., Poggi, L., Falk, J., Ryu, S., Kapsimali, M., Engel, U., Carl, M. (2017) Early commissural diencephalic neurons control habenular axon extension and targeting. Current Biology; 27:270-78.

Bernardos RL, Barthel LK, Meyers JR,Raymond PA, (2007) "Late-Stage Neuronal Progenitors in the Retina Are Radial Müller Glia That Function as Retinal Stem Cells", Journal of Neuroscience 27 June, 27 (26) 7028-7040; DOI: 10.1523/JNEUROSCI.1624-07.2007

Bernegger C, Blau N, (2002) "High frequency of tetrahydrobiopterin-responsiveness among hyperphenylalaninemias: a study of 1919 patients observed from 1988 to 2002", Molecular Genetics and Metabolism, Volume 77, Issue 4, December, Pages 304-313

Bickel H, Gerrard JW, Hickmans EM, (1953) "Influence of phenylalanine intake on phenylketonuria" Lancet, 2, pp. 812-819

BioPKU database (www.biopku.org) <<accessed 23.8.2017>>

Blau N, Bonafe L, Thöny B. (2001)a. Tetrahydrobiopterin deficiencies without hyperphenylalaninemia: Diagnosis and genetics of Dopa-responsive dystonia and sepiapterin reductase deficiency. Mol Genet Metab 74:172–185

Blau N, Heizmann CW, Sperl W, Korenke GC, Hoffmann GF, Smooker PM, Cotton RGH, (1992) "Atypical (Mild) Forms of Dihydropteridine Reductase Deficiency: Neurochemical Evaluation and Mutation Detection", Pediatric Research 32, 726–730; doi:10.1203/00006450-199212000-00021

Blau N, Hennermann JB, Langenbeck U, Lichter-Konecki U, (2011) "Diagnosis, classification, and genetics of phenylketonuria and tetrahydrobiopterin (BH4) deficiencies." Mol Genet Metab. 104 Suppl:S2-9. doi: 10.1016/j.ymgme.2011.08.017.

Blau N, Shen N, Carducci C. (2014). Molecular genetics and diagnosis of phenylketonuria: state of the art. Expert Rev Mol Diagn 14:655–671.

Blau N, Thöny B, Cotton RGH, Hyland K. (2001). Disorders of tetrahydrobiopterin and related biogenic amines. In: Scriver CR, Beaudet AL, Sly WS, Valle D, Childs B, Vogelstein B, editors. The metabolic and molecular bases of inherited disease. New York: McGraw-Hill. pp 1725–1776

Blau N., (2006), "Nomenclature and laboratory diagnostics of tetrahydrobiopterin deficiencies". In Blau N (ed.). PKU and BH4: Advances in phenylketonuria and tetrahydrobiopterin. Heilbronn: SPS Verlagsgesellschaft: pp. 555-567

Blau, N. (2016), Genetics of Phenylketonuria: Then and Now. Human Mutation, 37: 508–515. doi:10.1002/humu.22980

Braasch I, Schartl M, Volff JN (2007), "Evolution of pigment synthesis pathways by gene and genome duplication in fish" BMC E Vol. 2007, BMC Evolutionary Biology, 7:74 doi:10.1186/1471-2148-7-74

7. References

Brand M, Heisenberg CP, Jiang YJ, Beuchle D, Lun K, Furutani-Seiki M, Granato M, Haffter P, Hammerschmidt M, Kane DA, Kelsh RN, Mullins MC, Odenthal J, van Eeden FJ, Nusslein-Volhard C. (1996). Mutations in zebrafish genes affecting the formation of the boundary between midbrain and hindbrain. Development 123: 179–190.

Brenner M, Johnson AB, Boespflug-Tanguy O, Rodriguez D, Goldman JE, Messing A, (2001), "Mutations in GFAP, encoding glial fibrillary acidic protein, are associated with Alexander disease" Nature Genetics 27, 117 - 120 doi:10.1038/83679

Bringmann, A., Grosche, A., Pannicke, T., & Reichenbach, A. (2013). GABA and Glutamate Uptake and Metabolism in Retinal Glial (Müller) Cells. Frontiers in Endocrinology, 4, 48. http://doi.org/10.3389/fendo.2013.00048

Brown, D. D., Martz, S. N., Binder, O., Goetz, S. C., Price, B. M. J., Smith, J. C., & Conlon, F. L. (2005). Tbx5 and Tbx20 act synergistically to control vertebrate heart morphogenesis. Development (Cambridge, England), 132(3), 553–563. http://doi.org/10.1242/dev.01596

Burgoyne T, O'Connor MN, Seabra MC, Cutler DF, Futter CE (2015), Regulation of melanosome number, shape and movement in the zebrafish retinal pigment epithelium by OA1 and PMEL J Cell Sci 128: 1400-1407; doi: 10.1242/jcs.164400

Burlina A, Blau N. (2014). Tetrahydrobiopterin disorders presenting with hyperphenylalaninemia. In: Hoffmann FG, Blau N, editors. Congenital neurotransmitter disorders: a clinical approach. Hauppauge, NY: Nova Publishers Inc

Cajal S.R. (1899). Textura del sistema nervioso del hombre y de los vertebrados. Imprenta y Librería de Nicolás Moya, Madrid. Volume I, pages 80-95, 106-110.

Camp KM, Parisi MA, Acosta PB, Berry GT, Bilder DA, Blau N, Bodamer OA, Brosco JP, et al., (2014) "Phenylketonuria Scientific Review Conference: State of the science and future research needs", Molecular Genetics and Metabolism, Volume 112, Issue 2, Pages 87-122, ISSN 1096-7192, https://doi.org/10.1016/j.ymgme.2014.02.013.

Castello A, Fischer B, Eichelbaum K, Horos R,. Beckmann BM, Strein C, Davey NE, Humphreys DT, Preiss T, Steinmetz LM, Krijgsveld J, Hentze MW, (2012), Insights into RNA Biology from an Atlas of Mammalian mRNA-Binding Proteins, Cell, Volume 149, Issue 6, Pages 1393-1406, ISSN 0092-8674, http://dx.doi.org/10.1016/j.cell.2012.04.031.

Castello A, Fischer B, Frese CK, et al. (2016), Comprehensive Identification of RNA-Binding Domains in Human Cells. Molecular Cell. 63(4):696-710. doi:10.1016/j.molcel.2016.06.029.

Castello A, Horos R, Strein C, Fischer B, Eichelbaum K, Steinmetz LM, Krijgsveld J, Hentze MW. (2013), „System-wide identification of RNA-binding proteins by interactome capture." Nat Protoc. 8(3):491-500. doi: 10.1038/nprot.2013.020. Epub 2013 Feb 14.

Cepero Malo M, Duchemin A-L, Guglielmi L, et al. (2017), The Zebrafish Anillin-eGFP Reporter Marks Late Dividing Retinal Precursors and Stem Cells Entering Neuronal Lineages. Hitchcock PF, ed. PLoS ONE. 12(1):e0170356. doi:10.1371/journal.pone.0170356.

7. References

Cerveny KL, Cavodeassi F, Turner KJ, de Jong-Curtain TA, Heath JK, Wilson SW. (2010), The zebrafish flotte lotte mutant reveals that the local retinal environment promotes the differentiation of proliferating precursors emerging from their stem cell niche. Development (Cambridge, England). 137(13):2107-2115. doi:10.1242/dev.047753.

Chinta SJ, Andersen JK, (2005), "Dopaminergic neurons", The International Journal of Biochemistry & Cell Biology, Volume 37, Issue 5, Pages 942-946, ISSN 1357-2725, http://dx.doi.org/10.1016/j.biocel.2004.09.009.

Choi DW, Glutamate neurotoxicity and diseases of the nervous system, (1988), Neuron, Volume 1, Issue 8, Pages 623-634, ISSN 0896-6273, http://dx.doi.org/10.1016/0896-6273(88)90162-6.

Chow RL, Lang RA. (2001), Early eye development in vertebrates. Annu Rev Cell Dev Biol. 17:255-96.

Committee on Standardized Genetic Nomenclature for Mice. (1963). A revision of the standardized genetic nomenclature for mice. J. Hered. 54:159-162.

Coughlin CR, Hyland K, Randall R, Ficicioglu C., (2013), "Dihydropteridine reductase deficiency and treatment with tetrahydrobiopterin: a case report" JIMD Rep.10:53-6. doi: 10.1007/8904_2012_202.

Cox, A.G., Hwang, K.L., Brown, K.K., Evason, K.J., Beltz, S., Tsomides, A., O'Connor, K., Galli, G.G., Yimlamai, D., Chhangawala, S., Yuan, M., Lien, E.C., Wucherpfennig, J., Nissim, S., Minami, A., Cohen, D.E., Camargo, F.D., Asara, J.M., Houvras, Y., Stainier, D.Y., Goessling, W. (2016) Yap reprograms glutamine metabolism to increase nucleotide biosynthesis and enable liver growth. Nature Cell Biology. 18(8):886-96.

Chu, J., & Sadler, K. C. (2009). A New School in Liver Development: Lessons from Zebrafish. Hepatology (Baltimore, Md.), 50(5), 1656–1663. http://doi.org/10.1002/hep.23157

Das, G., Choi, Y., Sicinski, P., & Levine, E. M. (2009). Cyclin D1 fine-tunes the neurogenic output of embryonic retinal progenitor cells. Neural Development, 4, 15. http://doi.org/10.1186/1749-8104-4-15

Dianzani I, de Sanctis L, Smooker PM, Gough TJ, Alliaudi C, Brusco A, Spada M, Blau N, Dobos M, Zhang HP, Yang N, Ponzone A, Armarego WL, Cotton RG. (1998), "Dihydropteridine reductase deficiency: physical structure of the QDPR gene, identification of two new mutations and genotype-phenotype correlations." Hum Mutat.12(4):267-73.

Don EK, Formella I, Badrock AP, Hall TE, Morsch M, Hortle E, Hogan A, Chow S, Gwee SS, Stoddart JJ, Nicholson G, Chung R, Cole NJ. (2017), "A Tol2 Gateway-Compatible Toolbox for the Study of the Nervous System and Neurodegenerative Disease." Zebrafish. Feb;14(1):69-72. doi: 10.1089/zeb.2016.1321. Epub 2016 Sep 15.

Doudna JA, Charpentier E, (2014) "The new frontier of genome engineering with CRISPR-Cas9" Science28 Nov

7. References

Dyer MA, Cepko CL (2001), Regulating proliferation during retinal development. Nat Rev Neurosci. May;2(5):333-42.

Douglas G, Hale AB, Crabtree MJ, Ryan BJ, Hansler A, Watschinger K, Gross SS, Lygate CA, Alp NJ, Channon KM. (2015), A requirement for Gch1 and tetrahydrobiopterin in embryonic development. Developmental Biology. 399(1):129-138. doi:10.1016/j.ydbio.2014.12.025.

Eisen JS, Smith JC (2008), "Controlling morpholino experiments: don't stop making antisense" Development 135: 1735-1743; doi: 10.1242/dev.001115

El-Brolosy MA, Stainier DYR (2017), Genetic compensation: A phenomenon in search of mechanisms. PLoS Genet. Jul 13;13(7):e1006780. doi: 10.1371/journal.pgen.1006780.

Feng Xu, Yusuke Sudo, Sho Sanechika, Junpei Yamashita, Sho Shimaguchi, Shun-ichiro Honda, Chiho Sumi-Ichinose, Masayo Mori-Kojima, Rieko Nakata, Tadaomi Furuta, Minoru Sakurai, Masahiro Sugimoto, Tomoyoshi Soga, Kazunao Kondo, Hiroshi Ichinose (2014), "Disturbed biopterin and folate metabolism in the Qdpr-deficient mouse", FEBS Letters, 588 (21), 3 Nov, 3924–3931

Ferrara CT, Wang P, Neto EC, Stevens RD, Bain JR, et al. (2008) Genetic Networks of Liver Metabolism Revealed by Integration of Metabolic and Transcriptional Profiling. PLOS Genetics 4(3): e1000034. https://doi.org/10.1371/journal.pgen.1000034

Ficner R, Sauer UH, Stier G, Suck D., (1995), "Three-dimensional structure of the bifunctional protein PCD/DCoH, a cytoplasmic enzyme interacting with transcription factor HNF1." EMBO J. May 1;14(9):2034-42.

Ficner R, Sauer UH, Stier G, Suck D., (1995), "Three-dimensional structure of the bifunctional protein PCD/DCoH, a cytoplasmic enzyme interacting with transcription factor HNF1." EMBO J. May 1;14(9):2034-42.

Filippi, A., Mahler, J., Schweitzer, J., & Driever, W. (2010). Expression of the paralogous tyrosine hydroxylase encoding genes th1 and th2 reveals the full complement of dopaminergic and noradrenergic neurons in zebrafish larval and juvenile brain. The Journal of Comparative Neurology, 518(4), 423–438. http://doi.org/10.1002/cne.22213

Finsterwald C, Magistretti PJ, Lengacher S, (2015), Astrocytes: New Targets for the Treatment of Neurodegenerative Diseases. Curr Pharm Des ;21(25):3570-81

Flydal, M. I. and Martinez, A. (2013), Phenylalanine hydroxylase: Function, structure, and regulation. IUBMB Life, 65: 341–349. doi:10.1002/iub.1150

Fölling A., (1934), „Über Ausscheidung von Phenylbrenztraubensäure in den Harn als Stoffwechselanomalie in Verbindung mit Inbicillität" Ztschr Physiol Chem, 227 p. 169

Furujo M, Kinoshita M, Ichiba Y, Romstad A, Shintaku H, Kubo T.(2014), Clinical characteristics of epileptic seizures in a case of dihydropteridine reductase deficiency. Epilepsy & Behavior Case Reports. 2:37-39. doi:10.1016/j.ebcr.2014.01.007.

Gall JG, Pardue ML. (1969), Formation and detection of RNA-DNA hybrid molecules in cyctological preparations Proc Natl Acad Sci USA. 63(2):378-383.

7. References

Gasteiger E., Gattiker A., Hoogland C., Ivanyi I., Appel R.D., Bairoch A. (2003), ExPASy: the proteomics server for in-depth protein knowledge and analysis Nucleic Acids Res. 31:3784-3788

Geling A, Itoh M, Tallafuß A, Chapouton P, Tannhäuser B, Kuwada JY, B. Chitnis AB, Bally-Cuif L (2003), "bHLH transcription factor Her5 links patterning to regional inhibition of neurogenesis at the midbrain-hindbrain boundary" Development 130: 1591-1604; doi: 10.1242/dev.00375

Gerlai R. (2012). Using zebrafish to unravel the genetics of complex brain disorders. Curr. Top. Behav. Neurosci. 12 3–24

German DC, Manaye K, Smith WK, Woodward DJ, Saper CB. (1989), Midbrain dopaminergic cell loss in Parkinson's disease: Computer visualization. Ann Neurol. 26:507–514.

Gesemann M, Lesslauer A, Maurer CM, Schönthaler HB, Neuhauss SC. (2010), Phylogenetic analysis of the vertebrate Excitatory/Neutral Amino Acid Transporter (SLC1/EAAT) family reveals lineage specific subfamilies. BMC Evolutionary Biology. 10:117. doi:10.1186/1471-2148-10-117.

Ghosh S, Hui SP. (2016), Regeneration of Zebrafish CNS: Adult Neurogenesis. Neural Plasticity. 2016:5815439. doi:10.1155/2016/5815439.

Gross SS, Levi R., (1992), "Tetrahydrobiopterin synthesis. An absolute requirement for cytokine-induced nitric oxide generation by vascular smooth muscle." J Biol Chem. Dec 25;267(36):25722-9.

Grupp, L., Wolburg, H. and Mack, A. F. (2010), Astroglial structures in the zebrafish brain. J. Comp. Neurol., 518: 4277–4287. doi:10.1002/cne.22481

Haugeto O, Ullensvang K, Levy LM, Chaudhry FA, Honoré T, Nielsen M, Lehre KP, Danbolt NC. (1996), Brain glutamate transporter proteins form homomultimers. J Biol Chem. 271:27715–27722. doi: 10.1074/jbc.271.44.27715

Herbomel P, Thisse B, Thisse C, (2001), Zebrafish Early Macrophages Colonize Cephalic Mesenchyme and Developing Brain, Retina, and Epidermis through a M-CSF Receptor-Dependent Invasive Process, In Developmental Biology, Volume 238, Issue 2, Pages 274-288, ISSN 0012-1606, https://doi.org/10.1006/dbio.2001.0393.

Hester M. Wain, Elspeth A. Bruford, Ruth C. Lovering, Michael J. Lush, Mathew W. Wright, Povey S (2002), Guidelines for Human Gene Nomenclature Genomics 79(4):464-470

Himmelreich N, Kaufmann LT, Steinbeisser H, Körner C, Thiel C. (2015) Lack of phosphomannomutase 2 affects Xenopus laevis morphogenesis and the non-canonical Wnt5a/Ror2 signalling. J Inherit Metab Dis. Nov;38(6):1137-46. doi: 10.1007/s10545-015-9874-0. Epub 2015 Jul 4.

Howe DG, Bradford YM, Conlin T, Eagle AE, Fashena D, Frazer K, Knight J, Mani P, Martin R, Moxon SA, Paddock H, Pich C, Ramachandran S, Ruef BJ, Ruzicka L, Schaper K, Shao X, Singer A, Sprunger B, Van Slyke CE, Westerfield M. (2013). ZFIN, the Zebrafish Model Organism Database: increased support for mutants and transgenics. Nucleic Acids Res. Jan;41(Database issue):D854-60.

Hu, Z., Holzschuh, J., & Driever, W. (2015). Loss of DDB1 Leads to Transcriptional p53 Pathway Activation in Proliferating Cells, Cell Cycle Deregulation, and Apoptosis in Zebrafish Embryos. PLoS ONE, 10(7), e0134299. http://doi.org/10.1371/journal.pone.0134299

Huppertz I, Attig J, D'Ambrogio A, Easton LE, Sibley CR, Sugimoto Y, Tajnik M, König J, Ule J, (2014), iCLIP: Protein–RNA interactions at nucleotide resolution, In Methods, Volume 65, Issue 3, Pages 274-287, ISSN 1046-2023, https://doi.org/10.1016/j.ymeth.2013.10.011.

Ichinose H, Ohye T, Takahashi E, Seki N, Hori T, Segawa M, Nomura Y, Endo K, Tanaka H, Tsuji S, et al. (1994), "Hereditary progressive dystonia with marked diurnal fluctuation caused by mutations in the GTP cyclohydrolase I gene." Nat Genet. Nov;8(3):236-42

Imai F, Yoshizawa A, Matsuzaki A, Oguri E, Araragi M, Nishiwaki Y, Masai I. (2014), Stem-loop binding protein is required for retinal cell proliferation, neurogenesis, and intraretinal axon pathfinding in zebrafish. Dev Biol. Oct 1;394(1):94-109. doi: 10.1016/j.ydbio.2014.07.020. Epub 2014 Aug 5.

Ishikawa T, Imamura K, Kondo T, Koshiba Y Hara S, Ichinose H, Furujo M, Kinoshita M, Oeda T, Takahashi J, Takahashi, Inoue H (2016), "Genetic and pharmacological correction of aberrant dopamine synthesis using patient iPSCs with BH4 metabolism disorders" Hum Mol Genet. Oct 18. doi: 10.1093/hmg/ddw339.

J. Odenthal, K. Rossnagel, P. Haffter, R.N. Kelsh, E. Vogelsang, M. Brand, F.J. van Eeden, M. Furutani-Seiki, M. Granato, M. Hammerschmidt, C.P. Heisenberg, Y.J. Jiang, D.A. Kane, M.C. Mullins, C. Nusslein-Volhard (1996), Mutations affecting xanthophore pigmentation in the zebrafish, Danio rerio Development 123: 391-398;

Jaffe EK, (2017), "New protein structures provide an updated understanding of phenylketonuria." Mol Genet Metab. Aug;121(4):289-296. doi: 10.1016/j.ymgme.2017.06.005. Epub 2017 Jun 15.

Jäggi L, Zurflüh MR, Schuler A, Ponzone A, Porta F, Fiori L, Giovannini M, Santer R, Hoffmann GF, Ibel H, Wendel U, BallhausenD, Baumgartner MR, Blau N, (2008), "Outcome and long-term follow-up of 36 patients with tetrahydrobiopterin deficiency", Molecular Genetics and Metabolism, Volume 93, Issue 3, March 295-305, https://doi.org/10.1016/j.ymgme.2007.10.004.

Jean D, Ewan K, Gruss P. (1998), Molecular regulators involved in vertebrate eye development. Mech Dev. Aug;76(1-2):3-18.

Johnen G, Kaufman S., (1997), "Studies on the enzymatic and transcriptional activity of the dimerization cofactor for hepatocyte nuclear factor 1", Proc Natl Acad Sci U S A. Dec 9;94(25):13469-74.

Juers, D. H., Matthews, B. W., & Huber, R. E. (2012). LacZ β-galactosidase: Structure and function of an enzyme of historical and molecular biological importance. Protein Science : A Publication of the Protein Society, 21(12), 1792–1807. http://doi.org/10.1002/pro.2165

Kálmán M, (1998), "Astroglial architecture of the carp (Cyprinus carpio) brain as revealed by immunohistochemical staining against glial fibrillary acidic protein (GFAP)" Anat Embryol (Berl).

7. References

Karlsson J, von Hofsten J, Olsson PE. (2001), Generating transparent zebrafish: a refined method to improve detection of gene expression during embryonic development. Mar Biotechnol (NY). Nov;3(6):522-7.

Kassahn, K. S., Dang, V. T., Wilkins, S. J., Perkins, A. C., & Ragan, M. A. (2009). Evolution of gene function and regulatory control after whole-genome duplication: Comparative analyses in vertebrates. Genome Research, 19(8), 1404–1418. http://doi.org/10.1101/gr.086827.108

Kastenhuber E, Kratochwil CF, Ryu S, Schweitzer J, Driever W. (2010), Genetic dissection of dopaminergic and noradrenergic contributions to catecholaminergic tracts in early larval zebrafish. The Journal of Comparative Neurology. 518(4):439-458. doi:10.1002/cne.22214.

Kawahara A, Hisano Y, Ota S, Taimatsu K. (2016), Site-Specific Integration of Exogenous Genes Using Genome Editing Technologies in Zebrafish. Hatada I, ed. International Journal of Molecular Sciences. 17(5):727. doi:10.3390/ijms17050727.

Kim, H., Kim, K. and Yim, J. (2013), Biosynthesis of drosopterins, the red eye pigments of Drosophila melanogaster. IUBMB Life, 65: 334–340. doi:10.1002/iub.1145

Kimmel, C. B., Ballard, W. W., Kimmel, S. R., Ullmann, B. and Schilling, T. F. (1995), Stages of embryonic development of the zebrafish. Dev. Dyn., 203: 253–310. doi:10.1002/aja.1002030302

Kimmel, C.B., Grunwald, D.J., Walker, C., Westerfield, M., and Streisinger, G. (1985) Neuronal degeneration mutations that spare primary neurons in the zebrafish. Soc. Neurosci. Abstr.11:647

Kizil, C., Kaslin, J., Kroehne, V. and Brand, M. (2012), Adult neurogenesis and brain regeneration in zebrafish. Devel Neurobio, 72: 429–461. doi:10.1002/dneu.20918

Kopajtich, R., Murayama, K., Janecke, A. R., Haack, T. B., Breuer, M., Knisely, A. S., Harting, I., Ohashi, T., Okazaki, Y., Watanabe, D., Tokuzawa, Y., Kotzaeridou, U., and 16 others. (2016), Biallelic IARS mutations cause growth retardation with prenatal onset, intellectual disability, muscular hypotonia, and infantile hepatopathy. Am. J. Hum. Genet. 99: 414-422

Kroehne V, Freudenreich D, Hans S, Kaslin J, Brand M, (2011), "Regeneration of the adult zebrafish brain from neurogenic radial glia-type progenitors" Development 138: 4831-4841; doi: 10.1242/dev.072587

Kubo F, Takeichi M, Nakagawa S (2003), Wnt2b controls retinal cell differentiation at the ciliary marginal zone Development 130: 587-598; doi: 10.1242/dev.00244

Kwan, K. M., Fujimoto, E., Grabher, C., Mangum, B. D., Hardy, M. E., Campbell, D. S., Parant, J. M., Yost, H. J., Kanki, J. P. and Chien, C.-B. (2007), The Tol2kit: A multisite gateway-based construction kit for Tol2 transposon transgenesis constructs. Dev. Dyn., 236: 3088–3099. doi:10.1002/dvdy.21343

Lane, A. N., & Fan, T. W.-M. (2015). Regulation of mammalian nucleotide metabolism and biosynthesis. Nucleic Acids Research, 43(4), 2466–2485. http://doi.org/10.1093/nar/gkv047

Lee I, Hong W. (2004), "RAP--a putative RNA-binding domain" Trends Biochem Sci. Nov;29(11):567-70.

Lee J, Hollenberg S, Snider L, Turner D, Lipnick N, Weintraub H. (1995), Conversion of Xenopus ectoderm into neurons by Neuro-D, a basic helix-loop-helix protein. Science 268:836–844.

Lee J. (1997), Basic helix-loop-helix genes in neural development. Curr. Opin. Neurobiol. 7:13–20

Lei XD, Kaufman S. (1999), "Characterization of expression of the gene for human pterin carbinolamine dehydratase/dimerization cofactor of HNF1" DNA Cell Biol. Mar;18(3):243-52.

Li G, Li J, Tan B, Wang J, Kong X, et al. (2015) Characterization and Regulation of the Amino Acid Transporter SNAT2 in the Small Intestine of Piglets. PLOS ONE 10(6): e0128207. https://doi.org/10.1371/journal.pone.0128207

Lieschke GJ, Currie PD (2007), "Animal models of human disease: zebrafish swim into view" Nature Reviews Genetics 8, 353-367 May doi:10.1038/nrg2091

Lipton JO, Sahin M, (2014), The Neurology of mTOR, In Neuron, Volume 84, Issue 2, Pages 275-291, ISSN 0896-6273, https://doi.org/10.1016/j.neuron.2014.09.034.

Liu, B., Gao, H.-M., Wang, J.-Y., Jeohn, G.-H., Cooper, C. L. and Hong, J.-S. (2002), Role of Nitric Oxide in Inflammation-Mediated Neurodegeneration. Annals of the New York Academy of Sciences, 962: 318–331. doi:10.1111/j.1749-6632.2002.tb04077.x

Longhi R, Valsasina R, Butte C, Paccanelli S, Riva E, Giovannini M (1985) Cranial computerized tomography in dihydropteridine reductase deficiency. J Inherit Metab Dis 8 (3): 109–112. doi:10.1007/BF01819291.

Longo N. (2009). Disorders of biopterin metabolism. J Inherit Metab Dis 32:333–342

Lyons DA, Talbot WS. (2015), Glial Cell Development and Function in Zebrafish. Cold Spring Harbor Perspectives in Biology. 7(2):a020586. doi:10.1101/cshperspect.a020586.

Mahoko Furujo, Masako Kinoshita, Yozo Ichiba,Anne Romstad,Haruo Shintaku, and Toshihide Kubo, (2014), "Clinical characteristics of epileptic seizures in a case of dihydropteridine reductase deficiency", Epilepsy Behav Case Rep. 2: 37–39. Published online 2014 Mar 13. doi: 10.1016/j.ebcr.2014.01.007

Maita N, Okada K, Hatakeyama K, Hakoshima T (2002) Crystal structure of the stimulatory complex of GTP cyclohydrolase I and its feedback regulatory protein GFRP. Proc Natl Acad Sci U S A 99(3): 1212–1217. doi:10.1073/pnas.022646999.

Major RJ, Poss KD. (2007), Zebrafish Heart Regeneration as a Model for Cardiac Tissue Repair. Drug discovery today Disease models. 4(4):219-225. doi:10.1016/j.ddmod.2007.09.002.

Maragakis, N. J., Dietrich, J., Wong, V., Xue, H., Mayer-Proschel, M., Rao, M. S. and Rothstein, J. D. (2004), Glutamate transporter expression and function in human glial progenitors. Glia, 45: 133–143. doi:10.1002/glia.10310

Marcus RC, Delaney CL, Easter SS Jr., (1999), "Neurogenesis in the visual system of embryonic and adult zebrafish (Danio rerio). off." Vis Neurosci. May-Jun;16(3):417-24.

Marcus, R. C. and Easter, S. S. (1995), Expression of glial fibrillary acidic protein and its relation to tract formation in embryonic zebrafish (Danio rerio). J. Comp. Neurol., 359: 365–381. doi:10.1002/cne.903590302

Matthews RG, Kaufman S. (1980), Characterization of the dihydropteridine reductase activity of pig liver methylenetetrahydrofolate reductase. J Biol Chem 255:6014–6017.

McKeown KA, Moreno R, Hall VL, Ribera AB, Downes GB. (2012), Disruption of Eaat2b, a glutamate transporter, results in abnormal motor behaviors in developing zebrafish. Developmental biology. 362(2):162-171. doi:10.1016/j.ydbio.2011.11.001.

Medaka Expression Database: Alonso-Barba JI, Rahman R-U, Wittbrodt J, Mateo JL. (2015). MEPD: medaka expression pattern database, genes and more. Nucleic Acids Res. (http://mepd.cos.uni-heidelberg.de/mepd/) <<accessed 23.8.2017>>

Mencacci NE, Isaias IU, Reich MM, Ganos C, Plagnol V, Polke JM, Bras J, Hersheson J, Stamelou M, Pittman AM, Noyce AJ, Mok KY, Opladen T, Kunstmann E, Hodecker S, Münchau A, Volkmann J, Samnick S, Sidle K, Nanji T, Sweeney MG, Houlden H, Batla A, Zecchinelli AL, et al. (2014), Parkinson's disease in GTP cyclohydrolase 1 mutation carriers. *Brain*. 137(9):2480-2492. doi:10.1093/brain/awu179.

Mueller T, Wullimann MF, (2002), "BrdU-, neuroD (nrd)- and Hu-studies reveal unusual non-ventricular neurogenesis in the postembryonic zebrafish forebrain" Mechanisms of Development Volume 117, Issues 1–2, September Pages 123-135 https://doi.org/10.1016/S0925-4773(02)00194-6

Minghetti L, Levi G, (1998), Microglia as effector cells in brain damage and repair: focus on prostanoids and nitric oxide, In Progress in Neurobiology, Volume 54, Issue 1, Pages 99-125, ISSN 0301-0082, https://doi.org/10.1016/S0301-0082(97)00052-X

Nagashima M, Barthel LK, Raymond PA. (2013), A self-renewing division of zebrafish Müller glial cells generates neuronal progenitors that require N-cadherin to regenerate retinal neurons. Development (Cambridge, England). 140(22):4510-4521. doi:10.1242/dev.090738.

Ney DM, Blank RD, Hansen KE. (2014), Advances in the nutritional and pharmacological management of phenylketonuria. Current opinion in clinical nutrition and metabolic care. 17(1):61-68. doi:10.1097/MCO.0000000000000002.

Ng J, Papandreou A, Heales SJ, Kurian MA., (2015), "Monoamine neurotransmitter disorders--clinical advances and future perspectives." Nat Rev Neurol. Oct;11(10):567-84. doi: 10.1038/nrneurol.2015.172. Epub 2015 Sep 22.

Opladen T, Hoffmann GF, Blau N., (2012), "An international survey of patients with tetrahydrobiopterin deficiencies presenting with hyperphenylalaninaemia". J Inherit Metab Dis. Nov;35(6):963-73. doi: 10.1007/s10545-012-9506-x. Epub 2012 Jun 23.

Orphanet: an online rare disease and orphan drug data base. Copyright, INSERM 1997. Available on http://www.orpha.net. Accessed (20.10.2017).

Ozalp I, Coşkun T, Tokatli A, Kalkanoğlu HS, Dursun A, Tokol S, Köksal G, Ozgüc M, Köse R. (2001), "Newborn PKU screening in Turkey: at present and organization for future" Turk J Pediatr. Apr-Jun;43(2):97-101.

Pan YA, Livet J, Sanes JR, Lichtman JW, Schier AF. (2011), Multicolor Brainbow Imaging in Zebrafish. Cold Spring Harbor protocols. 2011:pdb.prot5546.

Park HC, Mehta A, Richardson JS, Appel B (2002). olig2 is required for zebrafish primary motor neuron and oligodendrocyte development. Dev Biol 248: 356–368

Parker MO, Brock AJ, Walton RT, Brennan CH. (2013), The role of zebrafish (Danio rerio) in dissecting the genetics and neural circuits of executive function. Frontiers in Neural Circuits. 2013;7:63. doi:10.3389/fncir.2013.00063.

Parkinson, J. (1917). An Essay on the Shaking Palsy. London: Sherwood,Neely, and Jones.

Petr, G. T., Sun, Y., Frederick, N. M., Zhou, Y., Dhamne, S. C., Hameed, M. Q., … Rosenberg, P. A. (2015). Conditional Deletion of the Glutamate Transporter GLT-1 Reveals That Astrocytic GLT-1 Protects against Fatal Epilepsy While Neuronal GLT-1 Contributes Significantly to Glutamate Uptake into Synaptosomes. The Journal of Neuroscience, 35(13), 5187–5201. http://doi.org/10.1523/JNEUROSCI.4255-14.2015

Pogge v Strandmann E, Senkel S, Ryffel GU., (2000), "Ectopic pigmentation in Xenopus in response to DCoH/PCD, the cofactor of HNF1 transcription factor/pterin-4alpha-carbinolamine dehydratase" Mech Dev. Mar 1;91(1-2):53-60.

Pollock RJ, Kaufman S. (1978), Dihydropteridine reductase may function in tetrahydrofolate metabolism.J Neurochem 31:115–123.

Ponzone A, Guardamagna O, Dianzani I, Ponzone R, Ferrero GB, Spada M, Cotton RG. (1993), Catalytic activity of tetrahydrobiopterin in dihydropteridine reductase deficiency and indications for treatment. Pediatr Res 33:125–128.

Ponzone, A., Spada, M., Ferraris, S., Dianzani, I. and de Sanctis, L. (2004), Dihydropteridine reductase deficiency in man: From biology to treatment. Med. Res. Rev., 24: 127–150. doi:10.1002/med.10055

Porta F, Mussa A, Concolino D, Spada M, Ponzone A. (2009). Dopamine agonists in 6-pyruvoyl tetrahydropterin synthase deficiency. Neurology 73:633–637

Poss, K. D., Keating, M. T. and Nechiporuk, A. (2003), Tales of regeneration in zebrafish. Dev. Dyn., 226: 202–210. doi:10.1002/dvdy.10220

Postlethwait JH, Yan Y-L, Gates MA, Horne S, Amores A, Brownlie A, Donovan A, Egan ES, Force A, Gong Z, et al. (1998), Vertebrate genome evolution and the zebrafish gene map. Nat Genet. 18:345–349

Protein Atlas Database: Uhlén M, Fagerberg L, Hallström BM, Lindskog C, Oksvold P, Mardinoglu A, Sivertsson Å, Kampf C, Sjöstedt E, Asplund A, Olsson I, Edlund K, Lundberg E, Navani S, Szigyarto CA, Odeberg J, Djureinovic D, Takanen JO, Hober S, Alm T, Edqvist PH, Berling H, Tegel H, Mulder J, Rockberg J, Nilsson P, Schwenk JM, Hamsten M, von Feilitzen K, Forsberg M, Persson L, Johansson F, Zwahlen M, von Heijne G, Nielsen J, Pontén F. (2015), "Tissue-based map of the human proteome."Science 347(6220):1260419. (http://www.proteinatlas.org/) <<Accessed 23.8.2017>>

Pujic Z, Malicki J. (2004), Retinal pattern and the genetic basis of its formation in zebrafish. Semin Cell Dev Biol. Feb;15(1):105-14.

Rao KVR, Jayakumar AR, Norenberg MD. (2003), Induction of the mitochondrial permeability transition in cultured astrocytes by glutamine. Neurochem Int 43: 517–523.

Recher G, Jouralet J, Brombin A, Heuzé A, Mugniery E, Hermel JM, Desnoulez S, Savy T, Herbomel P, Bourrat F, Peyriéras N, Jamen F, Joly JS (2013), "Zebrafish midbrain slow-amplifying progenitors exhibit high levels of transcripts for nucleotide and ribosome biogenesis" Development 140: 4860-4869; doi: 10.1242/dev.099010

Reifers F, Bohli H, Walsh EC, Crossley PH, Stainier DY, Brand M. (1998). Fgf8 is mutated in zebrafish acerebellar (ace) mutants and is required for maintenance of midbrain-hindbrain boundary development and somitogenesis. Development 125: 2381–2395.

Reinhardt R, Centanin L, Tavhelidse T, Inoue D, Wittbrodt B, Concerdet JP, Martinez-Morales JR, Wittbrodt J (2015), Sox2, Tlx, Gli3, and Her9 converge on Rx2 to define retinal stem cells in vivo. The EMBO Journal. 34(11):1572-1588. doi:10.15252/embj.201490706.

Robu ME, Larson JD, Nasevicius A, Beiraghi S, Brenner C, Farber SA, Ekker SC (2007), p53 Activation by Knockdown Technologies. Mullins M, ed. PLoS Genetics. 3(5):e78. doi:10.1371/journal.pgen.0030078.

Rosselli M, Keller PJ, Dubey RK., (1998), "Role of nitric oxide in the biology, physiology and pathophysiology of reproduction". Hum Reprod Update. Jan-Feb;4(1):3-24.

Rossi A, Kontarakis Z, Gerri C, Nolte H, Hölper S, Krüger M, Stainier DY (2015), Genetic compensation induced by deleterious mutations but not gene knockdowns. Nature. Aug 13;524(7564):230-3. doi: 10.1038/nature14580. Epub 2015 Jul 13.

Santoriello C, Zon LI. (2012), Hooked! Modeling human disease in zebrafish. The Journal of Clinical Investigation. 122(7):2337-2343. doi:10.1172/JCI60434.

Schallreuter KU, Kothari S, Hasse S, Kauser S, Lindsey NJ, Gibbons NC, Hibberts N, Wood JM. (2003)," In situ and in vitro evidence for DCoH/HNF-1 alpha transcription of tyrosinase in human skin melanocytes" Biochem Biophys Res Commun. Feb 7;301(2):610-6.

Schallreuter KU, Wood JM, Pittelkow MR, Gütlich M, Lemke KR, Rödl W, Swanson NN, Hitzemann K, Ziegler I., (1994), "Regulation of melanin biosynthesis in the human epidermis by tetrahydrobiopterin.,Science" Mar 11;263(5152):1444-6

Schmidt, R., Strähle, U., & Scholpp, S. (2013). Neurogenesis in zebrafish – from embryo to adult. Neural Development, 8, 3. http://doi.org/10.1186/1749-8104-8-3

Schnetz-Boutaud NC, Anderson BM, Brown KD, Wright HH, Abramson RK, Cuccaro ML, Gilbert JR, Pericak-Vance MA, Haines JL (2009). Examination of Tetrahydrobiopterin Pathway Genes in Autism. Genes, brain, and behavior. 8(8):753-757. doi:10.1111/j.1601-183X.2009.00521.x.

Scriver CR, Kaufman S. (2001), Hyperphenylalaninemia: Phenylalanine hydroxylase deficiency. In: Scriver CR, Beaudet AL, Valle D, editors. The metabolic and molecular bases of inherited disease. New York: McGraw-Hill; pp 1667–1724.

Sedel F, Ribeiro MJ, Remy P, Blau N, Saudubray JM, Agid Y. (2006), "Dihydropteridine reductase deficiency: levodopa's long-term effectiveness without dyskinesia." Neurology. Dec 26;67(12):2243-5.

Seeman P, Kapur S. (2000), Schizophrenia: More dopamine, more D2 receptors. Proceedings of the National Academy of Sciences of the United States of America. 97(14):7673-7675.

Segawa M, Nomura Y, Tanaka S, Hakamada S, Nagata E, Soda M, Kase M., (1988), "Hereditary progressive dystonia with marked diurnal fluctuation--consideration on its pathophysiology based on the characteristics of clinical and polysomnographical findings" Adv Neurol. 50:367-76. Review.

She P, Reid TM, Bronson SK, Vary TC, Hajnal A, Lynch CJ, Hutson SM, (2007), Disruption of BCATm in mice leads to increased energy expenditure associated with the activation of a futile protein turnover cycle. Cell Metab. 6:181–194. [PubMed: 17767905]

Shima, T., Znosko, W., Tsang, M. (2009), The characterization of a zebrafish mid-hindbrain mutant, mid-hindbrain gone (mgo). Dev. Dyn., 238: 899–907. doi:10.1002/dvdy.21916

Shin, S.-H., & Lee, Y.-M. (2013). Glyceollins, a novel class of soybean phytoalexins, inhibit SCF-induced melanogenesis through attenuation of SCF/c-kit downstream signaling pathways. Experimental & Molecular Medicine, 45(4), e17–. http://doi.org/10.1038/emm.2013.20

Si Q, Sun S, Gu, Y (2017), "A278C mutation of dihydropteridine reductase decreases autophagy via mTOR signaling" Acta Biochimica et Biophysica Sinica, Volume 49, Issue 8, 1 August Pages 706–712, https://doi.org/10.1093/abbs/gmx061

Sigrist CJA, de Castro E, Cerutti L, Cuche BA, Hulo N, Bridge A, Bougueleret L, Xenarios I. (2012), New and continuing developments at PROSITE Nucleic Acids Res. doi: 10.1093/nar/gks1067

Smooker PM, Gough TJ, Cotton RGH, Alliaudi C, de Sanctis L, Dianzani I. (1999), A series of mutations in the dihydropteridine reductase gene resulting in either abnormal RNA splicing or DHPR protein defects. Hum Mutat 13:503–504.

Smooker, P. M. and Cotton, R. G. H. (1995), Molecular basis of dihydropteridine reductase deficiency. Hum. Mutat., 5: 279–284. doi:10.1002/humu.1380050402

Sofroniew MV, Vinters HV. (2010), Astrocytes: biology and pathology. Acta Neuropathologica. 119(1):7-35. doi:10.1007/s00401-009-0619-8.

Stephens, W. Z., Senecal, M., Nguyen, M. and Piotrowski, T. (2010), Loss of adenomatous polyposis coli (apc) results in an expanded ciliary marginal zone in the zebrafish eye. Dev. Dyn., 239: 2066–2077. doi:10.1002/dvdy.22325

Stigloher C, Chapouton P, Adolf A, Bally-Cuif L, (2008), Identification of neural progenitor pools by E(Spl) factors in the embryonic and adult brain, Brain Research Bulletin, Volume 75, Issue 2, Pages 266-273, ISSN 0361-9230, http://dx.doi.org/10.1016/j.brainresbull.2007.10.032.

Streisinger, G., Walker, C., Dower, N., Knauber, D., and Singer, F. (1981) Production of clones of homozygous diploid zebra fish (Brachydanio rerio). Nature. 291(5813):293-296

Suárez I, Bodega G, Fernández B, (2002), Glutamine synthetase in brain: effect of ammonia, In Neurochemistry International, Volume 41, Issues 2–3, Pages 123-142, ISSN 0197-0186, https://doi.org/10.1016/S0197-0186(02)00033-5

Sumi-Ichinose C1, Urano F, Kuroda R, Ohye T, Kojima M, Tazawa M, Shiraishi H, Hagino Y, Nagatsu T, Nomura T, Ichinose H. (2001), Catecholamines and serotonin are differently regulated by tetrahydrobiopterin. A study from 6-pyruvoyltetrahydropterin synthase knockout mice. J Biol Chem. Nov 2;276(44):41150-60. Epub 2001 Aug 21

Swanson MS, Nakagawa TY, LeVan K, Dreyfuss G. (1987), Primary structure of human nuclear ribonucleoprotein particle C proteins: conservation of sequence and domain structures in heterogeneous nuclear RNA, mRNA, and pre-rRNA-binding proteins. Molecular and Cellular Biology. 7(5):1731-1739.

Taber KH, Hurley RA. (2008), Astroglia: not just glue. J Neuropsychiatry Clin Neurosci. 20:iv–129.

Takahashi Y, Manabe Y, Nakano Y, Yunoki T, Kono S, Narai H, Furujo M, Abe K (2017), Parkinsonism in Association with Dihydropteridine Reductase Deficiency. Case Reports in Neurology.9(1):17-21. doi:10.1159/000456610.

Tanaka K, Watase K, Manabe T, Yamada K, Watanabe M, Takahashi K, Iwama H, Nishikawa T, Ichihara N, Kikuchi T, Okuyama S, Kawashima N, Hori S, Takimoto M, Wada K.” (1997), Epilepsy and Exacerbation of Brain Injury in Mice Lacking the Glutamate Transporter GLT-1” Science13 Jun 1699-1702

Tao T, Peng J, (2009), Liver development in zebrafish (Danio rerio), In Journal of Genetics and Genomics, Volume 36, Issue 6, Pages 325-334, ISSN 1673-8527, https://doi.org/10.1016/S1673-8527(08)60121-6

TeSlaa JT, Keller AN, Nyholm MK, Grinblat G, (2013), “Zebrafish Zic2a and Zic2b regulate neural crest and craniofacial development” Developmental Biology, Volume 380, Issue 1, 73-86, http://dx.doi.org/10.1016/j.ydbio.2013.04.033.

Thisse C, Thisse B (2008), High-resolution in situ hybridization to whole-mount zebrafish embryos Nature Protocols 3, - 59 – 69 Published online: 20 December 2007 doi:10.1038/nprot.2007.514

Thisse, B., Thisse, C. (2004) Fast Release Clones: A High Throughput Expression Analysis. ZFIN Direct Data Submission (http://zfin.org).

Thöny B and Blau, N (2006) BIOMDB: Database of Mutations Causing Tetrahydrobiopterin Deficiencies In: Blau N. editor. PKU and BH4 – Advances in Phenylketonuria and Tetrahydrobiopterin 2006, SPS Verlagsgesellschaft

Thöny B, Auerbach G, Blau N. (2000), Tetrahydrobiopterin biosynthesis, regeneration and functions. Biochemical Journal. 347(Pt 1):1-16.

Thöny B, Neuheiser F, Kierat L, Blaskovics M, Arn PH, Ferreira P, Rebrin I, Ayling J, Blau N., (1998), "Hyperphenylalaninemia with high levels of 7-biopterin is associated with mutations in the PCBD gene encoding the bifunctional protein pterin-4a-carbinolamine dehydratase and transcriptional coactivator (DCoH)."Am J Hum Genet. Jun;62(6):1302-11.

Thöny B, Neuheiser F, Kierat L, Rolland MO, Guibaud P, Schlüter T, Germann R, Heidenreich RA, Duran M, de Klerk JB, Ayling JE, Blau N. (1998), "Mutations in the pterin-4alpha-carbinolamine dehydratase (PCBD) gene cause a benign form of hyperphenylalaninemia." Hum Genet. Aug;103(2):162-7.

Thöny, B. and Blau, N. a (2006), Mutations in the BH_4-metabolizing genes GTP cyclohydrolase I, 6-pyruvoyl-tetrahydropterin synthase, sepiapterin reductase, carbinolamine-4a-dehydratase, and dihydropteridine reductase . Hum. Mutat., 27: 870–878. doi:10.1002/humu.20366

Tönjes, M, Barbus S, Park, YJ, Wang W, Schlotter M, Lindroth AM, Pleier SV, Bai SHC, Karra D, Prio RM, Felsberg J, Addington A, Lemke D, Weibreicht I, Hovestadt V, Rolli CG, Campos B, Turcan S et al., (2013), "BCAT1 Promotes Cell Proliferation through Amino Acid Catabolism in Gliomas Carrying Wild-Type IDH1." Nature medicine 19.7 901–908. PMC. Web. 11 July (2017).

Trends in Genetics "Genetic Nomenclature Guide" (p. S.5-S.6; Elsevier Science Ltd., Cambridge, United Kingdom, 1998

Tripathi PP, Bozzi Y. (2015), The role of dopaminergic and serotonergic systems in neurodevelopmental disorders: a focus on epilepsy and seizure susceptibility. BioImpacts : BI. 5(2):97-102. doi:10.15171/bi.2015.07.

Van Calcar SC, Ney DM. (2012), Food Products Made With Glycomacropeptide, a Low Phenylalanine Whey Protein, Provide a New Alternative to Amino Acid-Based Medical Foods for Nutrition Management of Phenylketonuria. Journal of the Academy of Nutrition and Dietetics. 112(8):1201-1210. doi:10.1016/j.jand.2012.05.004.

Varughese KI, Skinner MM, Whiteley JM, Mathhews DA, Xuong NH, (1992), "Crystal structure of rat liver dihydropteridine reductase" Proc. Nati. Acad. Sci. USA Vol. 89, pp. 6080-6084, July

Verduzco, Daniel, James F. Amatruda. (2011), "Analysis of Cell Proliferation, Senescence and Cell Death in Zebrafish Embryos." Methods in cell biology 101 10.1016/B978–0–12–387036–0.00002–5. PMC.

W.Y. Chan, S. Kohsaka, P. Rezaie, (2007), The origin and cell lineage of microglia—New concepts, Brain Research Reviews, Volume 53, Issue 2, Pages 344-354, ISSN 0165-0173, http://dx.doi.org/10.1016/j.brainresrev.2006.11.002.

Walther DJ, Peter JU, Winter S, Höltje M, Paulmann N, Grohmann M, Vowinckel J, Alamo-Bethencourt V, Wilhelm CS, Ahnert-Hilger G, Bader M, (2003), Serotonylation of Small GTPases Is a Signal Transduction Pathway that Triggers Platelet α-Granule Release, Cell, Volume 115, Issue 7, Pages 851-862, ISSN 0092-8674, http://dx.doi.org/10.1016/S0092-8674(03)01014-6.

Wehman AM, Staub W, Meyers JR, Raymond PA, Baier H, (2005), Genetic dissection of the zebrafish retinal stem-cell compartment, Developmental Biology, Volume 281, Issue 1, Pages 53-65, ISSN 0012-1606, http://dx.doi.org/10.1016/j.ydbio.2005.02.010.

Werner ER, Blau N, Thöny B, (2011), "Tetrahydrobiopterin: biochemistry and pathophysiology " Biochemical Journal Aug 26 438 (3) 397-414; DOI: 10.1042/BJ20110293

Westerfield M. Fourth Edition. University of Oregon Press; Eugene: (2000). The Zebrafish Book. A Guide for the Laboratory Use of Zebrafish (Danio rerio)

Wiese S, Karus M, Faissner A (2012), "Astrocytes as a source for extracellular matrix molecules and cytokines" Front. Pharmacol., 26 June https://doi.org/10.3389/fphar.2012.00120

Williams RA, Mamotte CD, Burnett JR. (2008), Phenylketonuria: An Inborn Error of Phenylalanine Metabolism. The Clinical Biochemist Reviews. 29(1):31-41.

Woody RC, Brewster MA, Glasier C (1989) Progressive intracranial calcification in dihydropteridine reductase deficiency prior to folinic acid therapy. Neurology 39(5): 673–675.

Wu, S.-Y. S., Wang, H.-M. D., Wen, Y.-S., Liu, W., Li, P.-H., Chiu, C.-C.,Wen, Z.-H. (2015). 4-(Phenylsulfanyl)butan-2-One Suppresses Melanin Synthesis and Melanosome Maturation In Vitro and In Vivo. International Journal of Molecular Sciences, 16(9), 20240–20257. http://doi.org/10.3390/ijms160920240

Yamamoto K, Ruuskanen JO, Wullimann MF, Vernier P, (2010), Two tyrosine hydroxylase genes in vertebrates: New dopaminergic territories revealed in the zebrafish brain, In Molecular and Cellular Neuroscience, Volume 43, Issue 4, Pages 394-402, https://doi.org/10.1016/j.mcn.2010.01.006.

Yan, R.-T., Ma, W., Liang, L., & Wang, S.-Z. (2005). bHLH Genes and Retinal Cell Fate Specification. Molecular Neurobiology, 32(2), 157–171.

Ye J, Coulouris G, Zaretskaya I, Cutcutache I, Rozen S, Madden T (2012). Primer-BLAST: A tool to design target-specific primers for polymerase chain reaction. BMC Bioinformatics. 13:134.

Yuan, S., & Sun, Z. (2009). Microinjection of mRNA and Morpholino Antisense Oligonucleotides in Zebrafish Embryos. Journal of Visualized Experiments : JoVE, (27), 1113. Advance online publication. http://doi.org/10.3791/1113

Zebrafish atlas: http://zfatlas.psu.edu/, NIH grant 5R24 RR01744, Jake Gittlen Cancer Research Foundation, and PA Tobacco Settlement Fund; accessed 20.9.2017

Zebrafish information network (ZFIN); <<zfin.org>> accessed 9.1.2017 (see Howe et al., 2013)

Zhang H-P, Yang N, Armarego WLF. (1996), In vitro mutagenesis of human dihydropteridine reductase at the active site and at altered sites found in the reductase of deficient children. Pteridines 7:126–136.

Zhang Y, Chen K, Sloan SA, Bennett L, Schloze AR, O'Keeffe S, Phatnani HP, Guarnieri P, Cenada C, Ruderisch N, Denk S, Liddelow SA et al. (2014) An RNA-Sequencing Transcriptome and Splicing Database of Glia, Neurons, and Vascular Cells of the Cerebral

Cortex. The Journal of Neuroscience. 34(36):11929-11947. doi:10.1523/JNEUROSCI.1860-14.2014.

Ziegler, I. (2003), The Pteridine Pathway in Zebrafish: Regulation and Specification during the Determination of Neural Crest Cell-Fate. Pigment Cell Research, 16: 172–182. doi:10.1034/j.1600-0749.2003.00044.x

Ziegler I, McDonaldo T, Hesslinger C, Pelletier I, Boyle P, (2000), "Development of the Pteridine Pathway in the Zebrafish, Danio rerio*
JBC Papers in Press, April, 18, DOI 10.1074/jbc.M910307199

Zielonka M, Makhseed N, Blau N, Bettendorf M, Hoffmann GF, Opladen T. (2015), Dopamine-Responsive Growth-Hormone Deficiency and Central Hypothyroidism in Sepiapterin Reductase Deficiency. JIMD Reports. 24:109-113. doi:10.1007/8904_2015_450.

Zieminska, M Dolinska, J.W Lazzrewicz, J Albrecht (2000), "Induction of permeability transition and swelling of rat brain mitochondria by glutamine" Neurotoxicology, 21 pp. 295-300

Zucca FA, Basso E, Cupaioli FA, Ferrari E, Sulzer D, Casella L, Zecca L (2014), "Neuromelanin of the Human Substantia Nigra: An Update" Neurotoxicity Research January 2014, Volume 25, Issue 1, pp 13–23

Acknowledgement

This work is dedicated to all those who believed in me and supported me and for those I would like to propose a toast:

First and foremost, to Prof. Dr. Andreas Draguhn as first supervisor and Prof. Dr. Ana Martin-Villalba as second supervisor of my thesis. Thank you for the useful input and personal support throughout my thesis. Furthermore, to Prof. Dr. Stephan Frings and Dr. Mirko Völkers as third and fourth member of the examination commission.

Secondly to an amazing zebrafish expert and mentor, who guided me and supported me along my PhD (PD Dr. Matthias Carl).

Thank you for the support around the lab and their untouchable expertise (Prof. Dr. Georg F. Hoffmann, PD Dr. Jürgen Okun, Prof. Dr. Stefan Kölker, Prof. Dr. Nenad Blau, Prof. Dr. Matthias Hentze).

Next and no less important my family that stayed by my side during ups and downs within the 3 ½ years (Gabi Breuer, Julia Breuer, Joachim Breuer, Patricia Weinert, Martin Breuer, Tobias Benner). To my two wonderful ladies at home that never failed to cheer me up and give me strength even when things appeared hopeless (Merle Kochan, Arya).

To always having an open door and an open ear, with a solution at hand (PD Dr. Christian Thiel). To Team M&M (Matthias Zielonka), which could conquer every challenge and even the most difficult protocols!

I raise my glass to great friends I made (Nastassja Himmelreich, Patrick Feyh, Tim Weigand, Luca Guglielmi, Marlen Hutter) and family I lost (Wilhelm Breuer†). To those that greeted me every morning, including weekends, with a smile. To those who could stand my continuous ideas for experiments and their undefeatable enthusiasm (Alex, Sylvia, Brigitte, Sonja, Helga).

To those who have become more than just acquaintances (Rastislav Horos, Amol Tandon, Roland Imle, Nicolas Stützenberger, BeiTzu Wang, Bianca Dimitrov, Leander Hock, Nathalie Schell, Sabine Jung-Klawitter). To those who encouraged me from thousands of miles away (Jim Goddard, Carey Goddard, Michelle Ermter, Wolfgang Zimmermann). To those who support me no matter what and have always been there for me (Helena Schmitz, Familie Kochan, Familie Decker, Familie Igelhorst, Jojo&Konni)

And after all: To Us! To this incredibly journey, which I will cherish for the rest of my life.

Appendices

Supplemental A. Figures

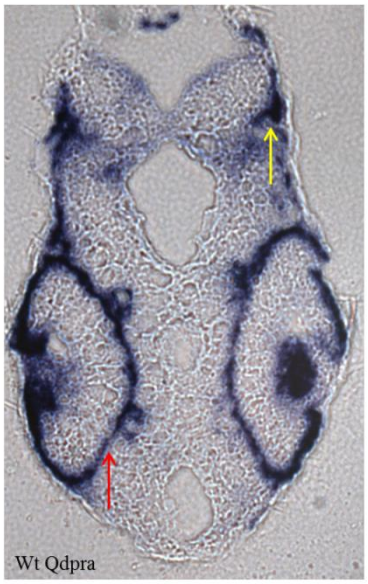

Supplemental Figure 1. WISH for *qdpra* at 24 hpf cryosection

Cryosection of 24 hpf zebrafish after WISH for *qdpra* shows exclusive expression in retinal pigment epithelium (red arrow) and NCC near the MHB (yellow arrow).

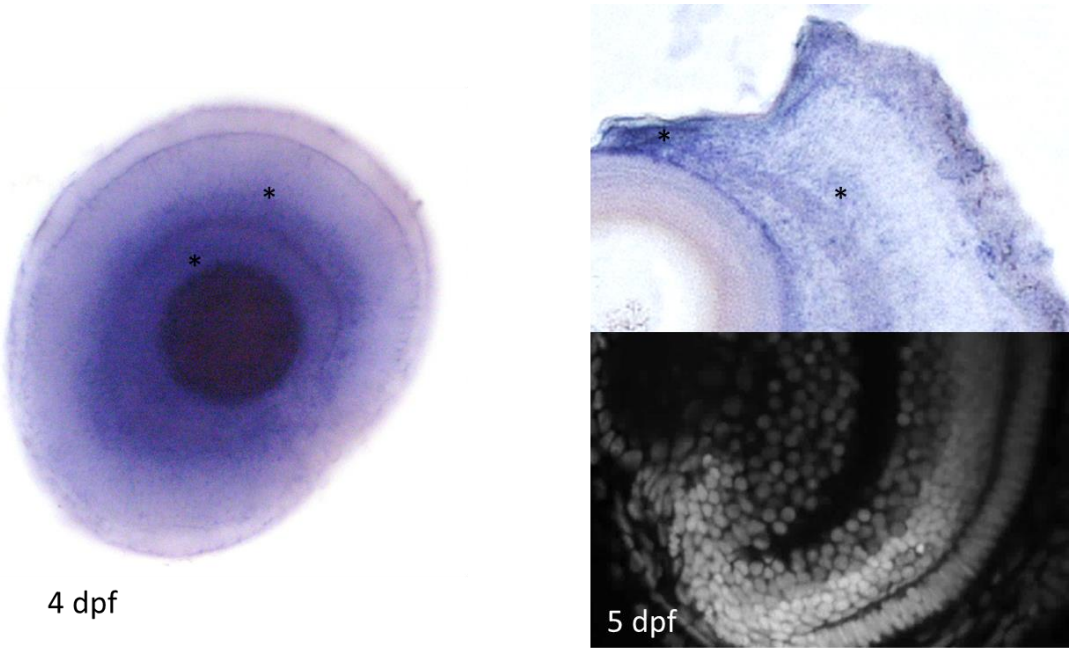

Supplemental Figure 2. WISH of 4 dpf Qdprb1 retina and Cryosection of 5dpf retina

WISH of 4 dpf retina stained for qdprb1 (lateral view), shows expression near CMZ and INL (asterisk). Cryosection of WISH for *qdprb1*, correlated to DAPI stain of 5 dpf retina, shows expression in CMZ and INL (asterisk)

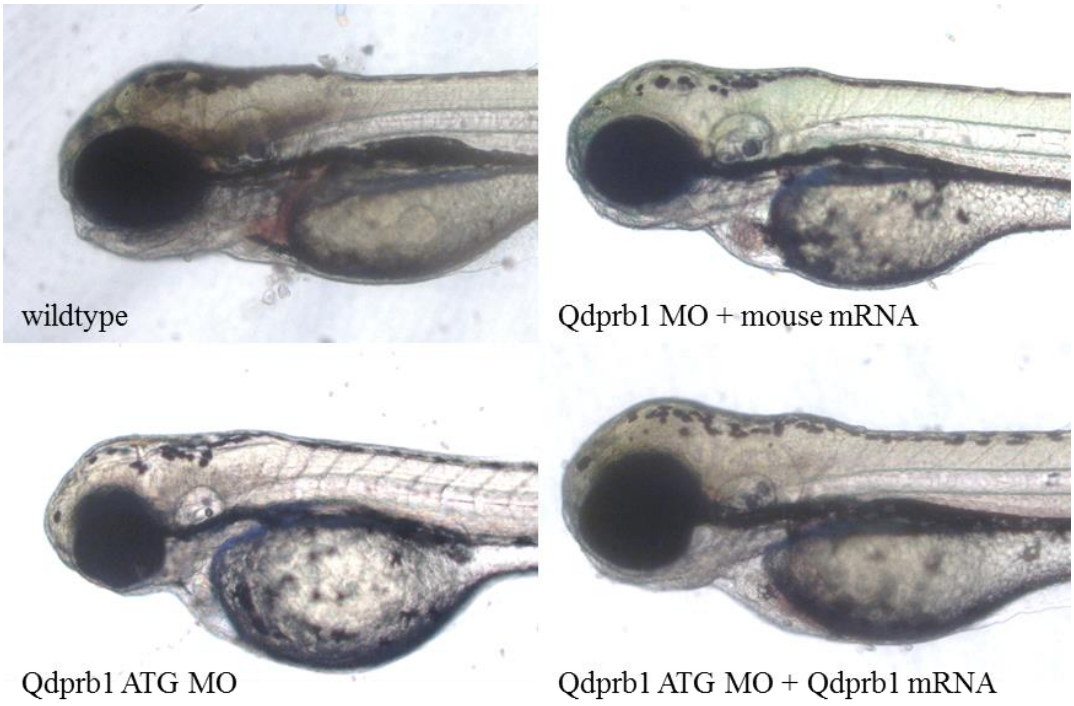

Supplemental Figure 3. Qdprb1 MO mouse rescue and ATG rescue

Morphology of 72 hpf embryos of wildtype (top left), Qdprb1 splice MO + mouse Qdpr mRNA (top right, showing partial rescue of the phenotype), Qdprb1 ATG MO (bottom left. Showing identical phenotype to Qdprb1 splice) and Qdprb1 ATG MO + qdprb1 mRNA (bottom right, showing complete morphological rescue)

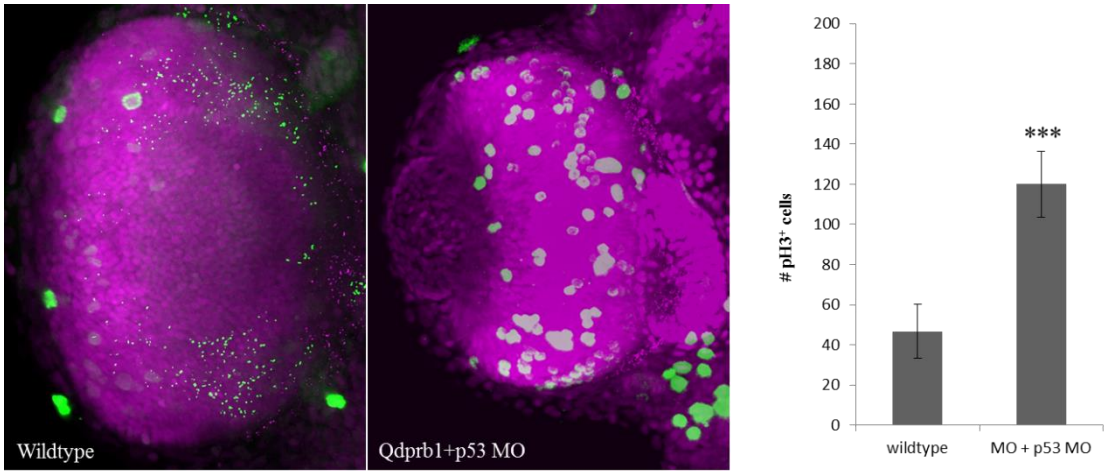

Supplemental Figure 4. pH3 antibody staining in retina of Qdprb1 MO + p53 MO injected embryos

pH3 antibody staining of wildtype (left) and Qdprb1 splice MO + p53 (middle), showing identical pattern observed in only Qdprb1 MO knockdown. Statistics (right) shows a significant increase in pH3 cells in half the retina

Supplemental B. Recipes

B.1 Recipes - ISH

4% PFA

- 20 g PFA to 500 ml DEPC-PBS
- Heat to 59 °C until dissolved
- Store in 50 ml Aliquots at -20 °C

DEPC H2O

- Add 1ml DEPC per 1L H_2O into autoclaved bottle. Stir for at least 2 h (best overnight)
- Autoclave to degrade DEPC
- Store RNAse free

DEPC-PBS

- 8.7g NaCl
- 0.272g KH_2PO_4
- 1.14g NA_2HPO_4
- Add 1000ml dH2O and 1ml DEPC
- Stir for at least 2 h
- Autoclave to degrade DEPC
- Store RNAse free

PBST

- 0,1% Tween 20 in PBS

Hybridization buffer

- 50% Formamide
- 5x SSC
- 0,1% Tween
- Add 5mg/ml tRNA and 50ug/ml Heparin for overnight hybridization

Blocking Buffer

- 2% Sheep Serum
- 10 mg/ml BSA
- In PBST

AP Buffer (50ml)

- 2ml NaCl (5M)
- 5ml $MgCl_2$ (1M)
- 10ml Tris (1M), ph 9.5
- 100µl Tween 20
- In DEPC-H_2O

Staining solution

- 10 ml AP buffer
- 200 µl NBT/BCIP solution (Roche)

B.2 Recipes - Cloning

10X LB (1L)

- 100 g Tryptone
- 50 g Yeast Extract
- 100 g NaCl
- Adjust to ph 7.5
- Autoclave

Dilute 1 in 10 for 1X LB

LB Agar (1L)

- 15 g Agar in 1X LB

B.3 Recipes – Antibody staining

PBS-Tr

- 1% Triton 1X PBS

Incubation Buffer

- 1% Triton
- 10% sheep serum
- 1% DMSO
- In 1X PBS

B.4 Recipes - Agarose Gel

1% gel

- 4g Agarose
- 400ml 1xTAE
- 20ul EtBr (10mg/ml)

10X TAE (1L)

- 48.4g Tris base
- 11.4ml glacial acetic acid
- 3.7g EDTA
- 1L H_2O

B.5 Recipes – RNA binding

10X MOPS (1L)

- 41.9g MOPS
- 8.2g Sodium acetate
- 3.72g EDTA
- Adjust to pH 7.0 with NaOH

500P lysis buffer

- 20mM Tris-HCl pH 7.5
- 500mM LiCl
- 0,5% NP-40
- 1mM EDTA
- 5mM DTT

100N buffer

- 20mM Tris-HCl pH 7.5
- 200mM LiCl
- 1mM EDTA
- 5mM DTT

PNK buffer

- 10mM Tris-HCl pH 7.5
- 50mM NaCl

PNK hot mix (1rxn)

- 27 µl PNK buffer
- +5 mM DTT
- 1 U/µl PN Kinase – 3 µl (of undiluted)
- 0,1 µCi/µl y-32-ATP – 0,3 µl when 250 µCi stock

Supplemental C. Primer

C.1 Primer - ISH

Table 15. Supplemental – Primer ISH

Name	Primer FW	Primer RW	Size fragment (bp)
Gch1	CTATTCTTCGGGGTCTCGGG	ACACCTAACATGGTGCTGGT	469
Gchfr	CACAGATCCGCCTGGAGACA	CAAACGTAAGACTGATGCACG	563
Gfap	TCCCAGCGTTCCTTCTCATC	TCAAATAGCACCGCTGACCA	1900
Pah	CGTGAGGACAACATCCCACA	GGGCTGAAGTTTAGGCTCGT	441
Qdpra	TGCGAACCGTGTCCTTGTTT	AACCATACCTGGAGTGGCGT	418
Qdprb1	GGTGAAGAGAAGGTTGACGC	TACCTGAAGGCGGTCTGCTT	451
Qdprb2	AGACAGTTTGTGTCAGAATCA	CCACTGTTCTGCCATTAGCG	771
Slc1a2a	CTCATCCACCCTGGAAACCC	GAAGCTGTTCCTAAGGCGGT	635
Slc1a2b	AATGCAGCACGATGAGGGAA	CCATAACCCCGGTGTATCCG	962
Slc1a3b	CCTTTGCCTGGGTGGATGAT	ACGTGAAGGGCTTTCTGAGG	331
Spra	CTCGTCAGTCCTTGGGGAAT	GAGCGTAGTTCAGCACTCGG	613
Sprb	CATCATCCGAGAGCGTGTGA	TGATGTTGACCACCGTCCTG	522
Th	TGAGGAGGAGAAGACTGGCA	TGTAAACCTCCCATGTGGCAT	494
Tph1a	CGAGATGGAGAATGTGCCGT	GCATTTCCTGACAGTGCGTG	747
Tph1b	TGCGGATCTTGCCATGAGTT	CCAGCCCCGTATGCTCTTAG	555
Tph2	TCTACGCAGCGACTAACCAC	ATTGGCATCGGAACAATGCG	461

C.2 Primer – qRT-PCR

Table 16. Supplemental - Primer for qRT-PCR

Name	Primer Fw	Primer Rv
Aqp4	TGGACACATTCAGGAGGTGC	GGACAAGCCAAAGCAAAGGG
Bcat1	CCATCATCTCACAAGGAAAACGG	GATGCATGGACAGGTTCCCA
Bcat2	GGAACCGAACTTCACTAGGT	TGCCGCCCATTTTGTACTCT
Ef1-α	TCCTCTTGGTCGCTTTGCTA	AAGAACACGCCGCAACCTT
Gch1	GGCCGGGTGCATATAGGTTA	TGGTGCTGGTCACAGTCTTG
Gfap	GTGTCCATGCTGGTGTCTCT	ATGCTGAAGGAGGAGATGGC
Gls2b	CGACTACTCGGGACAGTTCG	CCAGTTCCTGACAGAAGCGA
Glsa	ATGACAAGAGAAGGAAGGCAG	GCACCGTCTGAAGTGGTTTTC
Glula	CAACCTGGAACTCCCACTGAG	TACTGACGGACACCCCTTTG
Glulb	AGCCCTTCTTTTCCTGACCC	CGAGGAAGGAGGTTTGAAGCATA
Olig2	CACTGAACGCCATGGACTCT	CCATTGAGTCCTCCTCAGCG
Qdpra	GTCATTCACCGATCAAGCCG	CTGCGATGTACTCCAGTGGT
Qdprb1	GGTGAAGAGAAGGTTGACGC	GAGGAAGACCACTGTTCGGC
Qdprb2	TCTAGCAATCCTTCCGGAAACT	CACTGTTCTGCCATTAGCGG
Slc1a2a	GACTGGCTTCTGGATCGCTT	ATCGGCTGACAGGAGTTGTG
Slc1a2b	CCAGCCTGACAGTTGTGGAT	TTGTCATCGATGGGAGACGC
Slc1a3a	TGATACCCGTGTGTTGCTGT	AGGATTATTCCCACGATGACGG
Slc1a5a	CTGCATGTTTCCAGTGCGTC	CATGTGCGATCAACAAGCCA
Slc38a2	CTCCGTTAGTGTACCACGCA	GGCCAATGAAGGAGGGTCTC
Slc38a6	ACCACAGCATACAGACGGTG	CCATGGCATACGAGAGACCC
Slc38a7	GCATCACAGCTGGAGTGACA	TATTGCGCCCGATCAGCTTGT
Slc38a9	TCAAGAGAACAACGTCCGGG	AACAGAAGGAAGGTCCTCGC
Slc7a5	CAGGGGGTGACTACGCTTAC	TGACAGCGGTCAACAACAGTAT
Th	AGTAGCCAGCGTGACTTGTT	GTGCGCTGCAGGAATAGAGA
Vimentin	CCTGCGAGAGTCCATGAAGG	ATCTTCAGTGCCTCGGGTTC

C.3 Primer – Rescue

Table 17. Supplemental – Primer for Rescue mRNA

Name	Primer Fw	Primer Rv
Mouse 001 +RE sites	AGCGGATCCCTTTGGGGGCGGG GCACAGGCAGGGGCGGGTGTTC	AGCCTCGAGAGACATGAAGTGTG TTTATTAGGAAGAACACT
Qdprb1 mRNA	ACGACGGGATCCTGCATAACAC GGTCTCGTGCTCGTGAAGACAGA ATGGCAGC	CGTCGTTCTAGAATTAAAGTACGC TATATTTAATAGTCAGAATATAAC AGTACTCCAATTT

C.4 Primer – RT-PCR

Table 18. Supplemental – Primer for RT-PCR MO control

Name	Primer Fw	Primer Rv
Qdpra-splice Control	GTTGCCAGTATTGACATCGGAGC	TGGAGTGGCGTCCAGTGAAG
Qdprb1 splice Control	TGGGTTGCCTCTATTGATCT	TACAAATAGTGGAGGTCCATA

C.5 Primer – FLAG-Plasmid

Table 19. Supplemental – Primer for FLAG-DHPR generation

Name	Primer Fw	Primer Rv
DHPR Amplify	TGGCAGGAGCAGGATGGCG	CTAAAAATATGCTGGGGTGAGT TC
DHPR C-Terminus FLAG + Restriction site	ACGGGATCCATGGCGGCGG CGGCGGCTGCAGGCGAGGC GCGC	CGCGCGGCCGCCTACTTGTCGT CATCGTCTTTGTAGTCAAAATAT GCTGGGGTGAGTTCCGTCCTTCC TTC
DHPR N-Terminus FLAG + Restriction site	ACGGGATCCGCCACCATGGA CTACAAAGACGATGACGAC AAGGCGGCGGCGGCGGCTG CAGGCGAGGCGCGCCGG	CGCGCGCCGCCTAAAAATATGC TGGGGTGAGTTCCGTCCTTCCTT C

“Life is ours, we live it our way!”

(Metallica, 1991)